TESLA - COLLABORATION

Contributions to the CEC/ICMC '95

July 17 - 21, 1995 in Columbus, Ohio

August 1995, TESLA 95-21

INTRODUCTION

The Cryogenic Engineering Conference and International Cryogenic Materials Conference (CEC/ICMC), a biannual conference in the fields of superconductivity and cryogenics, was held in Columbus, Ohio, USA, July 17-21, 1995.

In the 95-meeting, there were 514 papers contributed into 66 technical sessions with the conference participants more than 700. To provide a forum which allows the superconductivity and cryogenics community at large to remain appraised of the status of major application, the conference program committee with support from the TESLA Collaboration specially organized a technical session entitled "TESLA", dealing with the various aspects of the TESLA project development.

The eleven papers (about the SRF cavities, cryostats, RF power input & HOM couplers, cryogenic systems of TESLA & TTF and T-R mappings) presented at the TESLA session (TU-A2 and TU-A3) are enclosed herewith for your information together with a contribution on cold compressors.

Quan-Sheng Shu (DESY)
Moyses Kuchnir (Fermilab)

August 8, 1995

Contributions to the CEC/ICMC'95 - Contents

Presented as an invited talk at the CEC/ICMC Conference, Columbus, Ohio USA, July 17-21, 1995.

TECHNICAL CHALLENGES OF SUPERCONDUCTIVITY AND CRYOGENICS IN PURSUING TESLA-TTF

Quan-Sheng Shu for the TESLA Collaboration

Deutsches Elektronen-Synchrotron (DESY)
Notkestrasse 85, 22607 Hamburg, Germany

ABSTRACT

TESLA (TeV Energy Superconducting Linear Accelerator) Collaboration is an international R & D effort towards the development of an e^+e^- linear collider with 500 GeV center of mass by means of 20 km active superconducting accelerating structures at a frequency of 1.3 GHz. The ultimate challenges faced by the TESLA project are (1) to raise operational accelerating gradients to 25 MV/m from current world level of 5-10 MV/m, and (2) to reduce construction costs (cryomodules, klystrons, etc.) down to $2,000/MV from now about $40,000/MV.

The TESLA Collaboration is building a prototype TESLA test facility (TTF) of a 500 MeV superconducting linear accelerator to establish the technical basis. TTF is presently under construction and will be commissioned at DESY in 1997, through the joint efforts of 24 laboratories from 8 countries. Significant progress has been made in reaching the high accelerating gradient of 25 MV/m in superconducting cavities, developing cryomodules and constructing TTF infrastructure, etc. This paper will briefly discuss the challenges being faced and review the progress achieved in the technical area of superconductivity and cryogenics by the TESLA Collaboration.

INTRODUCTION

There is a widespread consensus within the high energy physics community that the next electron positron collider would be built with a center of mass energy of 500 GeV and luminosity of a few times 10^{33} $cm^{-2}s^{-1}$. Such a collider would provide for top analyses and discovery reach up to a Higgs mass of ≈ 350 GeV. Worldwide, there are a number of groups pursuing different linear collider designs. The TESLA collaboration is an international R & D effort to develop a linear collider using superconducting accelerating structures (25 MV/m, Q_0=5x10^9) at low frequency (1.3 GHz)[1,2,3]. The TESLA collaboration consists of 24 institutes from 8 countries.

Advantages of TESLA

The technical advantages of superconducting RF cavities is their high Q value and low RF wall losses (less than Cu cavities by a factor of 10^5). It allows us to use large aperture structures operating at low frequency (1.3 GHz, L-band) with long macro pulse length and low peak power requirements. The large aperture has a beneficial consequence of substantially reducing transverse and longitudinal wake field effects, leading to relaxed Linac alignment and tolerances.

substantially reducing transverse and longitudinal wake field effects, leading to relaxed Linac alignment and tolerances.

Challenges of TESLA

Despite the attractive feature of the TESLA design, a major effort is needed to demonstrate that a linear collider can be built at a cost competitive with its normal conducting counterparts. The two technical challenges being faced and the key approaches to reach the ultimate goals can be summarised as follows [4,5]:

(1) Increase operational accelerating gradients of SRF cavities to 25 MV/m from current levels of 5-10 MV/m by eliminating field emission and thermal breakdown.

(2) Decrease structure cost by utilising multicell structure, long cryostat, high efficiency klystron and cost effective fabrication techniques.

We believe that the construction cost can be reduce to $2,000/MV compared to the current $40,000/MV. The TESLA Collaboration is building a test facility (TTF) of a 500 MeV superconducting linear accelerator to establish the technical base.

BASIC INFORMATION ABOUT TESLA AND TTF

TESLA Layout

The overall layout of the TESLA 500 is illustrated in Figure. 1 [1,6]. The electron beams (e^+ & e^-) are accelerated to 250 GeV by RF fields in each main linac. Each linac has an active accelerating legnth of 10,000m consisting of about 10,000 superconducting RF cavities. Total length of TESLA-500 is about 32 km. A discussion of the layout is introduced in the reference [6]. An overview of the main parameters of TESLA-500 is given in table 1.

As shown in Figure 1. TESLA is composed of many components. However, here we only introduce the technical issues relevant to cryigenic engineering. For convenience of discussion, we consider the TESLA-500 as a superconducting and cryogenic structure which is energized through thousands of high power RF couplers and cooled by a huge superfluid-He refrigeration system. The structure of the 20-kilometer active accelerating

Table 1. Parameters of TESLA-500

Linac energy	2x250 GeV	Luminosity	6×10^{33} cm^{-2}s^{-1}
Beam pulse current	8 mA	Bunch separation	0.7 μs
Number e/bunch	3.63×10^{10}	Bunch length	0.7 mm
Nu. of bunches/pulse	1130	Rep rate	5 Hz
RF pulse length	1.3 ms	Total Length (incl. inter. reg.)	32 km
Beam pulse length	0.8 ms	RF Freq.	1.3 GHz

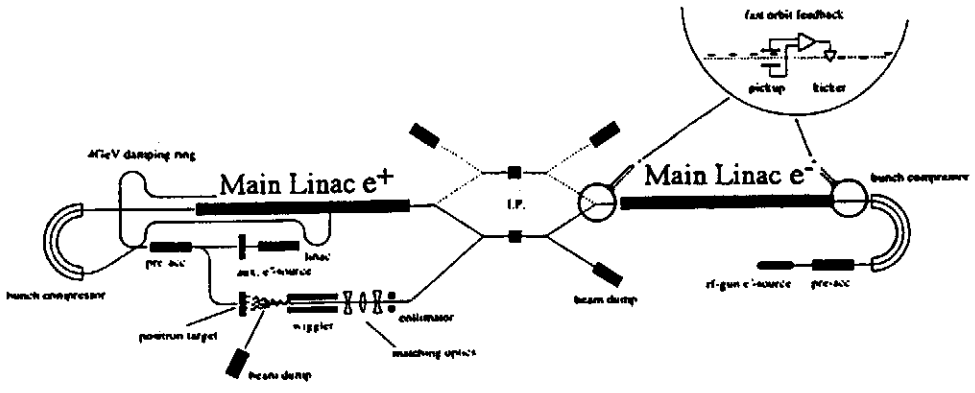

Figure 1. An overall layout for TESLA-500.

Table 2. TESLA-500 as a superconducting and cryogenic machine (consider SRF cavity as basic unit)

Unit	Group
9 SRF cavity cells	A cavity (including LHe vessel, RF couplers)
8 cavities (incl. quadr. packages)	A cryomodule of 12.2 m, and (4 cryomodule share one 10 MW klystron)
12 cryomodules	A string of 148 m, has an individual cryo-loop
12 strings	A TESLA subunit of 1830 m (one subunit has a 3.2 KW/2K cryo-plant)
16 subunits	The TESLA-500 (an active superconducting accelerating length of 20,000m)

machines is summarised in Table 2 with a SRF cavity (Eacc = 25 MV/m, Qo = $5x10^9$) as the smallest unit. The basic cryogenic structure unit is a cryomodule consisting mainly of 8 cavities. 4 cryomodules share a klystron of 10 MW peakpower. The heat load to 2K from a cryomodule is 21.4 W including dynamic (RF) and static losses [7]. To keep the TESLA machine in superconducting state, the total estimated cooling power is: 51 kW at 2 K, 37 kW at 4.5 K and 314 kW at 40-80 K [8]. Sixteen 2 K-refrigerators are needed to provide the cooling power distributed over the machine. The total liquid He inventory estimated in the TESLA machine is about 87,200 - 102,800 kg (depending on the version of cooling loops to be selected).

TTF Layout

Figure 2 is a schematic layout of the TTF consisting of an injector with a capture cavity, 15 MeV beam analysis area, TTF Linac with four cryomodules (the design requirement of the TTF cavities is Eacc = 15 MV/m and Q = $3x10^9$) and a high energy experimental area. The TTF is refrigerated by a He II refrigerator: 100 W at 1.8 K, 400 W at 4.5 K and 2000 W at 70 K (the refrigeration power will be expanded to 200 W at 1.8 K).

With the TTF, we will demonstrate and verify many technical issues, such as, cavity processing technologies, cavities performance, design and performance of couplers and cryostat, cryogenic operation, energy and position feedback, alignment, etc.

The TTF is also being considered for use as a Free Electron Laser Facility.

TESLA SRF CAVITIES

The TESLA SRF cavity is shown in Figure 3 and an overview of the main parameters is given in table 3. The TESLA cavities are made of high purity Nb sheets (2.8 mm thick) with a RRR of about 300. The cavity shape combining an elliptical iris and a spherical equator results in more satisfactory electromagnetic parameters than other combinations. Another consideration to TESLA cavity design is to minimize the ratio both of Epeak/Eacc (2.1) and Hpeak/Eacc (4.2 mT/MV/m) in order to reach the highest gradients [3,7].

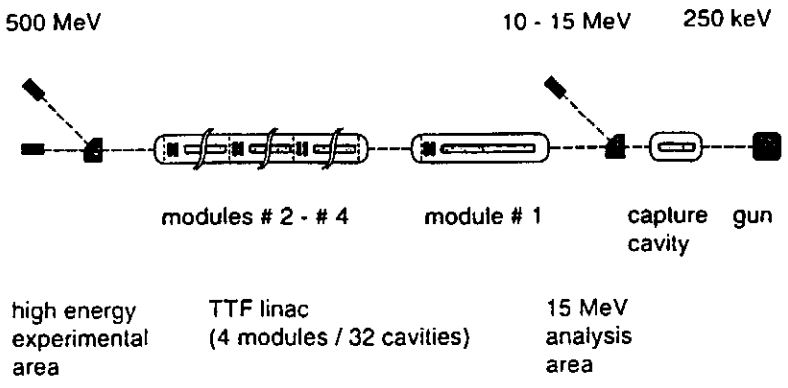

Figure 2. Schematic layout of the TESLA Test Facility (TTF)

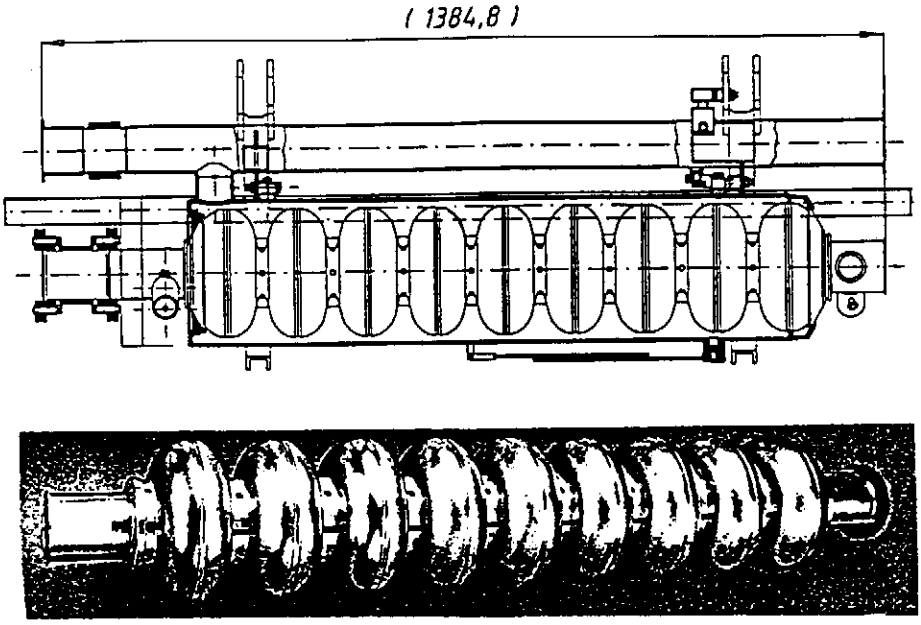

Figure 3. TESLA cavity with LHe vessel & 2K forward line, and a picture of the prototype cavity

Table 3. Parameters of the TESLA cavity

RF Freq.	1.3 GHz	Gradient	25 MV/m
Cavity cell	9	Cavity aperture	35 mm-radius
Effective length	1.035 m	Epeak/Eacc	2
Bpeak/Eacc	4.2 mT/MV/m	R/Q	1011 Ω/cavity
Peak RF power	206 kW/m	Stored energy	0.127 J/(MV/m)^2
Cryo load/module	21.4 W	G (Rs=G/Qo)	271
Coupling cell-cell	1.87%	HOM K(ll)	9.24 V/pC

The maximum cell number of 9 is determined by effective HOM damping requirement. There is one input power coupler and two HOM couplers for a cavity. Each cavity has a liquid He vessel with small LHe inventory which reduces the coldmass and allows a fast cooldown and warmup of the cavity.

QUEST FOR HIGHEST ACCELERATING GRADIENT -- AN ULTIMATE TASK

The TESLA collaboration aims for the highest operating gradients Eacc in SRF cavities using economically affordable approaches.

Theoretical Limit of Eacc

The limit magnetic field in RF is larger than Bc (type I superconductors) and Bc1 (type II) respectively, and is called superheating critical field Bsh. Table 4 gives the Bsh values of typical materials studied in SRF technology compared with the maximum surface field Bexp experimentally obtained so far[9]. Using a rule of thumb that 40 Gauss (4mT) is equivalent to 1 MV/m accelerating gradient in cavities with the TESLA shape, the theoritical limit for Nb by Bsh is then about 60 MV/m, and for Nb_3Sn, 100 MV/m[9].

Achievements and Limit in Operating Accelerators

Since the early 1970s, significant progress in the state of the art SRF accelerating cavities have been achieved. The operating accelerating gradients in more than 10 laboratories (such as Argonne[10], CEBAF[11], CERN[12], Cornell[13], Darmstadt[14], DESY[15],

Table 4. Critical field in DC and RF superconductivity

Materials	Tc [K]	Bcth [mT]	Bc1 [mT]	Bc2 [mT]	Bsh [mT]	Bexp [mT]
Sn	3.7	30.9	-	-	68	30.6
In	3.4	29.3	-	-	104	28.4
Pb	7.2	80.4	-	-	105	112
Nb	9.2	200	185	420	240	160
Nb_3Sn	18.2	535	20	2400	400	106

Bcth - thermodynamic critical field
Bsh - superheating critical field
Bexp - experimentally obtained maximum field
All data refer to values at T = 0 K

KEK[16], Saclay[17], etc.) and 400 structures reached 5-10 MV/m, compared to design goal of 5 MV/m. These achievements are attributed to anti-multipactor, round cell shape, high thermal conductivity Nb to avoid thermal breakdown (TB) and clean surface preparation to avoid field emission (FE). However, the excellent performance of the operating cavities is not adequate for the proposed TESLA machine. Tremendous efforts are still needed to comfortably reach the TESLA goals of Eacc ≥ 25 MV/m and Q ≥ $5x10^9$. The main obstacles still to overcome are FE and TB. Investigation and elimination of FE and TB have become one of the highest priorities in TESLA and TTF projects.

Understanding FE and TB

Significant efforts have contributed to understading and defeating FE and TB by the TESLA Collaboration.

Electrons on the cavity surface can be pulled out and accelerated in the cavity vacuum by RF electrical fields. These field emitted electrons absorb energy from RF fields and deposit the energy in their landing area on the cavity, resulting in degradation of Q value and limiting the Eacc. Studies with DC FE scanning microscope and in SRF cavities [18,19,20,21] indicate that most FE electrons come from submicro-size foreign particles of a metallic nature with irregular shapes. Some studies also found that the condensed gases and heat treatment at 200-600° C will activate FE [21, 22]. Thermal breakdown is due to imperfections of the RF surface. For a given imperfection, the thermal breakdown field

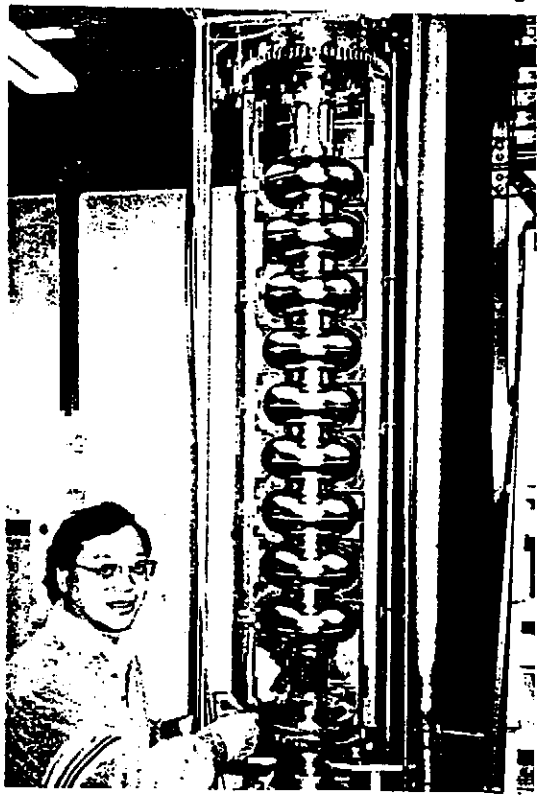

Figure 4. Rotating T-R mapping system for diagnostics of TESLA 9-cell cavities.

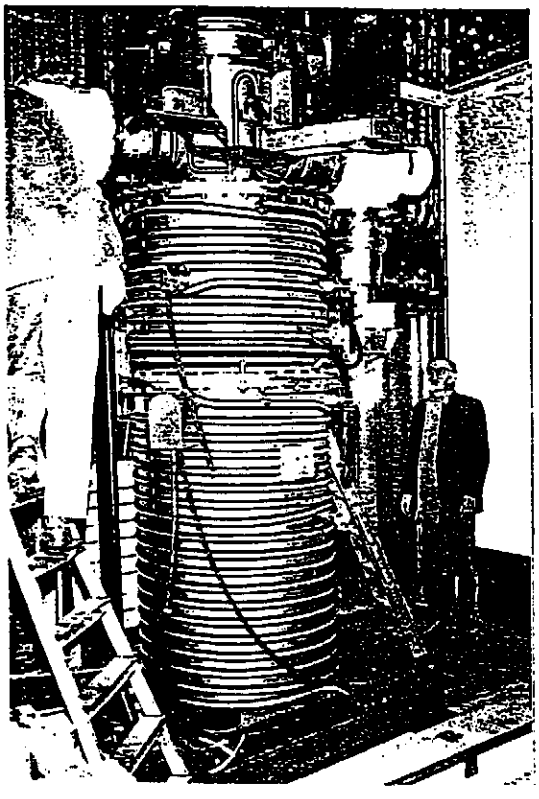

Figure 5. The ultahigh vacuum oven for Ti-gettering purification of cavities

scales roughly as the (thermal conductivity)$^{1/2}$. The residual resistance ratio (RRR) is used to characterise the thermal conductivity in a convenient way.

It is impossible to directly observe the FE and TB on the inner surface of cavities during RF operation. Therefore, the main approach to understanding the FE and TB of cavities is to study the hot spots and X-rays (induced by impacting FE electrons) generated on the cavity surfaces during RF operation. At DESY a rotating T-R mapping system for TESLA 9-cell cavities has been developed and more than 10,000 spots on the cavity can be investigated in one turn with 10° stepping. We have used it to successfully identify the TB location, trace the dynamic prograss of cavity quench, locate the heating areas by FE electrons and simulate the emitter locations [23].

Reducing FE and TB

For years in many laboratories around the world, there have emerged many comprehensive approaches for cavities processing in order to reach the highest possible gradient. Many of these approaches have been adopted, further developed and used by TESLA collaboration at DESY.

Reducing TB with UHV Oven.

Over the last 10 years the RRR of sheet Nb delivered by industry for cavities has been improved to 300 from 30 by better melting practices removing most of the dissolved impurities of O, N, H, C, etc. Cavities using these sheets produce a range of TB at 13 - 19 MV/m. Higher RRR of > 500 is desired for reaching a Eacc > 25 MV/m. Currently the way to increase RRR is to employ solid state gettering [19, 24]. In this technique, both the inside and outside surface of a prepared cavity are exposed to Ti vapors at 1400° C for 2-4 hrs. The oxygen which diffuses to the cavity surface is gettered by the evaporated layer. After improvement of RRR, both surfaces are etched to remove the foreign metal layer. Figure 5 is the UHV oven used at DESY (1400°C at 10^{-7} mbar). The control samples Nb indicate that RRR of 250-300 is raised to > 500 after the Ti-purification treatment. Several TESLA 9-cell cavities show Eacc increase to 20 - 26 MV/m.

Also the UHV oven has played an important role in reducing the FE and the hydrogen content of Nb, eliminating the "H-desease".

Figure 6. The clean room for cavity processing and assembling.

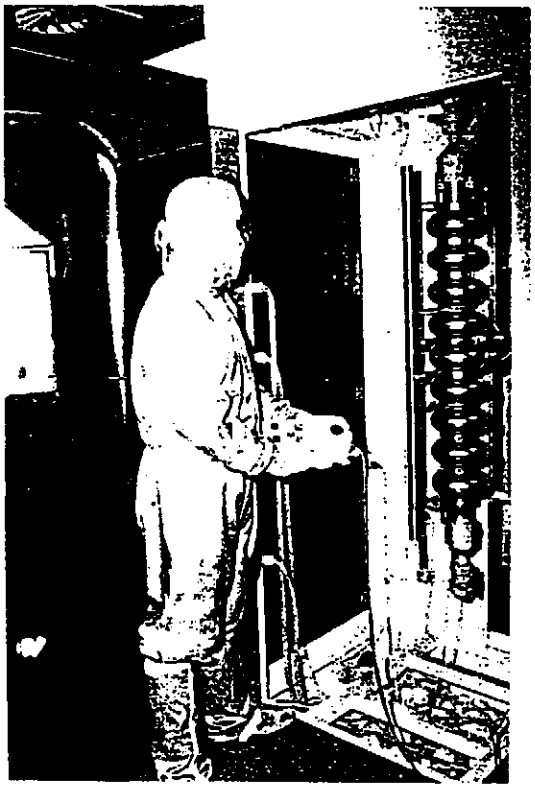

Figure 7. Chemistry and rinsing of cavity in the clean room

Cleaning Technology Defeating FE

Cleanning techniques similar to those utilized in semiconductor industry are used to remove all FE particles from the cavity's RF surfaces [25]. Cleanliness during chemical etching, water rinsing (high purity water of 15 MΩ-m) and assembling have played a importamt role in higher Eacc. The high pressure water rinsing (HPR) device made by CERN for the TESLA collaboration is very helpful in removing foreign particles which are difficult to remove by regular water rinsing. Several prototype TESLA cavities after HPR (without Ti-purification) produced Eacc > 15 MV/m.

We built a clean room of 300 m^2 with class 10 and 100 areas in 1993 for chemical etching, HPR, and cavity assembling (also we can load cavities into the UHV oven in a clean room area). The capability of HPR is as high as 200 bar. Figure 6 is a part of the clean room and Figure 7 shows the clean chemical etching of a TESLA cavity.

High Peak Power RF Processing - Last Chance to Reduce FE.

Despite how good a job performed to eliminate FE, there is always a possibility that particles escape removal and stay on cavities surfaces. Therefore a technique that can eliminate the emmiters in situ is highly desirable. The technique, called HPP - high power processing developed at Cornell University, is to apply a high power RF pulse to the cavity in situ and eliminate the FE through an explosive process [26]. The idea is to raise the electric field at an emitter as high as possible in a short time (μs - ms) which generates a very high FE current. The transient high current melts, evaporates and activates a RF spark to destroy the FE emitters. The high RF pulse power processing of cavities provides a final, effective way to destroy the remaining FE emitters[22]. At DESY a HPP facility has been used successfuly in raising Eacc. The peak klystron power is 4.5 MW with pulse length of 2 ms.

The key technologies we have used to rduce FE and TB can be summarized in Table 5.

Encouraging Achievements with TTF Project

With the above techniques, we significantly increase thermal conductivity and educe FE. Two 9-cell TTF prototype cavities reached respectively Eacc = 16 MV/m and 21 MV/m both with Q > $6x10^9$ in CW mode. The first series TTF 9-cell cavity (RRR=350) reached Eacc=26 MV/m in 1 ms RF power length (TESLA operational condition) and 22 MV/m in CW [27]. Also, a TTF injector cavity provided by Saclay reached 21MV/m, Q > $4x10^9$. Compared to the TTF goal of Eacc=15 MV/m and Q=$3x10^9$, these initial result is very encouraging. Continuing progress is expected with improvements in processing technologies and diagnostic testing. Some representative results are plotted in figure 8.

Table 5. Key technologies of cavities processing for highest Eacc

Techniques	Short Description	Impact on FE	Impact on TB	Results
Clean cavity handling	Class 10-100 clean room for chemistry, rinsing & assembling	Eliminating foreign particle contamination	Deep chemistry may remove some impurities	Good for Q and Eacc
Heat treatment + Ti-purification in UHV oven	Heat cavity at 1400 C for 1-4 hrs, Ti vapor coated in vacuum	Greatly reduce emitters existing on cavities	Improve RRR by a factor of 2, (improve K)	Substantially increase Q and Eacc
High pressure water rinse[24]	Rinse cavity by high purity water (15 MΩm) at 200 bar	Reduce emitters density		Increase Q and Eacc
High RF power processing	Apply high RF power pulse (1-2 MW, μs-ms) to cavity surface	Eliminate emitters in situ		Substantially increase Q and Eacc

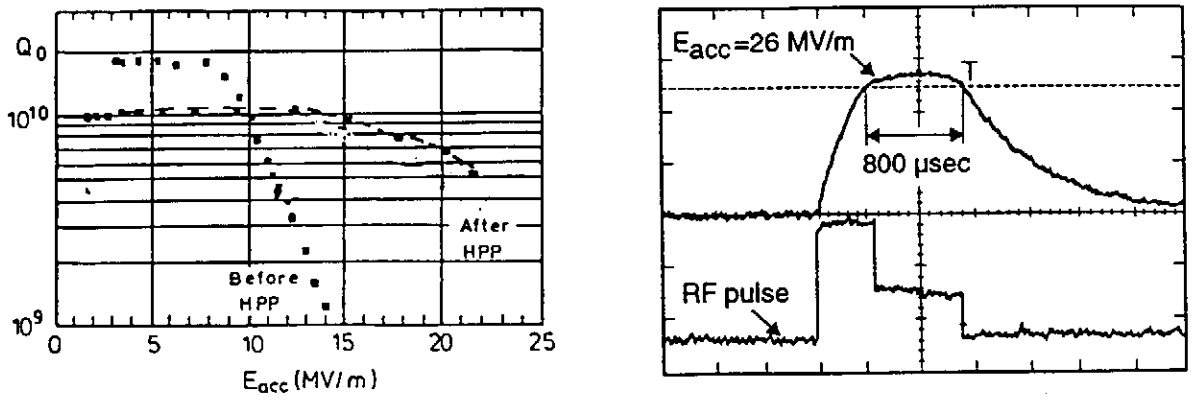

Figure 8. (A) Q vs. Eacc plots of TTF 9-cell cavity -1. (B) The performance of cavity D2 in pulse RF condition similar to TTF operation. 26 MV/m of Eacc is reached.

TESLA PROTOTYPE CRYOMODULE

The cryomodule is 12 m long and consists of 8 SRF cavities with LHe vessels, one quadrupole magnet package, associate fixtures (RF couplers, tuner, alignments, etc.) and a cryostat in which all the above components are housed. The TTF cryomodule also has some special requirements due to SRF cavity technologies. For instance:

(1) To eliminate FE, the eight cavities and quadrupole package must be assembled together in a clean room and be inserted in the cryostat as a single UHV tight unit.

(2) To improve cavity Q, magnetic shields are needed to reduce residual earth magnetic fields to less than 20 mGauss.

(3) Due to beam dynamic consideration, the axes of the cavities to the ideal beam axis need to be within ≤± 0.5mm.

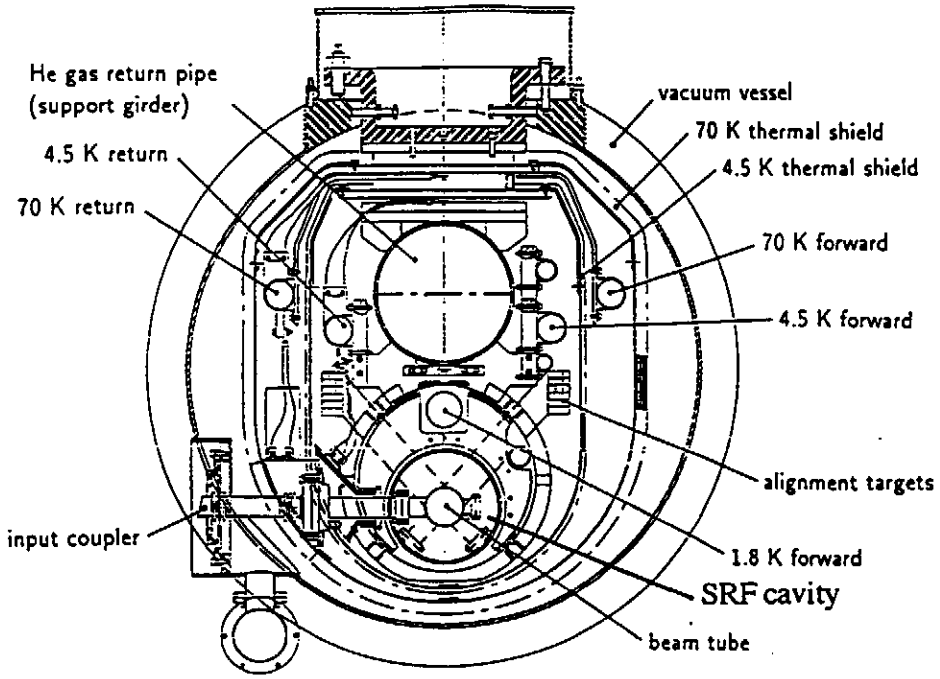

Figure 9. A cross section of TTF cryomodule.

Based upon cost effective design philosophy, most of the needs for keeping such special technical features must be addressed in the cryostat design. Figure 9 is a cross section of TTF cryomodule [3].

TTF Cryostat

The technical features and design details of the cryostat are discussed in the references [28, 29]. The total heat load to 2K from a cryomodule is estimated to be 21.4 W. The anticipated static heat load budget for one cryomodule is 4W at 2K, 14W at 4.5K and 120 W at 70K [28, 29 30]. Since dominate heat load in cryomodule is RF dynamic heating, nott the static heat leak, the primary interest of measuring the heat load is to verify the RF dynamic load. With the heat attributed to the RF loss, we can calculated the Q of each individual cavity or cavities. A comprehensive verification plan have been developed[3] (with about 135 thermometers, 2 accelerometers, etc.) that will allow us to study the heat leak through the power and HOM coupler and the thermal performance of the cryostat as well.

Special Magnetic Shield

The trapped magnetic flux from ambient fields (even less than 3 gauss) during cool down will seriously impact the cavity performance. The trapped flux will raise the RF power dissipation and gives an equivalent local residual resistance about $Rs \cong Rn(H/Hc2)\sin\alpha$. For a TESLA cavity (RRR=300, f=1.3 GHz), a conversion factor of 0.35 nΩ/mGauss closely matched experimental data. In order to get $Q = 5x10^9$ as specified for TESLA, surface resistance can not be larger than 25 nΩ, equivalent to 70 mGauss. Considering other contributions to the residual resistance and possibly increasing the Q, the remaining field around the TESLA-TTF cavities should be ≤ 20 mGauss. There are two shielding approaches in use: passive shields made of Cryoperm and active cancellation coil, both of which have been designed and examined[31].

Quadrupole Package

There is a quadrupole package [32] as shown in Figure 10, located at the end of each cryomodule, which includes: (1) a superferric quadrupole doublet (maximum gradient of 20 T/m and integrated gradient of 3T at 55.7 A) enclosed in a 4K LHe vessel, (2) two pairs of single layer dipole steering windings inside the quadrupole yoke bore, (3) a section of beam tube equipped with a beam position monitor (BPM) and HOM absorber (20 W), and (4) the He gas cooled power leads (0.1 g/s) for energising the magnets. At the end plate, there are two arms each holding reference targets for alignment.

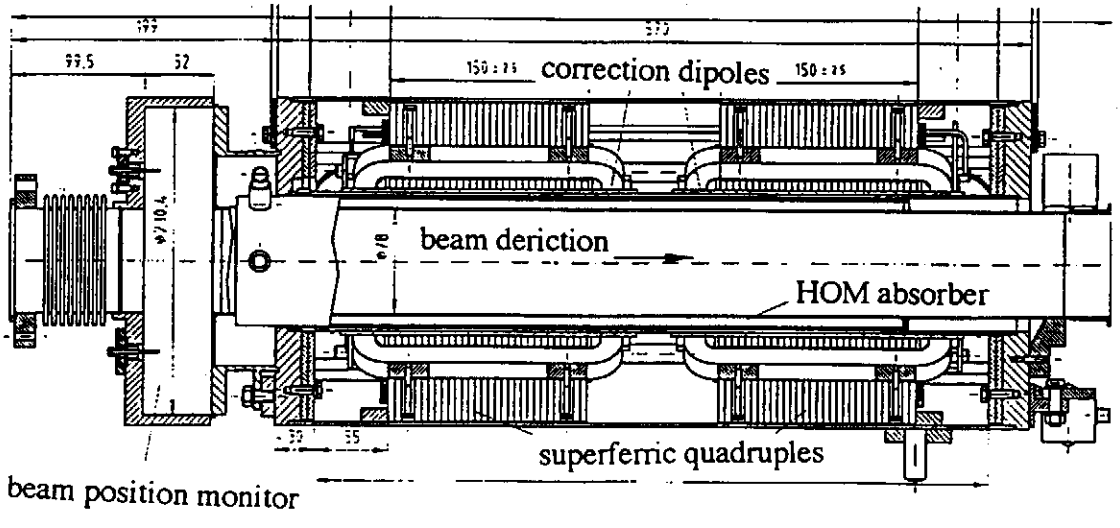

Figure 10. A quadrupole package.

Power and HOM Couplers

The TESLA input couplers [33, 34, 35]. are articulated with bellows to allow for the cavity moving during cooldown. The couplers also have an adjustable external Q of over a factor 10 range. The allowed RF heat load and heat leak are very low. All the above features make the coupler mechanically complicated. The input coupler is directly connected to the cavity cut off tube. It does not penetrate the LHe vessel, but is thermally anchored to the radiation shields with radiation cones. The thermal budget is 6W at 70 K, 0.5 W at 4.5 K and 0.06 W at 2 K. For TTF, two 5 MW peak power klystrons TH 2104 C from Thomson will power the four cryomodules and an extra 300 kW pulse klystron is needed for the injector .

To restrict the multi-bunch phenomena due to wakefields, the higher order modes (HOM) of the TESLA cavities must be damped (with Qext = 10^4-10^5) by two coaxial HOM couplers for each cavity [35]. The accelerating mode is not affected by the HOM couplers.

Capture Cavity

Besides the standard cryomodule there is an important cryo-component, called the capture cavity [36] in TTF. The capture cavity terminates the bunching upstream and provides the necessary energy for injection into the first cryomodule. The capture cavity is a standard TESLA 9-cell cavity and is installed in a separate cryostat at the end of the injector. It shares a common cryogenic feed box with the other four cryomodules. The capture cryostat only has an 80K insulation shield with 40 MLI layers. Epoxy-fiberglass rods are used instead of posts. The focusing superconducting solenoid magnet is conduction cooled from the 4K loop.

TTF STATUS

A 3000 m^2 of building, Hall III, has been assigned to host the TTF Linac and TTF infrastructure [5, 25]. We plan to deliver a beam through injector and first cryomodule with energy of about 140 MV/m by the end of 1995 (or early 1996). The complete 500 MeV TTF Linac will be commissioned in 1997. Figure 11 is an overview of the TESLA Test Facility.

For cavity processing, a clean room of 300m^2 (including a class 10 area); a chemistry etching facility with purity standards equal to semiconductor industry; a high pressure ultra-clean water rinsing system (18 MΩ-m, 200 bar); an UHV furnace with Ti-gettering

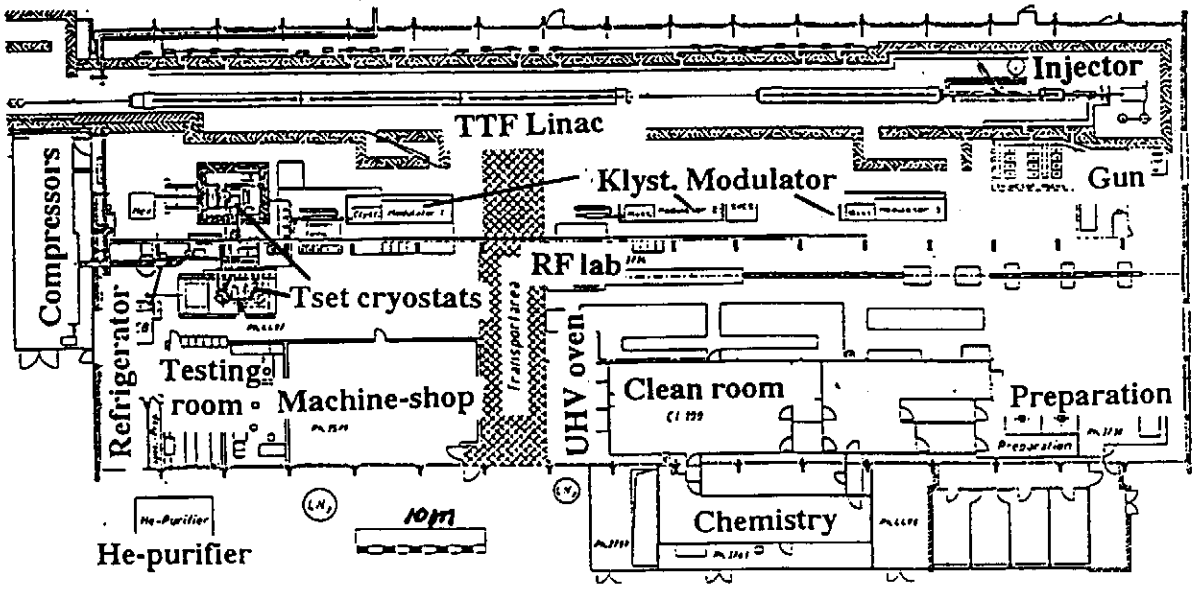

Figure 11. Overview of the TESLA Test Facility (TTF) at DESY.

purification fixture at about 1400° C, 10^{-7}mbar; a high power RF pulse processing system with up to 2 MW peak power; and a modulator and klystron of 4.5MW, 2ms have been installed and commissioned.

For testing, a LHe II cryogenic system with a warm vacuum compressor assembly for handling 10 g/s He at a pressure of 10 mbar and cooling capability of 100 W at 1.8K (at maximum liquefaction of about 5 g/s), 400W at 4.5K and 2000W at 70K is in normal operation. In the future, the plant will be expanded to 200 W at 1.8 K with 10 g/s liquefaction [30]. Two vertical test cryostats (one in use) and a horizontal test cryostat with RF system are installed. A rotating temperature and radiation mapping diagnostic system is also used to analyse the cavity performance. Control system is under development.

ACKNOWLEDGEMENTS

The author sincerely thanks many colleagues for the fruitful discussions and valuable information from CEBAF, CERN, Cornell, Darmstadt, DESY, INFN, KEK, Orsay and Saclay in the TESLA collaboration. This assistance enabled the author to contribute this paper to CEC/ICMC-95, Columbus Ohio, USA.

REFERENCES

1. H. T. Edwards, TESLA Parameters Update - TESLA 94-22, DESY, August, 1994.
2. R, Sundelin and M. Tigner, TESLA Parameters & Comparisions, Proc. 5th workshop on RFS, ED. by D. Proch, 1991, Hamburg, Germany
3 D. Edwards (editor), TESLA TEST Facility Linac - Design report, TESLA 95-01, DESY, March 1995.
4. D. Proch (editor), 5th workshop on RFS, ED. by D. Proch, 1991, Hamburg, Germany
5. M. Leenen, 4th European particle accelerator conf. 1994. to be published.
   H. Weise, 4th European particle accelerator conf. 1994. to be published.
6. R. Brinkmann, Proc. Particle Accelerator Conf. Dallas, USA, 1995, to be published.
7. D. Proch, DESY, private communication, 1995.
8. G. Horlitz, CEC/ICMC-95
9. W. Weingarten, CERN, private communication, 1995.
10. K. W. Shepard, et al, Proc. 6 th workshop on RFS, ed. by R. Sundelin, CEBAF, USA, 1994.
11. C. Reece, Proc. PAC-95 conf. Dallas, TX. USA, to be published.
12 G. Cavallari, et al, ibid ref. 10, 1994
13. H. Padamsee, et al, ibid ref. 10, 1994
14. H. D. Graef, et al, ibid ref. 10, 1994
15. B. Dwersteg, et al, 4th European particle accelerator conf. 1994. to be published.
16. K. Akai, ibid ref. 4, 1992
17 B. Bonin, et al, ibid ref. 5, 1994
18. H. Padamsee, Applied superconducting conf. Boston, 1994
19. Q. S. Shu, et al, IEEE transaction, Vol. 27, No. 2, 1991.
20. B. Bonin, et al, ibid ref. 10, 1994
21. G. Mueller , R. Roeth, ibid. ref. 4, 1992 and ref. 10, 1994.
22. Q. S. Shu, et al, IEEE transaction on magnetics, Vol. 25, No 2, 1989
23. Q. S. Shu, et al, Proc. PAC-95 conf. Dallas, TX. USA, to be published.and TU-A3 this conf.
24. H. Padamsee, et al, IEEE Tran. Mag. -21, 1007, 1985
    P. Kneisel, J. Less Common Metal, 139, 94, 1973.
    D. Trines, A. Matheisen, et al, TESLA - TTF Meetings, 1994 and 1995.
25. S. Wolff, Proc. PAC-95 conf. Dallas, TX. USA, to be published.
26. J. Graber, Ph. D. Dissertation, Cornell Univ. 1993.
27. W-D. Moeller, et al, TESLA internal meeting and TTF meeting, 1995.
28. T. Nicol, this conf. 1995.
29. F. Alessandria, this conf., 1995.
30. B. Petersen, et al, this conf. 1995.
31. M. Bolore, et al, TESLA Report, 94-23, 1994.
    H. Haiser, et al, TESLA internal meeting, 1995.
32 A. Koski, B. Bandelman, S. Wolff, MT-14, Finland, 1995.
33. K. Koepke, this conf., 1995.
34. M. Kuchnir, et al, this conf., 1995.
35. B. Dwersteg, TESLA internal meeting, 1994 and 1995.
    J. Sekutowicz, TESLA internal meeting, 1994 and 1995.
36. S. Buller, et al, this conf., 1995.

TESLA TEST FACILITY ALTERNATE CRYOSTAT DESIGN

T.H. Nicol

Fermi National Accelerator Laboratory
Batavia, IL, 60510, USA

ABSTRACT

Collaborators on the design of a Tevatron Superconducting Linear Accelerator (TESLA) are working toward construction of a test cell consisting of four full length cryostats, 12 meters long, each consisting of eight, 9-cell superconducting RF cavities. The purpose of this facility is to test all aspects of the accelerator system design; vacuum, cryogenics, RF, and electron source, prior to initiating construction of the full linac. The design for these cryostats pose many interesting challenges to cryostat designers. The systems must be capable of supporting all eight cavity structures within tight alignment tolerances, impose very low thermal heat loads on the 1.8K cryogenic system, provide strength and stiffness to resist structural loads during fabrication, shipping, and installation, and be manufactured at low cost. Several design options are being explored, each of which attempt to address requirements imposed by the reference design guidelines. This paper describes the design and analysis of one design alternative.

INTRODUCTION

During the course of early work by the TESLA collaboration, two working groups formed charged with the design of cryostats for use in the TESLA Test Facility (TTF). One group worked toward final development of ideas originating at DESY prior to the formation of the full collaboration. A second group worked on ideas based on the collective experiences gained during development of various cryostats at Fermilab, CEN-Saclay, DESY, INFN-Frascati, and E. Zanon SPA. The latter is an Italian industrial company which fabricated cryostats for HERA at DESY. This paper describes the baseline

Table 1. TTF Cryostat Miscellaneous Design Parameters	
Heat load to 1.8K	3 W
Heat load to 4.5K	14 W
Heat load to 70K	80 W
Vertical dynamic load	1 g
Lateral dynamic load	1 g
Axial dynamic load	1.8 g
Primary structural resonance	25 Hz
Cavity alignment tolerance	±0.5 mm

design, now fully developed and being fabricated for use in TTF as well as alternatives to various elements of that design in various stages of completion which are available for use if full testing of the baseline indicates any need for further development. Some of the more critical design specifications applicable to any cryostat design effort are outlined in Table 1.

OVERVIEW OF THE BASELINE DESIGN

The baseline design is described in the literature, but is briefly outlined here for reference.[1,2] Figure 1 illustrates a typical cross section through the

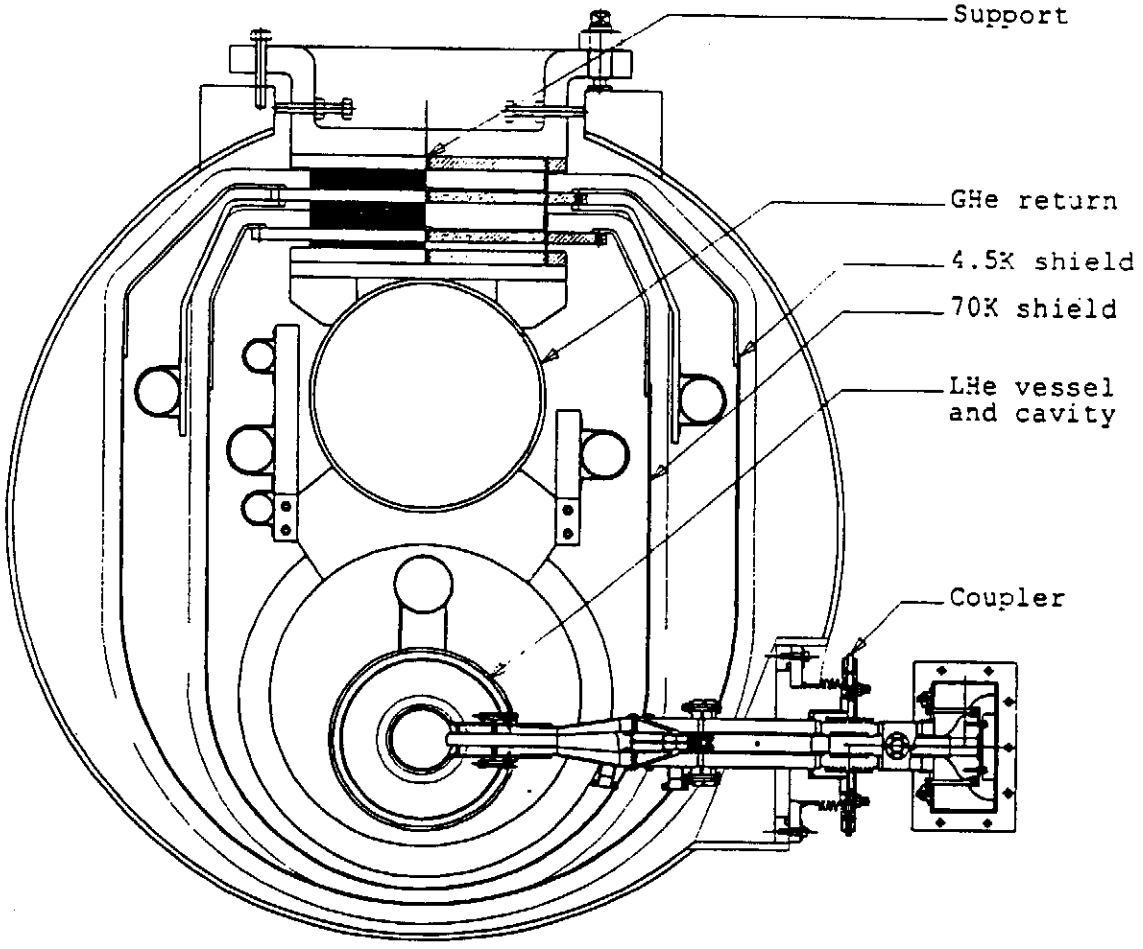

Figure 1. Baseline cryostat cross section

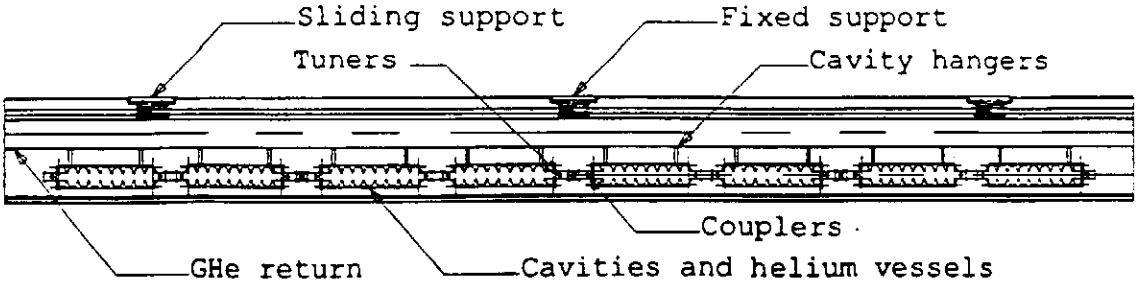

Figure 2. Baseline cryostat design longitudinal view

baseline cryostat. Figure 2 illustrates a longitudinal view of the same design. These figures are similar to, but not necessarily identical to the final design and do not include a depiction of the quadrupole due to lack of detail by this author.

Each cryostat contains eight superconducting RF cavities, their respective helium containment vessels, RF tuning systems, and input couplers, a gas helium (GHe) return header, two thermal radiation shields, cryogenic service pipes and connections, a structural support system, a single superconducting quadrupole, and vacuum vessel. The GHe return tube is attached to the vacuum vessel by means of three support posts similar to those developed for use in the Superconducting Super Collider (SSC) dipole magnets. The posts also serve to support the 4.5K and 70K thermal radiation shields, multilayer insulation, and cryogenic pipes. The cavities, helium vessels, and quadrupole are all hung from the GHe return tube. Input couplers which serve as coaxial connections between the RF system and the cavities are attached to one end of each cavity at each of the eight internal cavity interconnections. By virtue of there being three external supports and the use of the GHe return as a structural girder, the design of the input couplers must accommodate up to 15 mm of axial contraction during cooldown of the cryostat assembly.

GOALS OF THE ALTERNATE DESIGN

Alternatives to the baseline design have been encouraged throughout the collaborative effort as a means of ensuring that options exist should they become necessary at some point in the project. The following represent the main goals of the alternate cryostat design effort as well as a brief rationale for each. The content of the goals do not represent areas of concern with the baseline design, but rather are areas in which different design philosophies can be exercised without making significant perturbations to the general cryostat cross section.

- The design should accommodate a rigid or nearly rigid input coupler. This requires a minimum of four and possibly five supports and most likely implies "back-to-back" mounting of the input couplers, that is, two couplers at every other internal interconnect as opposed to one coupler at each internal interconnect as in the baseline design. The hope is that by minimizing the axial contraction during cooldown at the input coupler locations one can simplify the design of the coupler itself. These devices are very sophisticated and are prone to sparking and multipacting, some of

which may be due to bellows required to accommodate axial movement. No design may be truly rigid due to radial shrinkage and required allowances for assembly tolerances, however, flexibility requirements for these allowances are small.

- The design should attempt to structurally decouple the GHe return tube and the cavity vessels. Some concern exists that thermal distortions during cooldown will affect assembly alignment of the cavities.[3] It seems plausible to connect the cavity and helium vessel assembly directly to the supports as a means of minimizing changes in cavity alignment during cooldown.

- An attempt should be made to minimize the liquid helium inventory. Early helium vessel designs were substantially larger in design than the cavity to allow for two-phase flow over the top of the cavity. This resulted in a helium inventory significantly higher than that necessary to maintain the cavity temperature at 1.8K. Very early in the process of developing alternate designs, the helium vessel diameter was reduced significantly and a small connecting tube added above the vessel to allow for the same two-phase flow.[4] Since that time a very similar configuration was adopted for the baseline design. The revised vessel is shown in Figure 1. The large annular space around the helium vessel was necessary for the earlier design and has been retained in the TTF modules to minimize required design changes in other system components.

- The overall cryostat (vacuum vessel) diameter should be reduced as much as possible out of consideration for reducing overall cost and facilitating tunnel accessibility.

- Every effort should be made to minimize cost. It is safe to say this has also been a goal of the baseline design. Cost minimization in the alternate design is simply a continuation of that same philosophy.

- The axial and lateral suspension stiffnesses should be made as high as possible, while maintaining heat loads to the thermal intercepts at or below design limits. Although difficult to quantify specific goals, recent design studies and field tests on SSC dipoles at Fermilab indicate that high suspension system stiffness simplifies alignment and minimizes perturbations to system components during shipping and handling. Flexure of the GHe return defines the lowest frequency dynamic modes of the internal cryostat structure.[5] If the number of supports are increased and the GHe return is structurally decoupled from the cavity helium vessels it is possible to drive up the lowest modal frequencies.

CONSTRAINTS ON ALTERNATE DESIGNS

The goals in any design project must be consistent with a set of design constraints. The alternate cryostat design is no different. The constraints listed below represent a starting point for any responsible cryostat design effort which is aimed at providing alternatives to the TTF baseline.

- Any new design must be compatible with cavities being procured by DESY and INFN.

- The helium vessel should be modeled after that currently being designed at DESY, i.e. it should be of the same material, be nearly the same diameter, and interface to the cavity in the same way.

- The helium vessel and cryostat layout should be compatible with the cold tuning system being developed at CEN-Saclay.

- The piping system in any new design must be compatible with the TTF cryogenic system. It is too severe to dictate that any new design have exactly the same interconnect. However, it should have the ability to connect to a baseline cryostat with an adapter assembly.

- The design must include consideration of the quadrupole being designed at DESY.

- Cryomodule-specific design requirements must be met. For example, shipping and handling requirements must be met, heat loads should be consistent with those outlined in the design criteria, pipe sizes should be consistent with required flow rates, etc.

OVERVIEW OF THE ALTERNATE DESIGN

Figures 3 and 4 illustrate a cross section and longitudinal view of the alternate cryostat design for TTF. Clearly they are similar to their baseline counterparts in Figures 1 and 2, but there are some important differences. A detailed comparison of the baseline and any alternate cryostat design is not possible due to the fact that few detailed alternate designs exist. However, it is possible to describe design differences in general terms. The primary departures in design originate in the orientation and location of suspension system components. This departure is key because it gives rise to the ability to control cooldown contractions, the ability to decouple the GHe return from the balance of the internal components, and the ability to control the dynamic response.

As described above and shown in Figures 1 and 2, the baseline uses three supports located on the top of the vacuum vessel and connected to the GHe return at three points. The center attachment serves as the axial anchor point. The outboard two attachments are fixed vertically and laterally, but are free to slide axially to accommodate cooldown contraction. The cavity helium vessels are suspended from the GHe return by hangers.

In contrast, the alternate design uses five supports fixed rigidly to the bottom of the vacuum vessel. As shown in Figure 4, this allows rigid connections at one end of each cavity helium vessel which, in turn, enables one to contemplate couplers which need be flexible at levels significantly less than the 15 mm required by the baseline design. The GHe return is attached to a mounting bracket attached to the top of each support and allowed to "float",

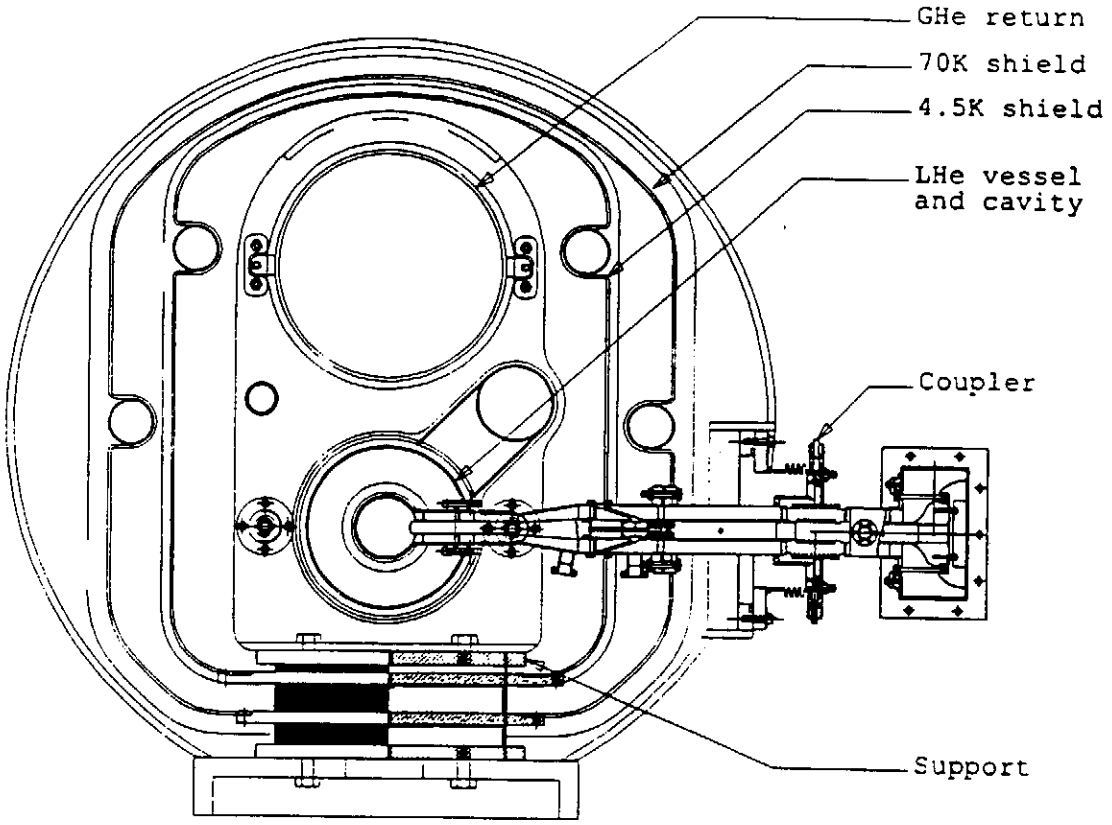

Figure 3. Alternate cryostat design end view

decoupled structurally from the cavity helium vessels. As a direct result of the bottom mounted supports, the effective stiffness of the suspension is increased from the point of view of the cavity vessels due to the reduced lever arm between the base of the support and the centerline of the cavity. The individual supports for each design are identical with the exception of the composite tube thickness. The thickness is scaled by the number of supports so that the conduction heat loads for each case are identical.[6]

There are of course potential problems with the alternate design. Support for the free ends of the cavity helium vessels and allowance for cooldown contraction are not as straightforward as in the baseline due to the alternate design not relying on the GHe return for structural support. The ends of the cavity helium vessels between supports must be connected to each other by a bridge to effect a rigid interconnection. In addition, the increased number of supports implies more penetrations through the thermal radiation shields, more supports, and more penetrations in the vacuum vessel. The advantages

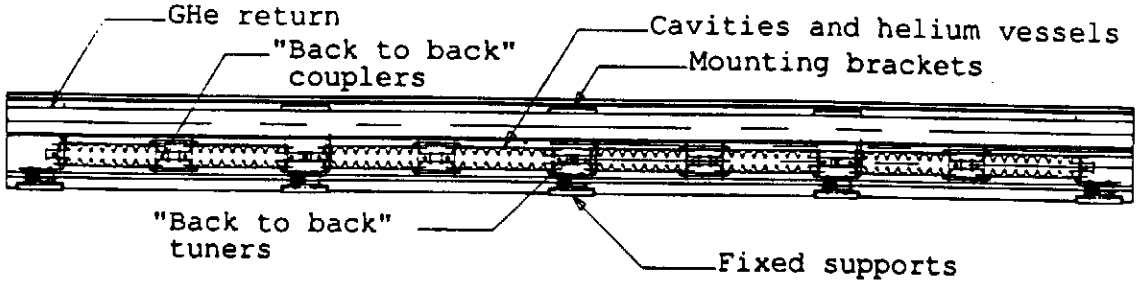

Figure 4. Alternate cryostat design longitudinal view

in terms of simplified input couplers and greater suspension system stiffness may prove worth the added complications. A responsible determination can only be made after a detailed design, analysis, and cost estimate is done.

SUMMARY

Fabrication of baseline design cryostats for TTF is well under way. The first completed cryomodule is scheduled to be shipped to DESY from Zanon in Schio, Italy in the fall of 1995. Every expectation exists that the baseline design will perform its intended function well and will meet the design specifications. As with any design and production process, the possibility exists that changes will be indicated for either the balance of the TTF cryomodules or for production modules for the remainder of the linac. In the event that either of those things happen, it is hoped that the body of work done on alternate designs can serve as a basis for implementing any required changes or incorporating added functionality.

ACKNOWLEDGMENTS

The author would like to thank the TESLA Collaboration for the opportunity to work on this project and especially fellow collaborators at Fermilab, DESY, INFN, CEN-Saclay, and Zanon for their constructive criticism, guidance, invaluable feedback, and sharing of experiences throughout the course of this design effort.

REFERENCES

1. D.A. Edwards, editor, "TESLA Test Facility Linac - Design Report," TESLA Collaboration Report 95-01, March 1995.
2. F. Alessandria, et al, "Design, Manufacture, and Test of the TESLA TTF Cavity Cryostat," presented at CEC/ICMC 1995.
3. T.H. Nicol, "TESLA Test Facility Cryostat Gas Helium Return Tube Thermal Gradient Analysis," TESLA Collaboration Report 94-12, May 1994.
4. H. Kaiser, Ge. Meyer, H.B. Peters, and G. Weichert, "Helium Vessel for the TTF Cavity," TESLA Collaboration Report 94-26, October 1994.
5. T.H. Nicol, "TTF Cryostat Modal Analysis," TESLA Collaboration Report 94-30, December 1994.
6. T.H. Nicol, "TESLA Test Cell Cryostat Support Post Thermal and Structural Analysis," TESLA Collaboration Report 94-01, January 1994.

DESIGN MANUFACTURE AND TEST OF THE TESLA-TTF CAVITY CRYOSTAT

F. Alessandria[1], G. Cavallari[2], M.Minestrini[3], T.H.Nicol[4], C. Pagani[1], R.Palmieri[5], S. Tazzari[6], G. Varisco[1]

[1]INFN sez. Milano, Milano,Italy
[2] INFN sez. Roma2, on leave of absence from CERN, Geneva
[3] INFN Laboratori Nazionali Frascati, Italy
[4] Fermi National Accelerator Laboratory, Batavia, IL. USA
[5] ENEA Centro di Frascati, Italy
[6] University of Roma Tor Vergata and INFN sez. Roma2, Roma Italy

ABSTRACT

The aim of the TESLA Test Facility (TTF) is to build and to operate a superconducting (SC) linear accelerator accelerating electrons to an energy of approximately 450MeV, to establish the technological basis for a SC accelerating structure of competitive cost, that could reliably achieve accelerating field of about 15MV/m. Eight individual nine-cell, 1300Mhz superconducting cavities, their RF equipment, a superferric quadrupole doublet and dipole steering coils and all diagnostic elements are combined in a 12m long accelerator module, housed in a single cryostat. The TTF linac consists of four such modules. Cavities are cooled by superfluid two-phase Helium at 1.8K and the quadrupole windings at 4.5K.

The liquid Helium distribution and cold gas recovery system are incorporated into the cryostat providing additional savings by the reduction of the number of transfer lines and other hardware on the outside of the cryostat enclosure.

The TESLA project

Factors determining the high cost of present SC cavity installations are their comparatively low accelerating field and that a single or few cavities have been housed in a separate cryostat with its own refrigeration circuit, thus requiring a relatively large number of cold to warm transitions and expensive distribution cold boxes; static losses, proportional to the number of transitions are a further cost factor. The TESLA accelerating structure and cryostat design philosophy has thus been to make individual accelerating modules as long as possible and combine then in strings fed by a single cold box, a technique similar to that used for SC magnets in large proton accelerators.

In the TESLA proposal eight individual nine-cell, 1300Mhz SC cavities, their RF equipment, a superferric quadrupole doublet and dipole steering coils and all diagnostic elements are combined in a 12m long accelerator module, housed in a single cryostat. Twelve cryomodules are combined into a 145 m subsection, individually fed by two phase

He; finally a separate cryoplant supplies a string of 12 subsections. A cryogenic unit would have a length of 1880 meters in TESLA.

The TTF accelerating structure will consists of four such modules.

Cryostat design

The scheme for cooling the TESLA prototype modules in the TTF test linac corresponds to the cooling process which is envisioned for a future TESLA linear accelerator. The cavities are in a 1.8K helium bath. Through the string of 4 modules between the feed box and the end box, an approximately uniform helium level is maintained. The regulation of the JT valve in the entrance of the modules is via the measurement of the liquid level in the end box. The He vapor at 1.8K returns back to the feed box via a 300mm diameter return line (HeGRP), which at the same time serves as the mechanical support of the cold mass. The design of this return line and the other process line is based on the dimensions of TESLA.

The cavity production technique has been carefully designed and specified to produce absolutely clean surfaces and to keep them such throughout the whole manufacturing and assembly process. This poses significant constraints on the design and assembly together in a clean room as they have to be inserted in the cryostat as a single UHV tight unit.

The design solutions have been chosen for simplicity and ease of fabrication; thus putting some constraints onto other RF components. To minimize the costs, machining on large items such as vacuum vessel and He gas return pipe has been limited to a few vacuum flanges requiring precise positioning. The long string of accelerator modules with a common insulation vacuum minimizes the number of warm to cold transitions. All refrigeration piping run inside the cryostat thus avoiding costly external transfer lines.

The cryostat vacuum vessel, Fig. 5, of carbon steel is evacuated to a pressure of 10^{-6} mbar. The design critical over pressure is 1.25 bar. It is the main mechanical structure and a number of constraints have been put on the shape: position of the power coupler flanges $\pm$1mm, cylindricity tolerance $\leq$3mm. The actual shape of the prototype vessel is shown in Fig. 1.

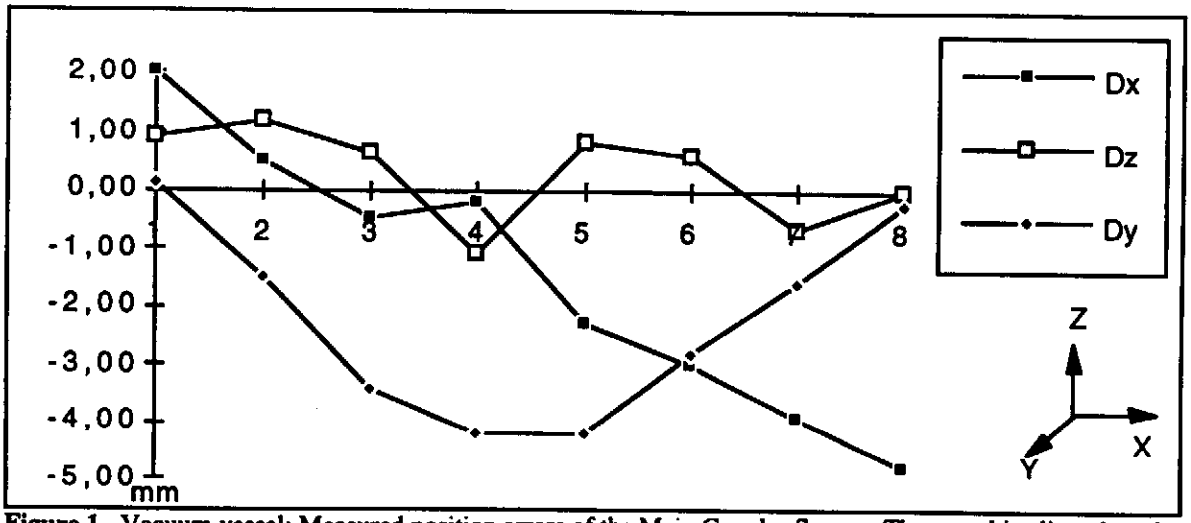

Figure 1. Vacuum vessel: Measured position errors of the Main Coupler flanges The vessel is aligned on the x axis, on the abscissa the cavity number

The 300 mm Helium gas return pipe, required to recover the 16mbar cold gas evaporated from the 1.8K He bath, is also used as the main support beam for the accelerator module. The overall weight of items hanging from the pipe is about 2300Kg. The HeGRP operating pressure is specified to be 2 Bar, the test pressure 3 Bar .

The HeGRP is supported from above by three support posts that provide the necessary thermal insulation; posts are fastened to large flanges on the upper part of the vacuum

vessel, by means of adjustable suspension brackets. The scope of the adjusting mechanism is to allow for the accelerator module axis to be brought into its proper position, independent of the absolute position of the vacuum vessel flanges on which it rests.

In the longitudinal direction the center post is fixed to the vacuum vessel while the two end brackets are allowed to move to accommodate differential shrinkage during temperature cycling. The posts consist of fiberglass pipe terminated by two shrink fit stainless steel flanges. At intermediate positions, optimized to minimize heat leak, two additional shrink fit flanges are provided to allow intermediate heat shield connections to 4.2K and 70K.
Seven additional cooling pipes run through the cryomodule (Fig. 5):

1.8K two phase line forward supply
2.2 K pressurized He forward, to supply downstream modules
4.5 K pressurized He forward, to cool the quadrupole lens
4.5 K Pressurized He return, to cool the 4.5K shield
70 K He forward, also used to cool the quadrupole beam tube
70 K He return, also used to cool the 70K radiation shield
a warm-up/cool-down line

All pipe connections in between modules are welded; bellows are provided to mechanical decouple modules and to allow for thermal contraction.

Alignment

Another very significant requirement, deriving from beam dynamics considerations, is the overall alignment requirements. The axes of the 8 cavities must stay aligned to the ideal beam axis to within $\pm$ 0.5 mm and those of quadrupoles to within + 0.1 mm over the entire length of the accelerator; in addition the vertical mid plane of the lens must stay aligned to the vertical direction to $\leq \pm$ 0.1 mrad. Cavity positions will be monitored during cool down with optical marks and wire positions monitors (WPM) installed on each cavity of the first prototype. The cavities and the quadrupole are aligned at room temperature before insertion in the vacuum vessel. Reference Taylor-Obson spheres on the posts are then used to align the cold mass in the vacuum vessel.

Modal analysis

The accelerator repetition rate is 10Hz and the RF cycle lasts 1.4 msec. Lorenz forces at 10Hz, induced in the cavities by the RF radiation pressure, may excite mechanical resonance. The aim of the TTF cryostat modal analysis [1] is thus twofold. First to evaluate the static behavior, mainly deflection, due to the lumped masses of the cavities, the quadrupole and the weight of the GHe return tube itself. Fig 2 gives the results.

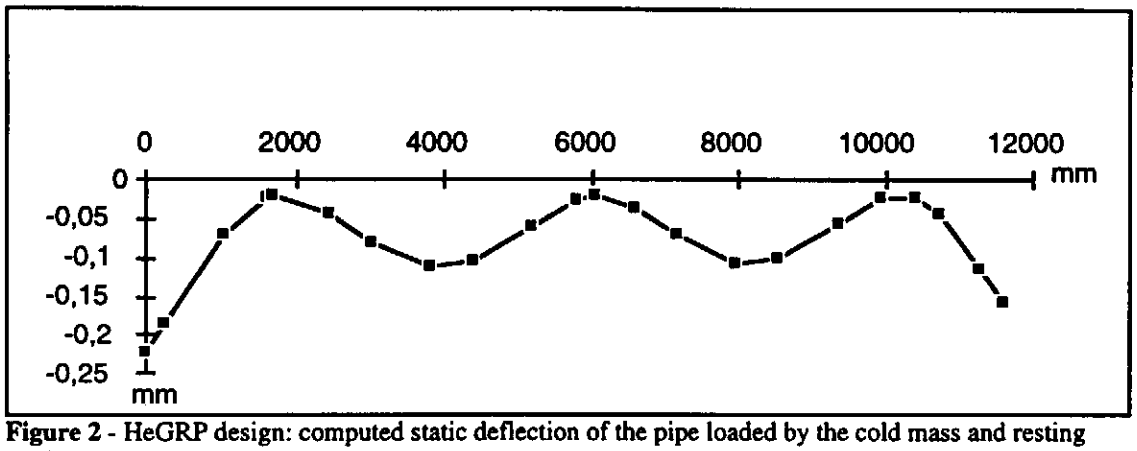

Figure 2 - HeGRP design: computed static deflection of the pipe loaded by the cold mass and resting on three posts

Secondly to extract all the translational modes. The accelerator repetition rate being 10Hz, all mode above 20 Hz are considered non dangerous. The analysis yielded 12 modes below 100Hz. The modes, frequencies and deflections planes are summarized in table 2. Nearly all the first 12 modes are associated with flexure of the GHe return pipe. The exception is mode 6 at 26.7Hz. This mode is almost exclusively associated with lateral deflections of the support posts. It is of course possible to determine deflections at resonance only with a specific input load spectrum.

Table 1 - HeGRP Modal Analysis

mode no.	freq. (Hz)	defl. plane
1	18,7	x-y
2	20,3	x-z
3	21,7	x-z
4	22,1	x-y
5	25,4	x-y
6	26,7	x-z
7	27,6	x-z
8	41,9	x-y
9	49,6	x-y
10	54,0	x-z
11	76,0	x-z
12	101,3	x-z

Heat treatment

Concern has been expressed about thermally induced distortions of the HeGRP. Specifically, the issue involves thermal gradients which can occur in this tube from flow stratification during cool down. These thermal gradients induce mechanical distortions and thermal stresses in the tube and impose structural loads on the support system[1]. In a stress free tube the bending stresses resulting from thermal bow are small compared to the yield strength. However, residual stresses from fabrication of the tube and welding of various cryostat components to the tube imply that some parts of the tube may in fact be on the verge of yield. Any additional stresses will result in permanent deformation of the tube. The finished HeGRP has been heat treated to 550 C to relieve stresses, Fig. 4. The thermal cycle was specified such as to avoid carbide precipitation.

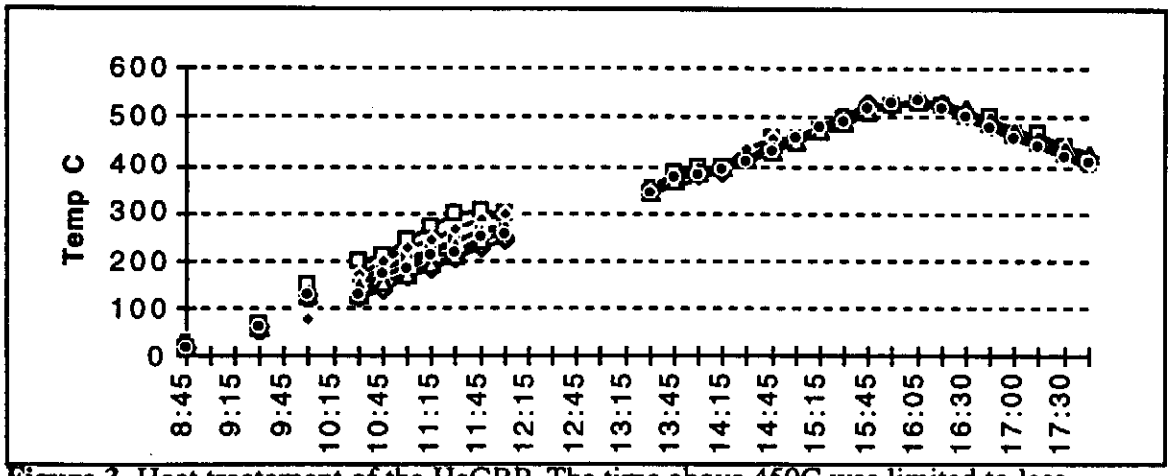

Figure 3. Heat treatement of the HeGRP. The time above 450C was limited to less than 3 hours.

After heat treatment, the shape of the HeGRP standing on two supports has been measured with optical means[3], cooled down with LN_2 and re-measured after warm up.

Within the measurement precision of 0.15mm no permanent deformations induced by the cool down cycle have been spotted but a deviation from straight line of ± 1.5mm. The HeGRP was closed with welded flanges, connected to inlet and outlet lines and inserted in a horizontal vacuum vessel. The inlet pipe went all along the HeGRP at the cylinder axis with nozzles every 200mm. Filling with LN_2 was stopped when liquid poured out of the exit line, i.e. when the HeGRP was half full. Temperature gauges were installed at the outer side of the pipe, three on the top and three on the bottom. While the bottom part was at the LN_2 temperature for more then 8 hours, the top part cooled down to only 160K, Fig. 4. It can be explained by a full stratification of the GN_2 inside the HeGRP due to the very slow gas speed.

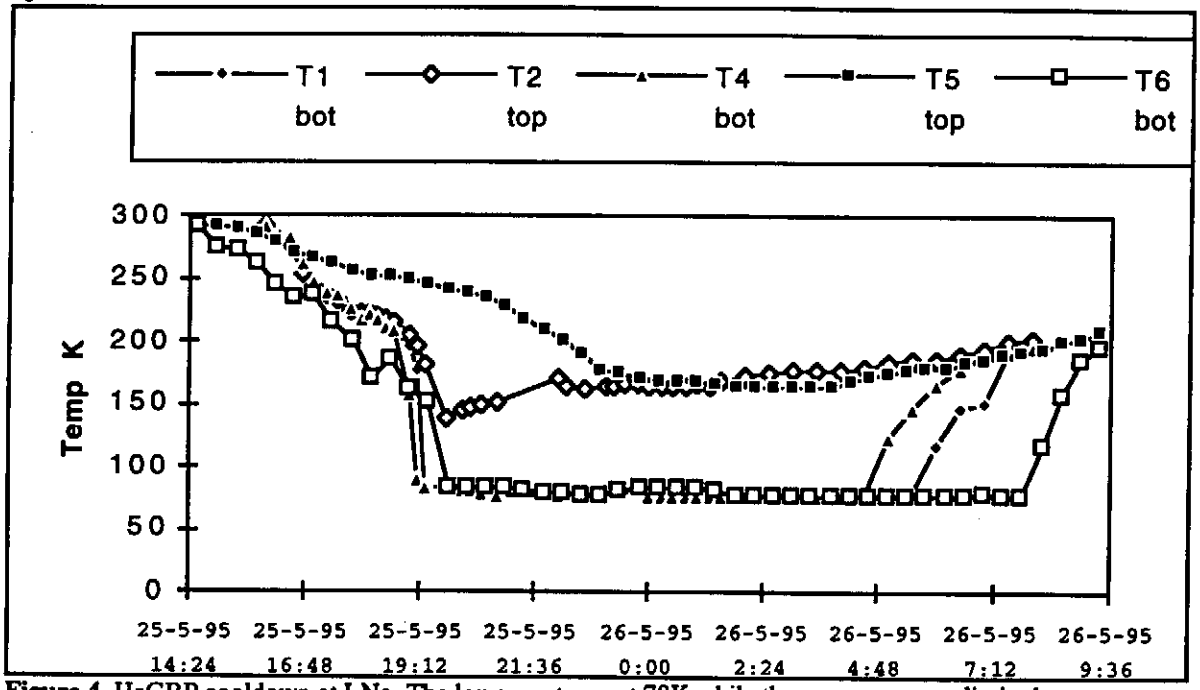

Figure 4. HeGRP cooldown at LN_2. The lower part was at 78K while the upper part was limited to 180K due to stratification of the GN_2

Radiation shields

Two aluminum radiation shields are provided at intermediate nominal temperatures of 4.2K and 70K. Each shield is made in two halves. The half-shield upper sections, 5mm thick, are supported by the post intermediate flanges: they are bolted onto the center post but can slide on the end posts, to avoid build up of excessive forces on the posts during thermal cycling, when temperature differences of 100 K can develop between different points of the shield sections. The shields are cooled by means of flexible copper braids at regular intervals to the centerline of the shield upper section; the braids are directly connected to the cooling pipes and their cross section is such as to keep the ΔT between shield connection and pipe to $\leq$ 10 K and $\leq$ 2K for the 70K and the 4.5 K levels respectively. The lower half-shields, 3mm thick, are bolted to the upper-half and are cooled by conduction.

The Al 6082 thermal conductivity been measured at 4.2K[3]. The 3mm and the 5mm thick Al sheets have 11 W/mK and 18W/mK respectively. Measurements on different samples cut across and along the rolling direction have given the same values: we conclude this difference to come from the bulk material itself. These values are above the figures assumed for the thermal budget design by at least a factor of 5.

Super insulation

All surfaces at 70K and 4K facing surfaces at ambient temperature or 70K respectively are covered with multi layer insulation (MLI). Ten and thirty layers of MLI are provided on

the 4 K and 70 K shields respectively. The estimated heat loads are $0.03W/m^2$ and $0.9W/m^2$. The He vessel, the HeGRP and the quadrupole 4K feed lines have a 5 layer blanket, to reduce heat transmission in case of vacuum failure.

The anticipated static and dynamic heat load budget for a single cryomodule is shown in table 2.

Table 2:	Estimated cryogenic losses (W)		
	2 K	4.5 K	70 K
Static losses	2,80	13,90	76,80
Total losses at 15MV/m	15,40	15,20	125,00
Total losses at 25MV/m	21,40	16,00	136,00

Diagnostics

PT1000 and Cernox-1030 temperature sensors will be installed at various places of the cold mass. The Cernox sensors are thin film resistors, are very stable over repeated thermal cycling and can withstand the high radiation doses expected around the SC cavities. The sensors are calibrated from room temperature to 1.7K with a number of calibration points according to the final operating temperature. In the first cryomodule we will install 92 Cernox and 43 PT1000 sensors to qualify the cryogenic design.

Magnetic shield

In order to reach their nominal performance level [5], the superconducting cavities of TESLA must be cooled in a magnetic field $\leq 2mT$, this corresponds to a field 20 to 40 times smaller than the ambient magnetic field. To achieve this shielding level it is intended to use a mixed scheme combining a Cryoperm tube around the cavity Helium vessel and a string of Helmoltz coils around the cryomodule vacuum vessel. The former, and the carbon steel vacuum vessel will mainly shield the transverse component of the ambient field, the latter will shield the longitudinal component. The longitudinal demagnetization factor of a long cylinder, as it is the case for a string of TESLA cryomodules, approaches unity.

Acknowledgments

The TTF community at DESY, Hamburg, have participated to the cryostat design with many fruitful discussions and advices. W. Weingarten and C. Dalmas of CERN have kindly performed the thermal conductivity measurements. One of us (G.C.) thanks INFN for the hospitality.

References

1.- T. Nicol: TTF Cryostat Modal Analysis; TESLA Rep. 94-30
2.- T. Nicol: TTF cryostat: HeGRP thermal analysis; TESLA Rep. 94-12
3.- F. Wei: Private communication; 1995
4.- W. Weingarten: private communication, 1995
5.- M. Bolore et al.: Magnetic Shielding of the TESLA TTF SC Cavities; TESLA Rep. 94-23
6.- D.A. Edwards ed.: TESLA Test Facility Linac - Design Report; TESLA Rep. 95-01

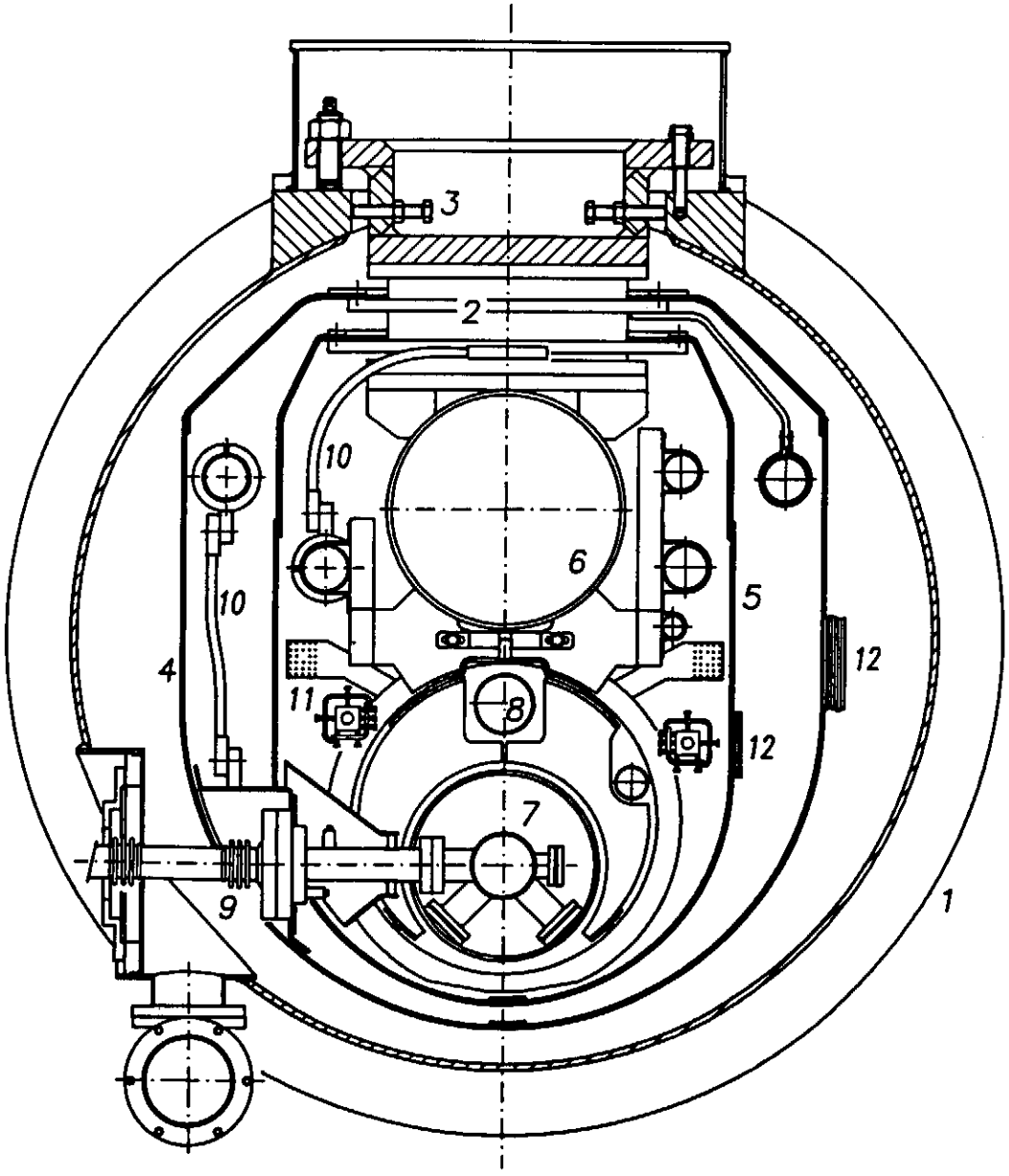

1	VACUUM VESSEL	7	CAVITY
2	COMPOSITE POST	8	1.8 K LHe SUPPLY
3	SUPPORT BRACKET	9	MAIN COUPLER
4	70 K SHIELD	10	Cu BRAIDS
5	4.5 K SHIELD	11	ALIGNEMENT TARGETS
6	1.8 K He GAS RETURN PIPE	12	ML INSULATION

Figure 5 – CRYOSTAT CROSS SECTION AT CAVITY

IV-A2-7

THE TESLA 500 CRYOGENIC SYSTEM LAYOUT

G. Horlitz,[1] T. Peterson[2], D. Trines[1]

[1]Deutsches Elektronen-Synchrotron DESY
Notkestraße 85, 22603 Hamburg, Germany
[2]Fermi National Accelerator Lab.
P.O. BOX 500, Batavia, IL 60510, USA

ABSTRACT

The superconducting 2 x 250 GeV e^+e^- linear accelerator TESLA is composed of a series of high frequency resonators (cavities), fabricated of high purity niobium. It has to be operated at a temperature of ca. 2 K. A nominal refrigeration power of about 51 KW at 2 K, 37 KW at 4.5 K and 314 KW at 40/80 K is required. The cooling power has to be distributed over a distance of more than 30 km. Different aspects of the cryogenic system are discussed.

INTRODUCTION

The TESLA project has been presented previously [1]. Two linacs of about 15 km length, producing 250 GeV electrons and positrons respectively, will be installed collinearely, separated by a ca. 2 km long interaction zone (fig. 1). The cryogenic system, maintaining the operating temperature of 2 K, will be described in the following chapters.

GENERAL LAYOUT

Cavities

Basic elements of the linac are cavities, consisting of nine cell high purity niobium RF-resonators, welded into cylindrical containers of titanium (fig. 2). Details of this design are presented in other sessions of this conference [2; 3]. The space between the cavity and the cylinder will be completely filled with superfluid liquid He at temperatures below 2 K, in order to maintain the desired operating temperature.

Modules

A module (12.2 m length) is an assembly of 8 cavities mounted into a common vacuum cylinder together with one quadrupole and one absorber for higher order mode (HOM) losses at an end. Two concentric heat shields, one at 4.5 K, and a second one at a

temperature between 40 K and 80 K, protect the cavities. All cold supply and return lines go through the modules as well [fig. 3]. The TESLA 500 cavities will be connected directly to the 0.3 m return tube The 100 mm two phase tube of the TTF cryostats is eliminated. The exact number of quadrupoles in the machine is not yet fixed. Probably only one quadrupole every second or every third module will be installed.

Strings
12 modules are arranged in a string. At the end of the string there will be a supply box, the other end is terminated by an end box (fig. 4, Detail A). The total length of a string including the boxes is 148 m.

Subunits
An assembly of 12 strings is a subunit (fig. 4). It will be supplied by one common refrigerator . The resulting length of 1830 m for each subunit is tolerable from the point of view of pressure drops within reasonable tube sizes.
The "geographical" length of subunits in fig. 5 differs somewhat from the "cryogenic" length in fig. 4 due to the location of the refrigerators.

The machine
Based on an accelerating gradient of 25 MV/m, for an end energy of 250 GeV an active length of 10000 m per linac is required, which means a mechanical length 14908 m (8 subunits, space factor 0.671). The total length of the system, including 2 km interaction region, amounts to ca. 32 km (Fig 5).

HEAT LOADS

An estimate of heat loads for modules and cavities has been given recently [4]. Static and total (dynamic) loads are summarized in Tab. 1. Higher order mode (HOM) losses are partially transferred to the cavity helium, a large fraction escapes out of the cavities and travels through the beam pipe from where it has to be removed by means of absorbers in the quadrupoles, cooled by the 40/80 K shield helium.

The values marked "n" in Tab. 1 represent the calculated actual estimates ("nominal"). The whole system was designed with safety factors of about 1.5 for all three temperature levels. The "design" values are marked "d".

Tab. 1
TESLA heat loads
(n = normally expected values; d = design values; stat = HF-power off; dyn = HF-power on)

Temperature	2 K		4.5 K		40/80 K		
	stat	dyn	stat	dyn	stat	dyn	W
Module n	2.8	21.4	13.9	16.0	76.8	136.0	W
d	4.2	32.1	20.9	24.0	115.2	204.0	W
String n	43.0	266.2	166.8	192.0	921.6	1632.0	W
d	64.5	399.3	250.2	288.0	1382.4	2448.0	W
Subunit n	521	3200	2007	2309	11070	19595	W
d	782	4800	3011	3500	16605	30000	W
TESLA n	8336	51200	32112	37000	177120	313500	W
d	12512	76800	48168	56000	265680	480000	W

The equivalent room temperature power inputs have been evaluated, taking into account conversion factors of 800; 250; 25 W/W for T = 2.0; 4.5; 60 K respectively. They are listed in Tab. 2.

Tab. 2

TESLA ambient temperature electrical power input in mega watt

Temperature		2 K		4.5 K		40/80 K		Σ input	
		stat	dyn	stat	dyn	stat	dyn	stat	dyn
Subunit	n	0.42	2.56	0.50	0.58	0.28	0.49	1.2	3.6
	d	0.63	3.84	0.75	0.88	0.42	0.75	1.8	5.5
TESLA	n	6.7	41.0	8.0	9.3	4.4	7.8	19.1	58.1
	d	10.0	61.4	12.0	14.0	6.6	12.0	28.6	87.4

THE CRYOGENIC SYSTEM

The generalized flow scheme is shown in fig. 4. A refrigerator (to be described elsewhere in this conference [5]) produces supercritical helium ($p \cong 5.4$ bar, $T \cong 4.5$ K) in point 1.
The whole mass flow enters first the 4.5 K quadrupole line at point 3, passes all quadrupoles in the subunit and returns from the end through the 4.5 K shields to point 5. A fraction is further cooled to 2.2 K in the heat exchanger HX6. It enters the 2.2 K supply line through point 2. The rest of the flow is expanded into the bath precooler HX5. ($T \cong 4.3$ K, $p \cong 1.1$ bar).

From point 6, a 40 K/18 bar flow is deviated for the 40/80 K shield cooling. After the passage through the shields and the HOM-absorbers in series it returns with $T \cong 80$ K, $p \cong 17$ bar at point 7.
At every string, about 1/12 of the 2.2 K supply flow is expanded through Joule Thomson valves into the supply boxes. From here, a two phase flow moves through the 0.3 m diameter return tube back to the end box of the string.
The heat from the cavities is transferred to the liquid in the return tube through vertical connection tubes between cavities and return tube (fig. 6) by means of the internal heat conduction process in He II [6]. In the tube, all heat flow is removed by evaporation of liquid at its surface.
For steady state operation the flow rates in the strings have to be controlled depending on the heat loads. At the end of each string, all liquid has been converted into vapor. The level is kept constant by means of a level controller LC acting on the JT-valve.
The end box of each string is mechanically combined with the supply box of the next one. A wall in the lower part seperates the two adjacend liquid levels, the vapor passes through (fig.4 Detail:A).
In point 8 the vapor returns to the heat exchanger HX 6 via a connection tube (0.3 m diameter, ca. 54 m length) and a buffer tank. The return gas temperature is about 1.9 K, its pressure ca. 30 mbar.
At point 9, the helium is warmed up to ca 3.4 K. Cold compressors (4 stages) are used to raise the pressure to the inlet pressure of the main compressor group (ca. 1.0 bar).
Driving forces for the liquid through the strings are the gradients of vapor pressure $\partial p/\partial x$ and liquid level $\partial h/\partial x$. Various flow conditions have been investigated under the

assumption of independent flow of liquid and vapor in the return tube [7]. Fig. 7 displays pressure, temperature and liquid level in the return tube under different loads.

Table 3 gives massflow rates (m), temperatures T and pressures p at different points in the system.

Table 3

Thermodynamic data at different points of the flow scheme

normal heat loads n				design heat loads d		
No.*	m [kg/s]	T [K]	p [bar]	m [kg/s]	T [K]	p [bar]
1	0.371	4.5	3.9	0.560	4.5	5.4
2	0.160	2.2	3.0	0.242	2.2	3.0
3	0.211	4.5	3.9	0.318	4.5	5.4
5	0.210	5.3	3.04	0.317	5.43	3.1
6	0.0945	40.0	18.0	0.142	40.0	18.0
7	0.0945	80.0	17.58	0.142	80.0	17.0
8	0.160	1.98	0.0297	0.242	1.958	0.0276
9	0.160	3.38	0.027	0.242	3.38	0.025
11	0.0133	2.00	0.0313	0.0202	2.00	0.0313

* position numbers of flow scheme Fig. 4

Cool down/warm up procedures

Cooling will be performed in several steps. Starting at room temperature, helium of about 80 K will be supplied through the 2.2 K line. At point 10 (fig. 4, Detail A) cool down lines parallel to the strings are branched. Every cavity is connected to these lines by means of narrow tubes, the flow resistances of which are large compared to all longitudinal resistances. This assures an approximately uniform flow distribution through the cavities, returning through the common 0.3 m return line. A parallel cooling of all cavities of one subunit is estimated to reach 80 K within some hours. Faster cooling, if desired, is possible, if the cooling capacity is concentrated to only one or two strings at the same time. In order to prevent cold exhausting gas penetrating to the next strings not yet to be cooled, the 2 K line must be closed at the end and the gas returns through valve VX and the 80 K return line. The cooling will be continued with running turbines and decreasing temperatures until the cavity temperatures are at about 4.5 K. At this level the filling of the cavities can be executed through the JT valves and the return line. Once having filled the whole system with 4.5 K liquid the cold compressors can start to establish final pressure and temperature.

Alternative circuit

An interesting alternative solution is presented in fig. 8. Here, the whole massflow for the string is injected through one single JT-valve at the end in point 12. Subdivision into strings is only necessary for cool down/warm up processes. The advantages of this system are: only one JT-valve with control loop hardware and software instead of 12, only 2 boxes at the ends of the subunit. The overall length of a subunit reduces to 1812 m. Flow conditions have been calculated for this system as well [6]. Pressures and temperatures are very similar to fig. 7, the much smoother level behavior is shown in fig. 9.

A disadvantage may be that a higher liquid level at the JT-valve end of the string is required for driving the total string liquid rate through the full length of the unit. This causes a higher amount of liquid being stored in the return line.

The estimated amounts of helium in a subunit are listed for both solutions in Tab. 4 under design conditions.

Tab. 4

Helium stored in different sections of a TESLA unit

Circuit section	A [kg]	B [kg]
Liquid in the return tube	262.2	1630.7
Vapor in the return tube	95.7	85.8
Cavaties and other tubes	6662	6624
Total He-mass per subunit	7025	8346

A = 12 JT-valve version
B = 1 JT-valve version

SUMMARY

A possible cooling scheme for TESLA has been worked out and is proposed here. Also many requirements are unique, the limits of the present state of the art are certainly reached, but not exceeded. For future optimisation of the system, experiences from CEBAF, LEP 2, LHC and especially from TTF will be of essential value. Furthermore, it has to be investigated, whether the simplicity of the alternative scheme has drawbacks for operation or cooldown.

REFERENCES

1. G. Horlitz, T. Peterson, D. Trines, A 2 Kelvin Helium II Distributed Cooling System for the 2 x 250 GeV e^+e^- Linear Collider TESLA, Proc. 15. Intern. Cryog. Eng. Conf. Genova, 1994, p. 131
2. Q. S. Shu, D. Trines, Technical Challenges of Superconductivity and Cryogenics in Persuing TESLA Test Facility (TTF), Proc. CEC/ICMC 1995, to be published
3. T. Nicol, TESLA Test Facility Cryostat Design, Proc. CEC/ICMC 1995, to be published
4. D. A. Edwards (Editor) TESLA Test Facility LINAC-Design Report, TESLA-Report No. 95-01, p. 228
5. M. Kauschke, C. Haberstroh, H. Quack, Safe and Efficient Operation of Multistage Cold Compressor Systems, Proc. CEC/ICMC 1995, to be published
6. T. Peterson, Notes about the Limits of Heat Transport from a TESLA Helium Vessel with a Nearly Closed Saturated Bath of Helium II, TESLA-Report No. 94-18
7. G. Horlitz, Computer Simulation of Pressures, Temperatures and Liquid Levels in a 1830 m TESLA Subunit under different Conditions and System Configurations, TESLA-Report No. 94-17, to be updated and published Sept. 1995

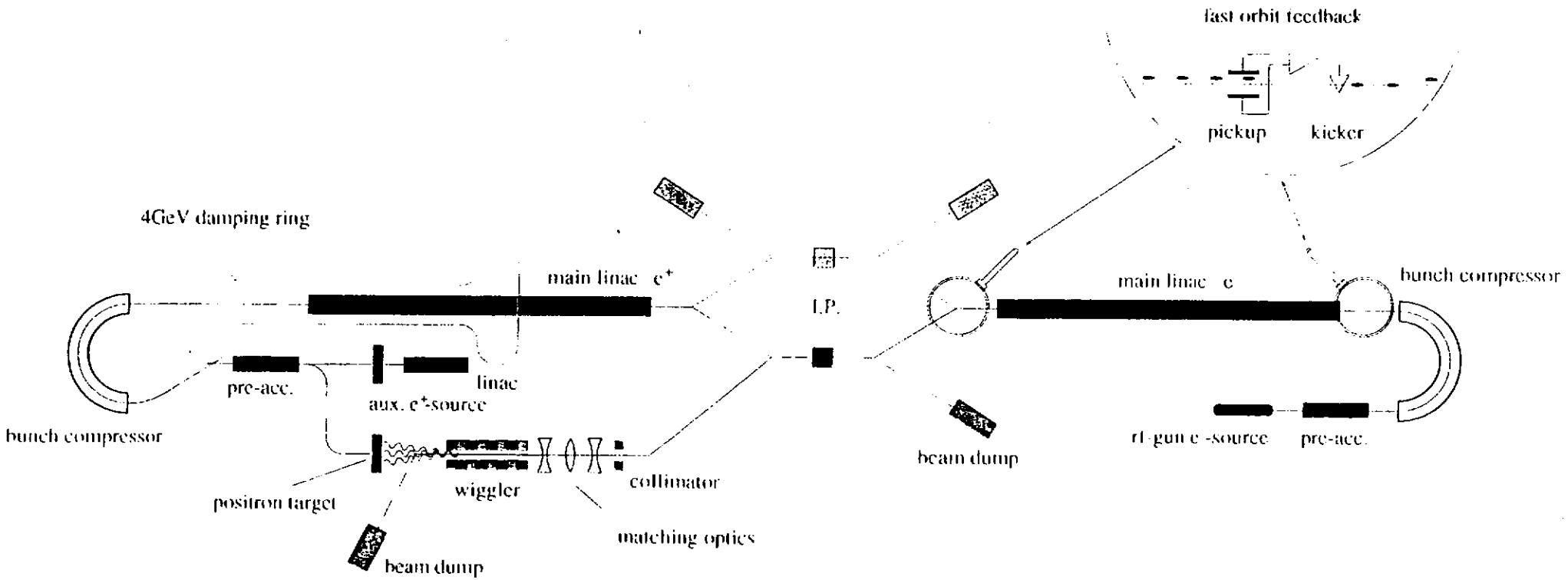

Fig. 1 TESLA General Layout

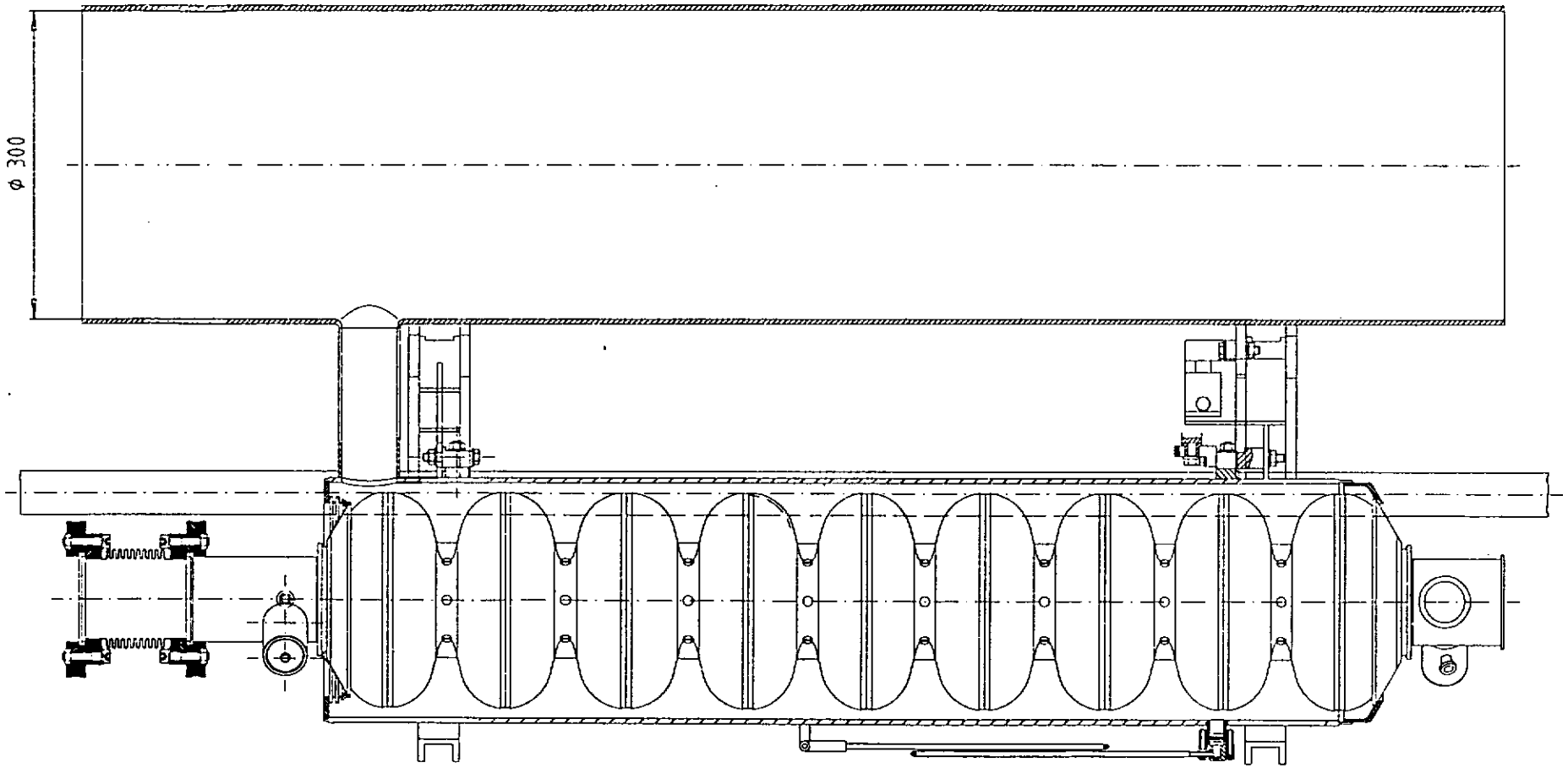

Fig. 2 TESLA Cavity and Vapor Return Tube

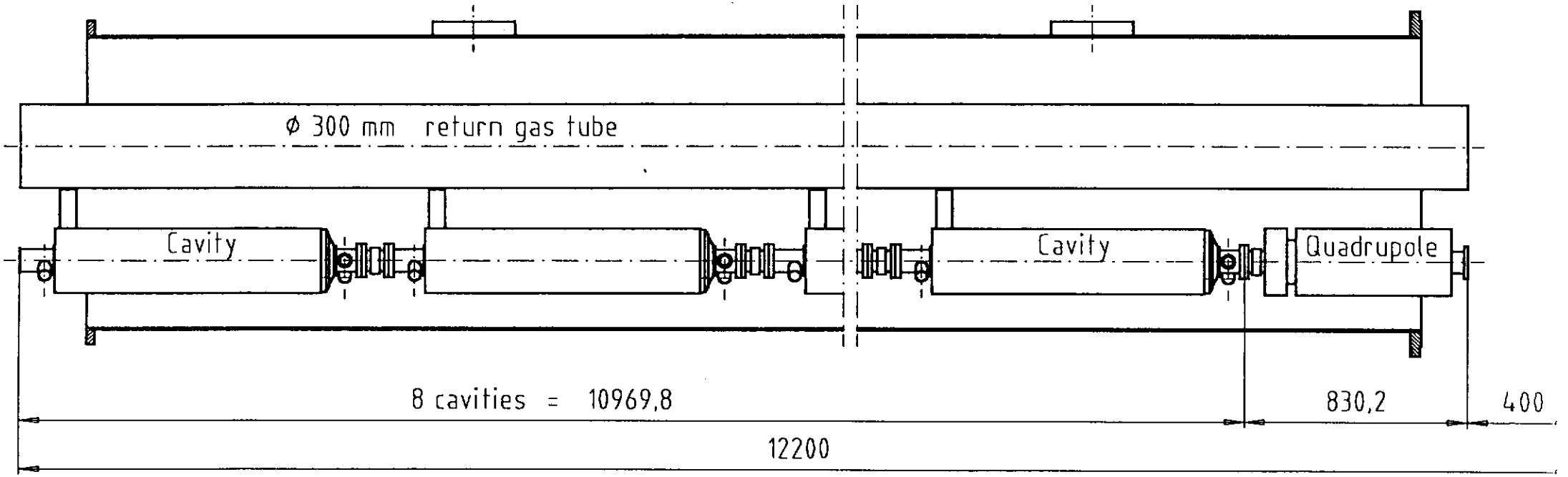

Fig. 3 TESLA Module

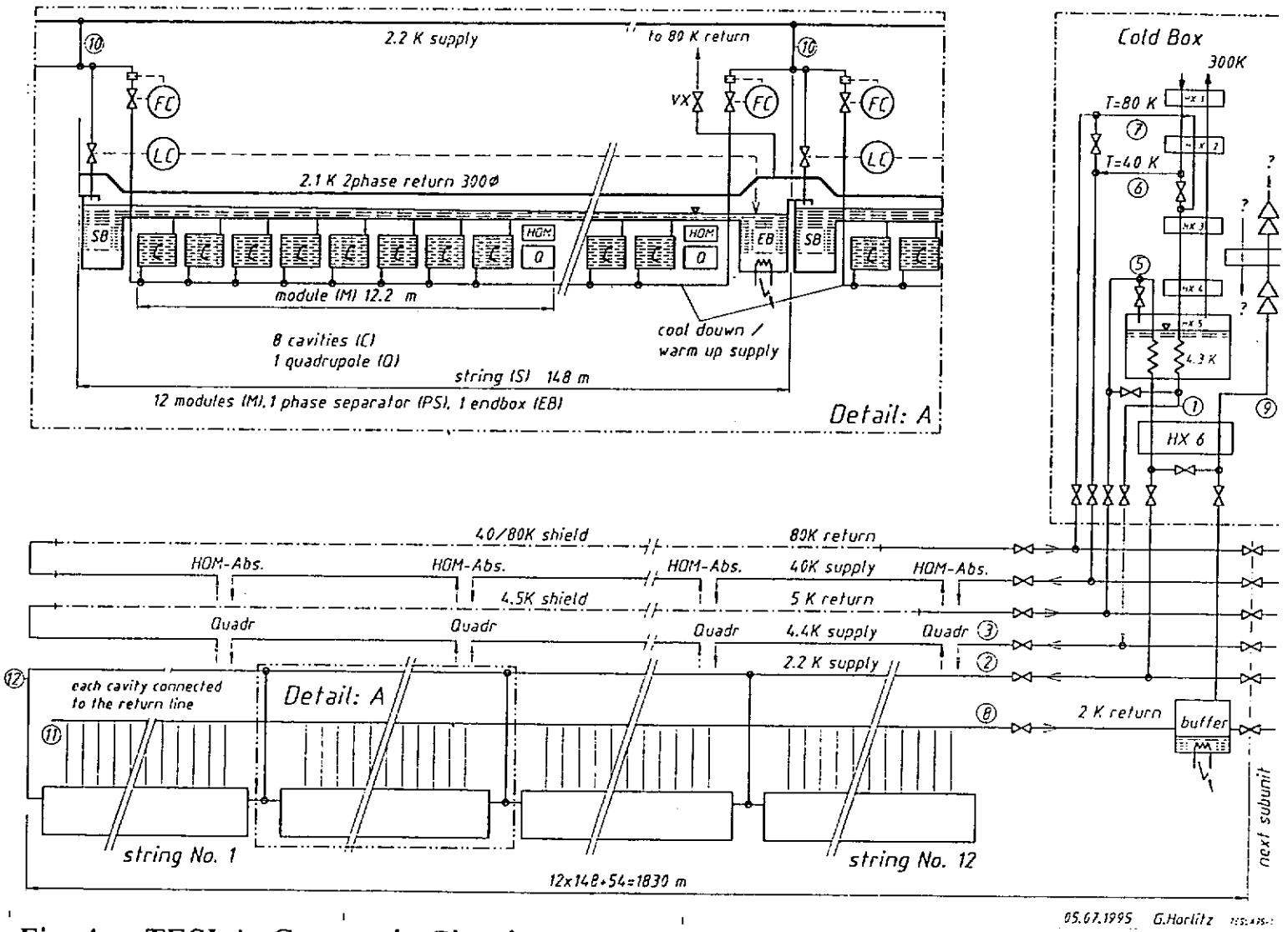

Fig. 4 TESLA Cryogenic Circuits
(version with one JT-valve for each string)

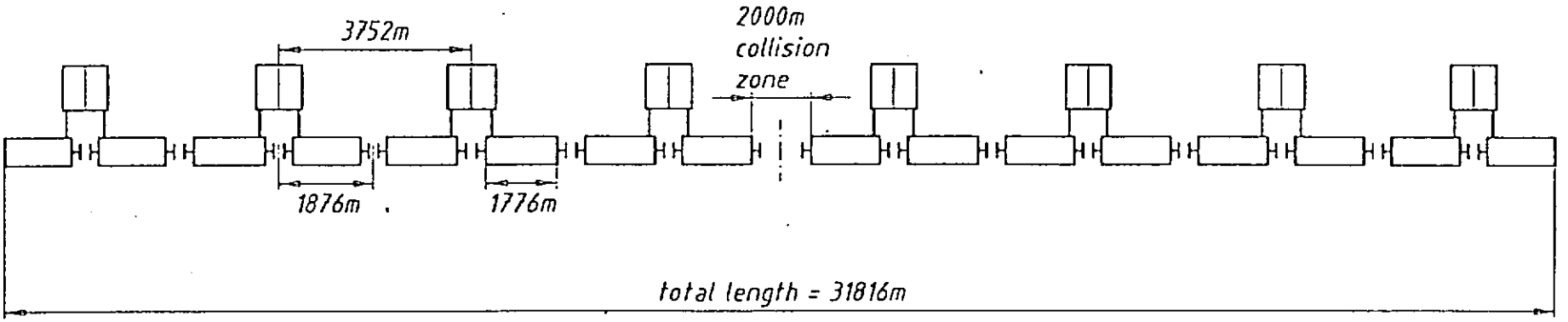

required: 8 Cooling stations a 2 refrigerators

capacity of one Refrigerator	total
$\dot{q}_{2.0}$=5000 W	80000 W
$\dot{q}_{4.5}$=4200 W	67200 W
$\dot{q}_{60}$=30000 W	480000 W

04.07.1995 G.Horlitz

Fig. 5 TESLA Cryogenic System
(General layout and subdivisions)

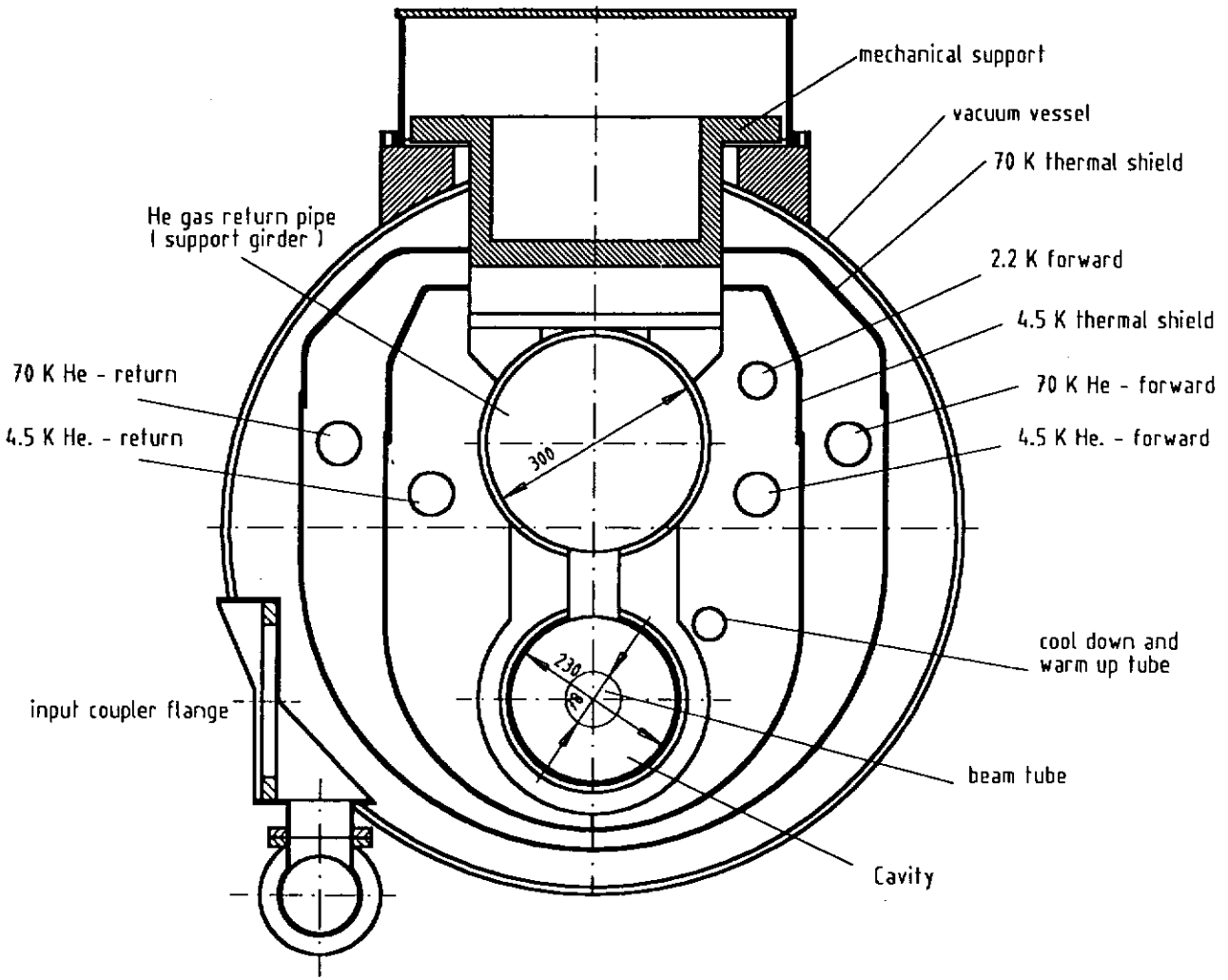

Fig. 6 TESLA Cryostat Cross Section

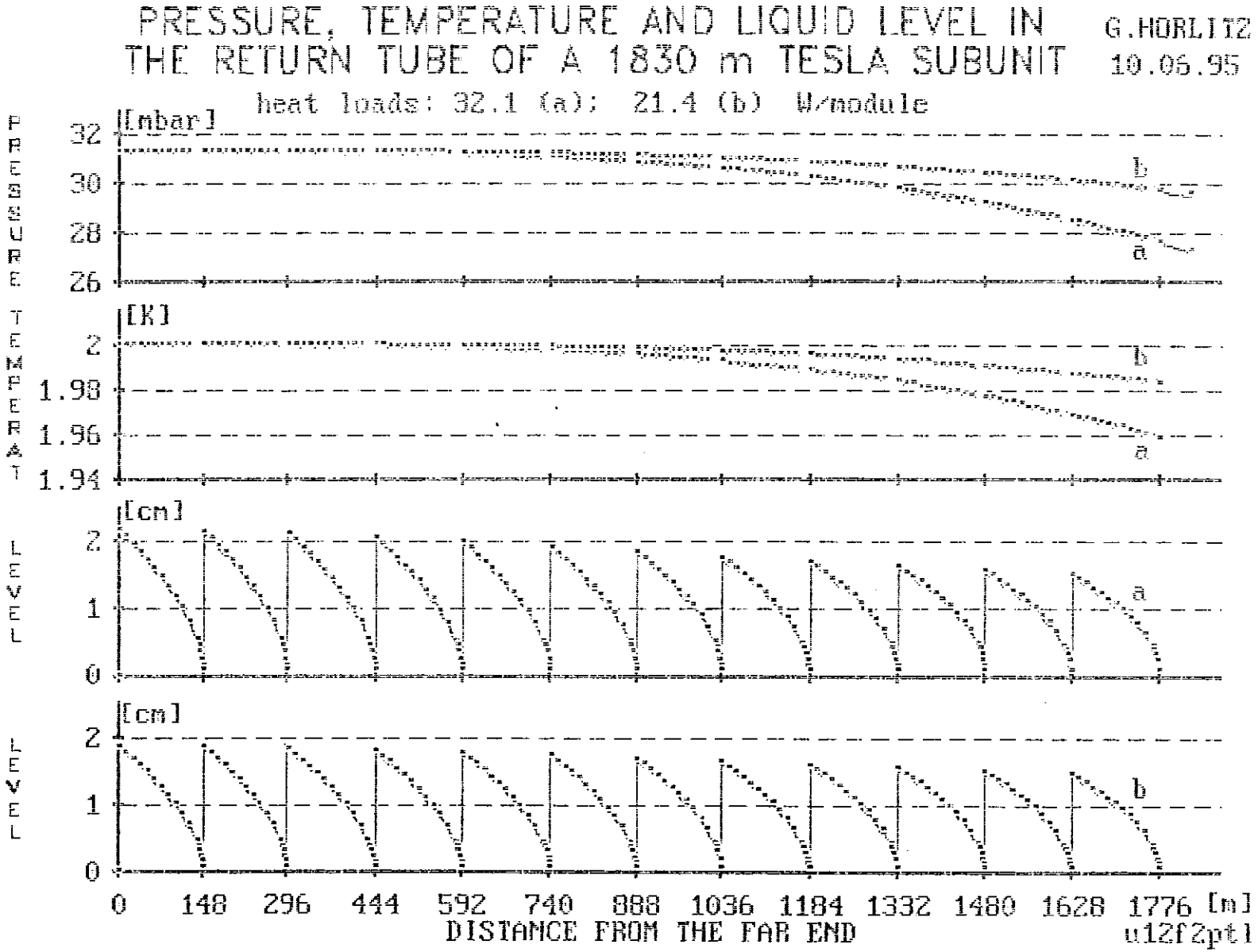

Fig. 7 Flow Parameters in the Return Tube
(1 JT-valve for each 148 m string)

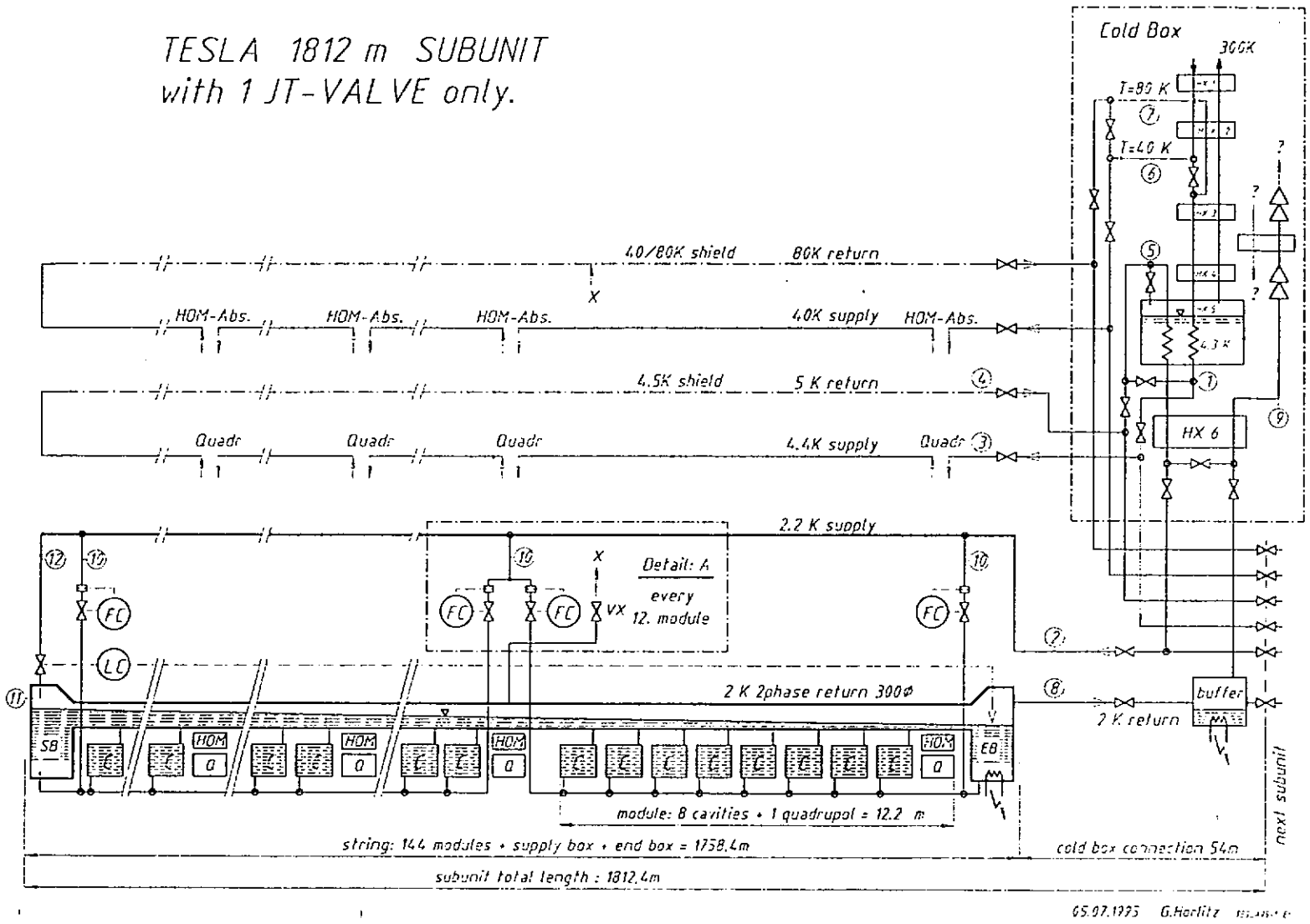

Fig. 8 TESLA alternative Subunit Flow Scheme
(1 JT-valve for the whole unit)

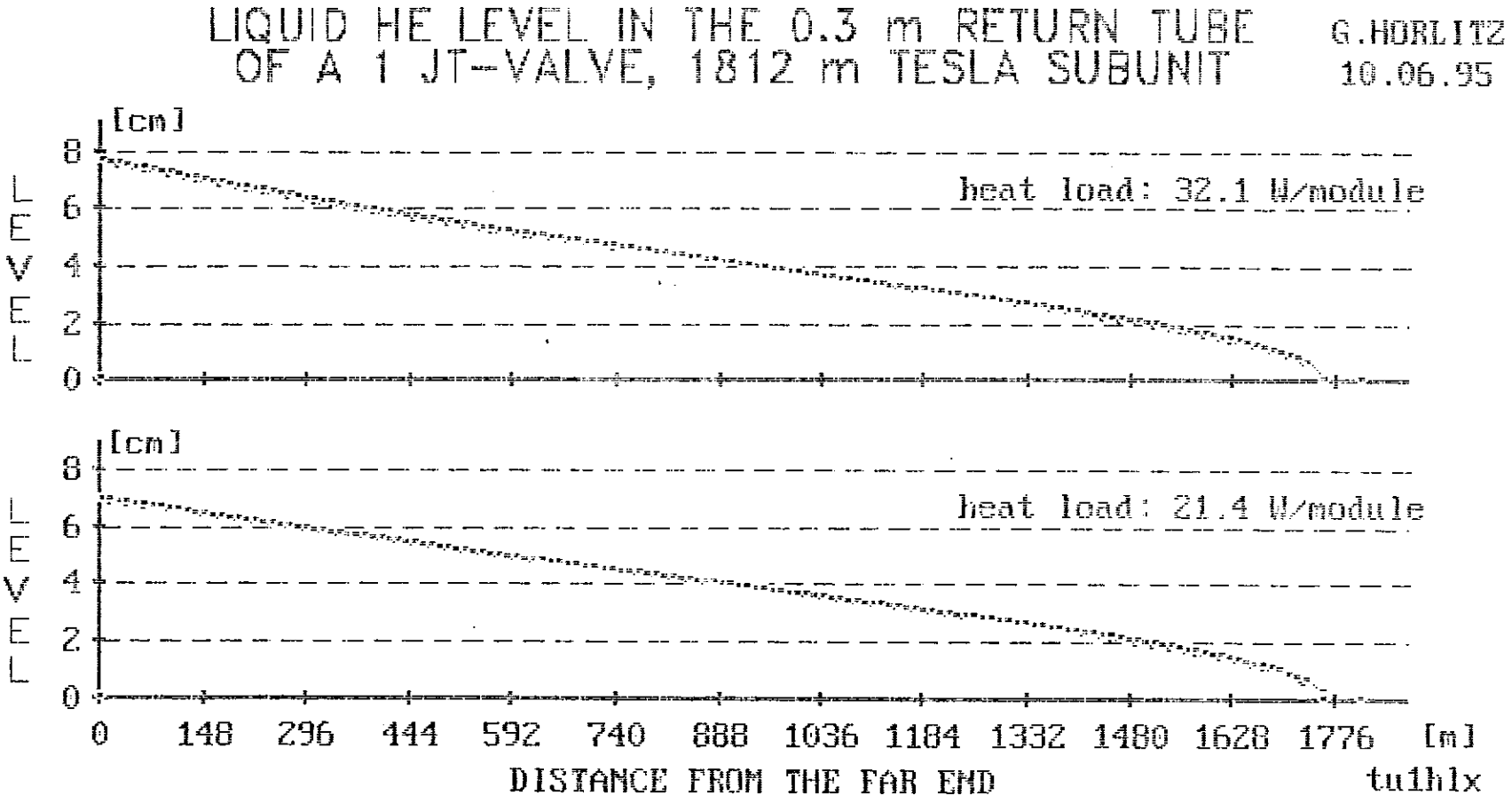

Fig. 9 Liquid He-Level in the Return Tube
(only 1 JT-valve at the far end of the subunit)

DESIGN OF POWER AND HOM COUPLERS FOR TESLA

Karl Koepke, for the TESLA Collaboration

Fermi National Accelerator Laboratory
P.O. Box 500, Batavia, Illinois 60510, USA

ABSTRACT

The basic TESLA accelerating structure is a 1 m long, 9-cell superconducting cavity operating at a frequency of 1.3 GHz and an accelerating gradient of 25 MV/m. Each of these cavities has one fundamental mode power input coupler and two higher order mode (HOM) couplers. The rf requirement of the input coupler is a peak power of 200 kW for 1.3 ms at a 10 Hz repetition rate. The input coupler must also accommodate a 15 mm cavity motion during cryostat cool down and must minimize the cryogenic heat load with and without rf power present. The HOM couplers must extract from the cavities the beam induced HOM energy that does not propagate to the rf absorbers located at the end of each cryomodule. Two distinct input couplers and two distinct HOM couplers designs have been produced. Their design criteria and performance will be reported.

INTRODUCTION

TESLA [1] (TeV Energy Superconducting Linear Accelerator) is one of a family of proposed e^+e^- linear colliders[2] with a CM collision energy of 500 GeV. TESLA is unique among these proposed accelerators in that it uses superconducting rf accelerating cavities. The basic TESLA accelerating cavity[3] is shown in Figure 1. It consists of 9 cells that are dimensioned to operate in the standing wave π mode of the TM_{010} passband at a frequency

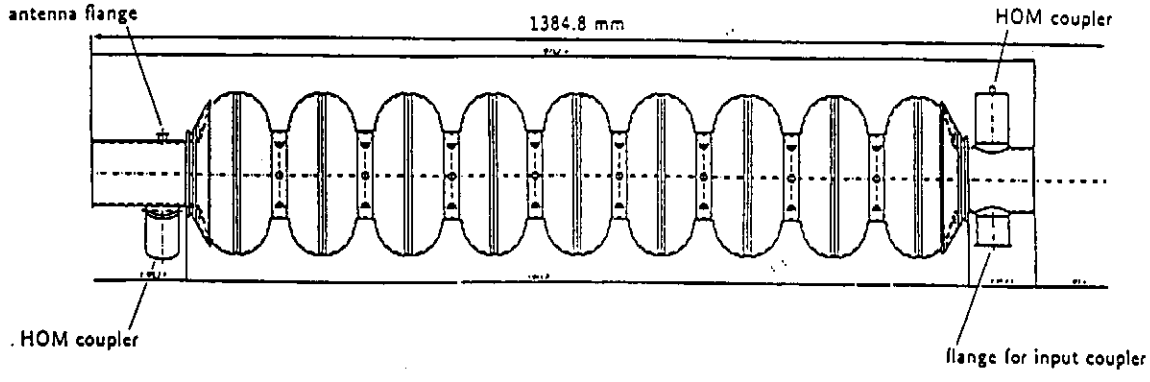

Figure 1. TESLA 9-cell superconducting cavity with coupler locations.

of 1.3 GHz. The cells, bore tube and flanges are fabricated out of high purity niobium sheets (RRR=300).

The basic rf power source[4] for TESLA is a 1.3 GHz klystron capable of producing a peak power up to 5 MW (100 kW average) at the TESLA duty cycle. The klystron rf output passes thru a circulator and is then split approximately equally by directional couplers into 16 WR650 waveguide channels to power 16 cavities. The input couplers transmit the rf power from the waveguide at room temperature to the cavity at 1.8 K. The circulator protects the klystron from the rf power that is reflected due to mismatches in the rf circuit, primarily from the cavity, but also due to imperfections in the waveguides and input couplers.

Each 9-cell cavity is energized by a single power input coupler to which 1.3 ms long rf pulses with a peak power of 200 kW are applied at a 10 Hz rate. The accelerating gradient of 25 MV/m is reached 0.5 ms after the rf pulse is applied. At this time, 800 beam bunches, spaced 1 μs apart, are injected into the cavities and accelerated. Each beam bunch contains 5 10^{10} particles. The input coupler must also tolerate a 1 MW peak power pulse at reduced pulse length and repetition rate for in situ peak power reprocessing of 9-cell cavities after installation in the cryostat or after a vacuum failure.

As the beam bunches traverse the cavities, they excite higher order mode (HOM) resonances in the cavities. The electromagnetic fields of this induced HOM energy interact with the beam, causing beam instabilities, emittance growth and energy spread. The HOM energy is also an unacceptable 1.8 K heat load and in extreme cases can cause thermal breakdown of the superconducting cavities (quench) unless the HOM energy is extracted from the cavities. Approximately 70 % of the HOM energy in the TESLA cavities is expected to be above the beam tube cutoff frequency and will be absorbed by broad band rf absorbers located at the end of each cryomodule. The remaining HOM energy and some HOM energy above cutoff but trapped between the cavities will be extracted by the HOM couplers. Each 9-cell cavity has 2 HOM couplers for this purpose.

The basic TESLA cryogenic unit is the 12 m long cryomodule[5]. Each cryomodule contains eight 9-cell cavities plus beam focusing and steering magnets. Each 9-cell cavity within the cryomodule is contained within its own 1.8 K vessel. These vessels are filled by gravity with 1.8 K liquid He from the 1.8 K liquid He supply pipe located above the cavities. The cryomodule also contains 4.5 K and 70 K radiation shields. The He supply lines for these shields also serve as heat intercepts for devices that penetrate to the 1.8 K region, e.g., supports, input couplers, etc. The input coupler and 2 HOM couplers of each cavity are attached to the bore tube of the cavity outside of its 1.8 K vessel. This results in a simplified mechanical structure and eliminates a source of He leaks as all the coupler joints within the cryomodule have vacuum on both sides. However, the large number of cells per cavity makes it more difficult to obtain a uniform accelerating field in time for the next accelerated beam bunch and to couple adequately to all the HOM excited within the cells.

An international collaboration has assembled a TESLA Test Facility (TTF) at DESY, Hamburg, Germany, to demonstrate the technical viability of TESLA. TTF already has the infrastructure to clean, assemble and test superconducting cavities. The present effort is to produce 4 complete cryomodules that will be part of a 500 MeV test linac. As part of this effort, DESY[6] and Fermilab[7] have each developed an input coupler, and DESY[8] and Saclay[9] have each developed a HOM coupler.

INPUT COUPLERS

The two TESLA input coupler versions are shown in Figure 2 and Figure 3. Although they differ in detail, they both satisfy the same electrical , mechanical and cryogenic requirements.

Waveguide-Coax Transition

This component transforms the TE_{10} mode transmitted by the WR650 waveguide into the TEM mode transmitted by the coaxial line of the coupler. This transformation needs to be achieved with minimum reflections (matched at 1.3 GHz) for rf efficiency and diagnostic reasons. The magnitude and phase of the reflected power are an important indicator of coupler and cavity performance. The Fermilab input coupler utilizes a

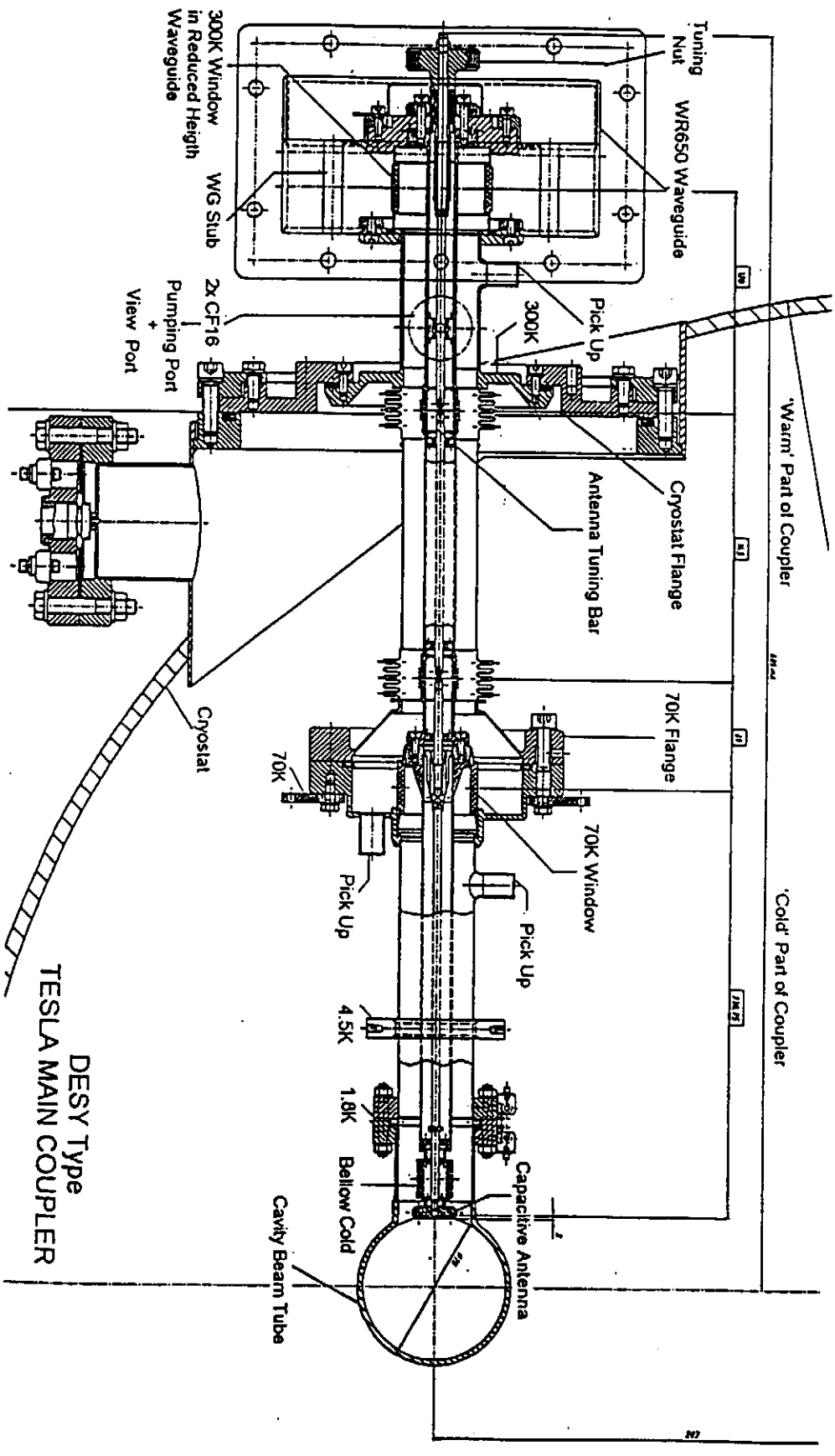

Figure 2. DESY designed TESLA power input coupler.

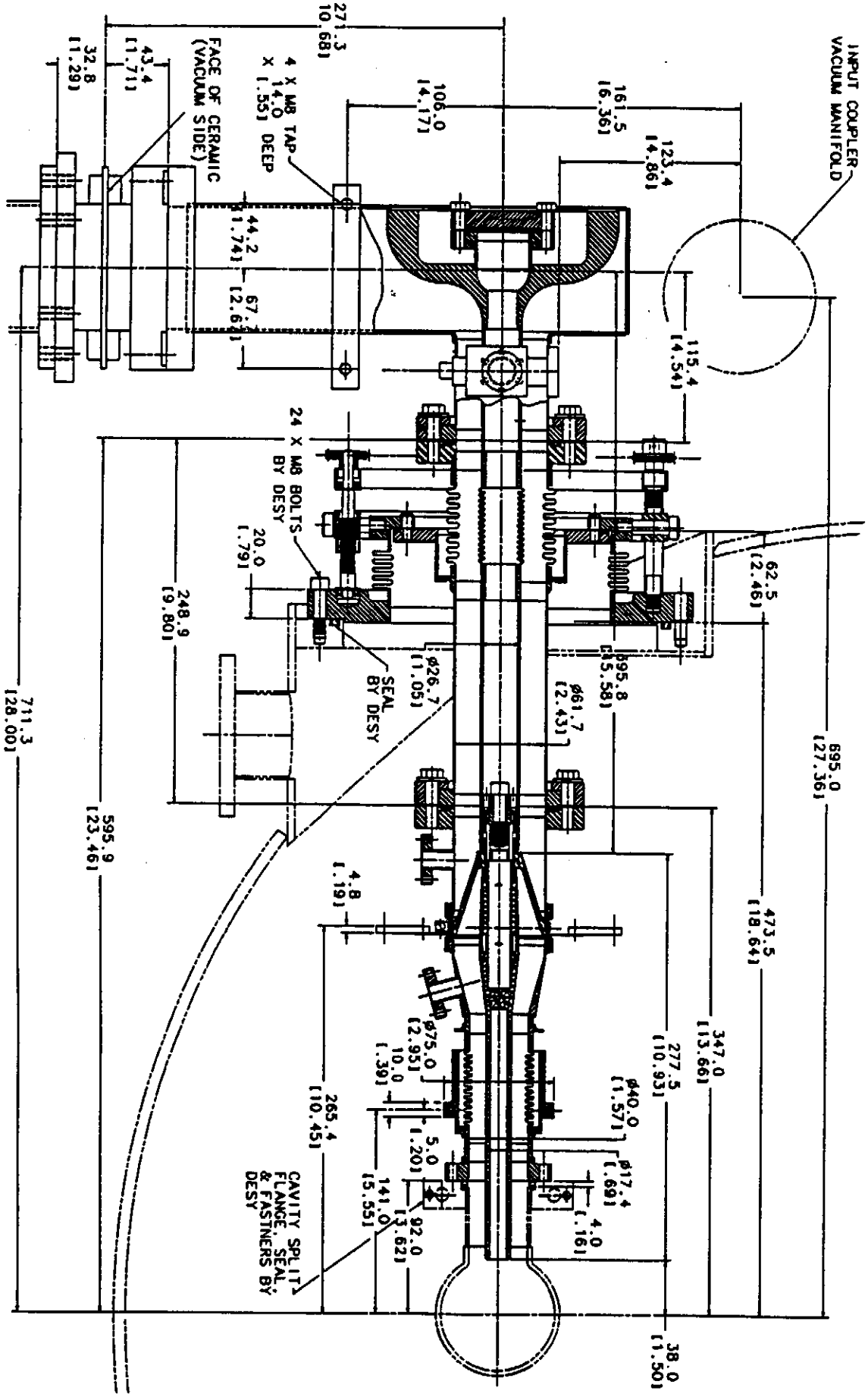

Figure 3. Fermilab designed TESLA power input coupler.

"doorknob" transition. The Hewlett Packard code, HFSS (High Frequency Structure Simulation), has been used to calculate the shape of the "doorknob" to assure a match at 1.3 GHz. The DESY transition uses a "flattened doorknob"; the WR650 waveguide tapers to a reduced height WR650 section. It is matched by two posts located in the reduced height waveguide upstream of the warm rf window.

Warm Window

This component isolates the atmosphere in the waveguide from the upstream vacuum of the coupler. The Fermilab warm window is a commercial "pillbox" type, located immediately upstream of the "doorknob" transition and matched by two posts upstream of the window. The DESY warm window is cylindrical and mounted within the waveguide transition and concentric with the inner coax conductor. Both windows are fabricated out of high purity Al_2O_3 (>99%) and are "thin" to minimize rf losses.

Cold Window

Both coupler versions have a cold rf window located close to the cavity. This window isolates the coupler vacuum from the ultraclean vacuum of the cavity. The cold window is attached to the cavity in the clean room and prevents contamination of the cavity by micron sized particles during subsequent handling and installation into the cryostat. The windows are "thin" and constructed out of high purity Al_2O_3. Both the Fermilab and DESY cold windows are matched to the coaxial line at 1.3 GHz. The Fermilab window is conical in shape. The DESY window is cylindrical.

Coaxial Lines

Both coupler versions utilize a 50 Ω coaxial line to transmit the rf from the waveguide transition through the vacuum vessel of the cryostat. The coaxial line terminates on the bore tube at a point outside of the 1.8 K vessel that surrounds the cavity. The cold end of the outer coaxial conductor is cooled to 1.8 K by conduction through the niobium bore tube, connection tube, and flange. The static heat load and rf heat loads to the 1.8 K volume are minimized by 4.5 K and 70 K heat intercepts located slightly upstream of the 1.8 K flange and at the cold window respectively. The Fermilab coaxial line upstream of the cold window has an outer diameter of 6 cm and is fabricated out of thin walled stainless steel for mechanical rigidity and minimum heat conduction. The inner surfaces in contact with rf are plated with approximately 10 μm of copper. The coaxial line tapers to 4 cm after the cold window. The inner conductor of the 4 cm coaxial section is thick walled copper to keep the temperature at the inner conductor tip approximately equal to the 70 K temperature at the cold window. The DESY coaxial line diameter is 4 cm over its whole length. It is also constructed out of copper plated stainless steel with a copper inner conductor tip at its end.

Bellows

Depending on their position in the cryomodule relative to the centrally located fixed suppport, the 9-cell cavities move up to 15 mm during cool down. Both coupler versions have bellows on the inner and outer coaxial parts of the coupler to allow this motion. When warm, the coupler is kinked. When cold, the coupler straightens to its nominal operating position. The bellows are hydroformed stainless steel and copper plated where necessary to reduce the rf surface resistance.

Coupling Adjustment

Coupling to the 9-cell cavity needs to be adjustable to compensate for cavity performance variations. The nominally required external Q is $3\ 10^6$. The external Q of both coupler versions is adjustable approximately a factor of 10 around this value by adjusting the position of the coupler's inner conductor relative to the bore tube center. The Fermilab coupler achieves this by varying the length of the outer conductor bellow nearest to the bore tube. The DESY coupler adjusts the inner conductor bellow nearest to the bore tube. As the impedance of the 9-cell cavity changes as a function of accelerating

field and accelerated beam current, the coupler is matched for the nominal accelerating voltage and beam current. During the rise time of the accelerating voltage in the 9-cell cavity and for beam currents other than the nominal beam current, a fraction of the rf power applied to the input coupler is reflected at the cavity-coupler interface and is absorbed by the rf load attached to the circulator. When the input coupler is matched to the cavity, the rf power going into the coupler is completely absorbed by the accelerated beam.

Heat Load

The heat loads into the 1.8 K, 4.5 K and 70 K heat sinks have been estimated by a one dimensional program that divides the coaxial conductors into segments and then performs an energy balance on each segment. The program uses temperature dependent tables for the thermal conductivity and electrical resistivity of stainless steel and copper to calculate heat conduction and rf heating. At cryogenic temperature, the 10 μm copper plating dominates not only the rf loss but also the heat conduction. The thickness of the copper plating, the RRR value of the copper, and the copper surface quality are therefore critical. The rf skin depth must also be adjusted for the anomalous skin effect. The calculated heat load[10] during full rf duty cycle operation is essentially identical for the two input coupler designs; approximately .06 W, .6W, and 6.0 W to the 1.8 K, 4.5 K, and 70 K heat intercept points.

Standing Wave

The input couplers are overcoupled until beam is injected into the cavity. At the beginning of the rf pulse, all of the rf is reflected back from the tip of the inner conductor. The resulting standing wave pattern has a voltage maximum equal to twice the voltage of the traveling wave. The maximum repeats every half wave length with the first occurring approximately at the tip of the inner conductor. The voltage amplitude modulation of the standing wave decreases as the cavity accelerating field rises, reaches zero, and then rises again with a quarter wave phase shift. Beam is injected at the time when the standing wave modulation amplitude is zero and the beam maintains the coupler matched for the remaining duration of the rf pulse. The rf windows of the Fermilab coupler have been placed at voltage minimum locations. The DESY coupler has its cold window at a voltage maximum, the warm window at a voltage minimum. All of the rf windows have been coated with a few nanometers of TiN to reduce multipactoring. The TiN reduces the secondary electron coefficient of the surface. The Fermilab couplers will also have the copper plated surfaces coated with TiN.

HOM COUPLERS

Two types of HOM couplers have been developed for testing at TTF, one with a flange to allow demounting of the HOM coupler from the bore tube, the other welded to the bore tube. The demountable HOM coupler was developed by CE Saclay and is similar to the HOM coupler used on the LEP cavities but scaled to the 1.3 GHz TESLA fundamental frequency. A sketch of the demountable HOM coupler is shown in Figure 4. The welded HOM coupler (Figure 5) was developed at DESY. It is based on the HOM coupler used on the 4-cell HERA cavities.

Unlike the fundamental mode input coupler that needs to be matched at 1.3 GHz to maximize the power available for beam acceleration, the HOM couplers contain a rejection filter at this frequency to prevent loading of the cavity's accelerating gradient and to prevent an excessive heat load in the HOM cable that connects the HOM coupler to the load external to the cryostat. This filter must have sufficient bandwidth to permit pretuning at room temperature without impairing damping of adjacent HOM frequencies.

The mode families identified as possible sources of beam blowup are: TE_{111} (1622 MHz - 1789 MHz, TM_{110} (1800 MHz - 1889 MHz), TE_{121} (3076 MHz - 3114 MHz), TM_{011} (2380 MHz - 2454 MHz), and TM_{012} (3720 MHz - 3857 MHz). The HOM couplers can provide damping over the frequency range, 1.8 GHz to 10 GHz, as their transfer functions are essentially flat over this range. The external Q for a particular HOM passband frequency depends on the HOM field amplitude at the location of the HOM coupler and the orientation of the HOM coupler. Depending on the HOM passband, coupling can be

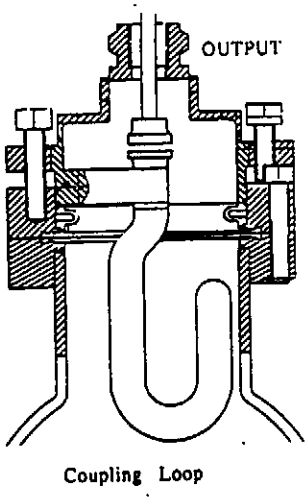

Figure 4. Demountable HOM coupler.

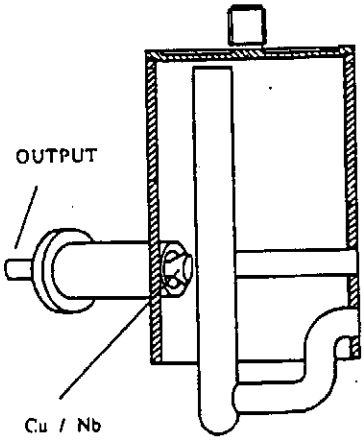

Figure 5. Welded HOM coupler.

predominantly to the electric or magnetic HOM fields. To assure proper coupling to the above HOM families, two HOM couplers per 9-cell cavity are placed on the bore tube outside of the cavity helium vessel. The demountable HOM couplers are separated by an azimuthal angle of 115°, the welded HOM coupler at an angle of 150°. These angles are the optimal position for these couplers relative to the summed impedances of the eight highest (R/Q) HOM dipole passbands.

The fundamental frequency rejection filter of the demountable HOM coupler is formed by the inductance of the loop and the capacitance of the loop end to the outer conductor. Final tuning of the rejection frequency is accomplished with a single convolution bellow located above the demounting flange joint. A capacitive probe extracts the HOM power at the top of the coupler. The fundamental frequency rejection filter for the welded HOM coupler is formed by the inductance of the inner conductor pin and the capacitance of the pin gap to the top surface of the coupler. This rejection filter is tuned by an inelastic deformation of the coupler's top. A capacitive probe extracts the HOM power at the side of the coupler. Both HOM couplers can adjust Qext at 1.3 GHz to larger than 10^{11}.

The HOM couplers are cooled by conduction to the bore tube. The demountable HOM coupler has an additional thermal shunt to 1.8 K at the coupling loop support post location as the thermal conduction through the demounting flange joint proved to be inadequate. To minimize rf heating, caused primarily by currents at the fundamental mode frequency, the inner and outer conductors of the HOM couplers are fabricated out of niobium. The coupler temperature must therefore be maintained below 9 K to avoid a quench and thermal runaway.

PERFORMANCE

Two prototypes of the Fermilab input coupler have been tested up to a peak power of 70 kW, the highest 1.3 GHz power currently available at Fermilab. The tests were performed without a cavity. The cold windows of the couplers were cooled by immersing the couplers in an open dewar containing LN up to the 70 K intercept point and the coupler ends were terminated with a 4 cm diameter closed pipe. The first coupler was tested with a 50 kW standing wave and two inner conductor tip lengths; the first placed the cold window at a voltage maximum of the standing wave pattern, the second at a minimum. This exposed every part of the coupler to the voltage equivalent of a 200 kW traveling wave. The second prototype input coupler was tested up to 70 kW with the cold window placed at a standing wave minimum. The vacuum trip level during conditioning was set at 2 10^{-6} Torr. Photomultipliers and electron probes detected light and electrons early in the conditioning period. This activity was conditioned away after 2 weeks of operation. These couplers are presently at DESY where they are scheduled to be tested at full power.

The cold rf window of the DESY input coupler has been tested in a three half wavelength long coax resonator. The window was placed at the standing wave voltage maximum at the resonator's center and tested with a 100 kW peak power standing wave.

This is equivalent to the voltage of a 400 kW peak power traveling wave. The observed vacuum, light, and electron activity was removed by conditioning.

Both HOM couplers have been tested at DESY and CE Saclay with copper models of the 9-cell TESLA cavity. The copper cavity tests confirmed that both HOM couplers have sufficient damping of the HOM passbands that were considered as possible emittance growth sources. 1.5 GHz models of the HOM couplers were also tested on a single cell 1.5 GHz superconducting cavity at CE Saclay. Both couplers worked properly up to 12.5 MV/m in cw mode. This represents a significant safety margin for 25 MV/m operation at the 1.3 % TESLA duty cycle.

SUMMARY

Twelve Fermilab designed input couplers are presently being assembled at Fermilab. Three DESY designed input couplers have been ordered from industry. These input couplers are expected to start arriving at DESY within a few weeks. They will be conditioned in a fixture that tests two couplers in series, and after successful testing, will be assembled to 9-cell cavities that have been preconditioned in a vertical dewar. Testing of the HOM couplers is already in progress at full rf power during conditioning of 9-cell cavities in a vertical dewar.

ACKNOWLEDGMENTS

Fermilab is operated by the Universities Research Association under contract to the U.S. Department of Energy. The couplers were developed at CE Saclay, DESY and Fermilab primarily by the following individuals: M. Champion, S.Chel, B. Dwersteg, A. Mosnier and J. Sekutowicz.

REFERENCES

1. H. Edwards, Proc. 6th Workshop on RF Superconductivity, CEBAF, Vol.1, p.361 (1993).
2. J. Rossbach, Proc. 1992 Linear Acc. Conf., Ottowa, Vol.1, pg. 25.
3. D. Proch, Proc. 6th Workshop on RF Superconductivity, CEBAF, Vol.1, p.382 (1993).
4. A. Gamp, Proc. 6th Workshop on RF Superconductivity, CEBAF, Vol.1, p.492 (1993)
5. A. Tazzari, F. Alessandria, F. Castagna, L. Catani, M. Ferrario, M. Minestrini, T. Nicol, Proc. 6th Workshop on RF Superconductivity, CEBAF, Vol.1,p.440 (1993).
6. B. Dwersteg, G. Weichert, N. Adelt, Proc. 6th Workshop on Superconductivity, CEBAF, Vol.2, p.1144 (1993).
7. M. Champion, Proc. 6th Workshop on RF Superconductivity, CEBAF, Vol.1, p.406 (1993).
8. J. Sekutowicz, Proc. 6th Workshop on RF Superconductivity, CEBAF, Vol.1, p.426 (1993).
9. S. Chel, A. Mosnier, M. Fouaidy, T. Junquera, contributed to 4th European Particle Accelerator Conference, London, June 1994.
10. T. Peterson, TESLA Report 93-37, available from DESY.

CRYOSTAT FOR TESTING RF POWER COUPLERS

M. Kuchnir, M.S. Champion, K.P. Koepke and J.R. Misek

Fermi National Accelerator Laboratory*
Batavia, IL, 60510, USA

ABSTRACT

Similar to the power leads of accelerator superconducting magnets, the power couplers of accelerator superconducting cavities are components that link room temperature to superfluid helium temperature for the purpose of energy transfer. Instead of conducting kiloamperes of current they guide megawatts of RF power between those two temperatures. In this paper we describe a cryostat designed for testing the performance of these components and measuring their heat loads. A special feature of this cryostat is its minimum liquid inventory that considerably simplifies safety related requirements. This cryostat is part of a Fermilab facility contributing to the international collaboration working on TESLA (TeV Electron Superconducting Linear Accelerator). This facility is now operational and we will be presenting specifications as well as performance data on the cryostat as well as the first pair of power couplers tested with it.

INTRODUCTION

One of the TESLA (TeV Electron Superconducting Linear Accelerator)[1] essential components is the **Input RF Power Coupler** that transmit the 1.3 GHz Power from room temperature to the 1.8 K environment of the superconducting accelerating cavities. These articulated coaxial transmission lines have a wave-guide to coax transition at room temperature, a ceramic window at 78 K, and an outer conductor extremity connected to the superconducting beam-tube between the cavities.

In order to test the power handling capability of these power couplers and measure their heat loads on the refrigeration system we designed the cryostat described here. It measures their heat loads by thermal sinking them through heatmeters .[2] A resonant ring containing a single cell superconducting cavity between two power couplers is used with the available 100 kW power source in order to test them RFwise up to the 1 MW power level required for HPP (High Power Processing)[3] of the TESLA cavities in situ. This arrangement is schematically shown in figure 1. The cavity together with the colder segments of the couplers are attachable to the cryostat as an evacuated unit. A special container for shipment of this unit was also built. This allows for the chemical surface treatment of the cavity and clean room assembly of this three components unit to be performed at already existing facilities of participants in the TESLA collaboration.

In this paper we describe the cryostat, its operation and one of the first tests using it. This test verified the cryostat operation and measured the static heat load of the two

* Fermi National Accelerator Laboratory is operated by Universities Research Association, Inc. under contract with the U.S. Department of Energy.

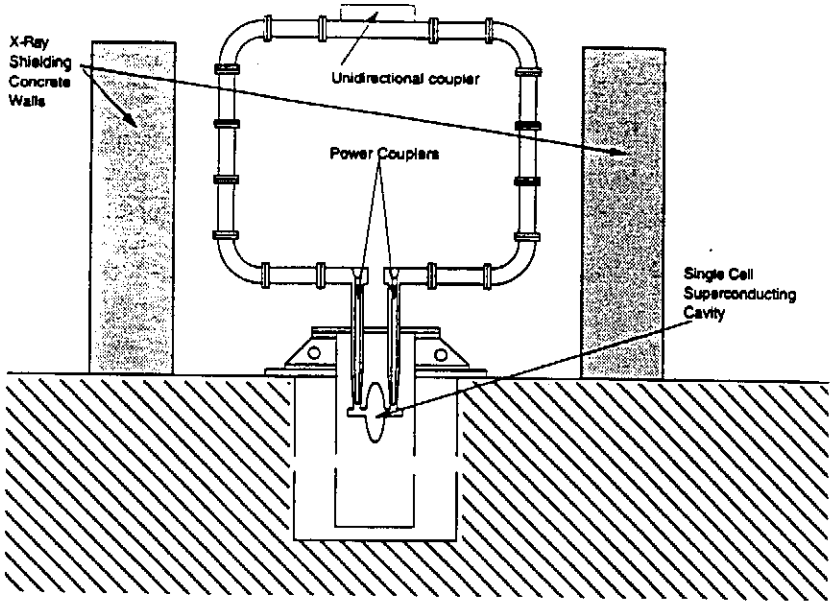

Figure 1. Resonant ring testing concept

power couplers in use. Performance under RF power was precluded by the lack of the required chemical treatment of the superconducting cavity.

CRYOSTAT DESCRIPTION

The length of the cryostat is dictated by the power couplers length. As a consequence it is rather short (0.7 m), also the separation between the couplers is dictated by simulation to the TESLA cavity cell-coupler distance resulting in a axis to axis distance of (0.203 m). This cryostat fits in an existing sunken dewar of 0.44 m internal diameter that is used here just as a vacuum vessel.

In order to make the cryostat inherently safe and avoid need for boiler code certifications etc. the liquid He inventory is minimized to 1.6 liters and the operation is based on continuously flowing cryogens from a liquid N_2 trailer and a liquid He 500 liter storage dewar.

The cryostat is formed by a **stainless steel top plate**, a **copper LN_2 plate** with its **aluminum shield** that surrounds a **copper LHe plate** and its **aluminum shield** that in turn surrounds the **pure niobium piece**. The surrounding is not complete since race track shaped holes in the copper plates are needed for the couplers, plumbing lines and instrumentation cables. The gaps remaining in these holes are closed for infrared radiation purposes with closer fitting multilayered insulation mats. Four G11CR fiberglass-epoxy rods form the **structural frame** that holds together the plates and the cradle holding the niobium piece. Figure 2 presents these components in a simplified schematic. The simplification required for figure 2 substitutes by a single stainless steel bellows the rather sophisticated mounting system of the **power coupler** to the top plate. This mounting system allows the motions required for RF tuning of the coupler to the TESLA cavities as well as the resonant ring in this test arrangement besides taking care of thermal expansion differentials.

The **stainless steel top plate** is 2.54 mm thick. Besides the circle of bolts that seals it to the dewar and the two flanges for the coupler adapters it has 10 penetrations and 4 blind screw holes for the set of G11CR fiberglass-epoxy rods. Pairs of these penetrations are for the LHe transfer lines, LN_2 lines, rotary feedthroughs, electrical wires and fiber optic feedthroughs, vacuum and pump out ports. The penetrations for LHe transfer lines are equipped with Cajon fittings for 12.7 mm OD transfer lines. These rigid U shaped transferlines have 6.35 mm ID and are used for both the incoming liquid and the exiting cold gas from the copper plate and cryopump (Exhaust).

The penetrations for the LN_2 lines and the LHe Vent line are double walled elbows using the insulating vacuum to prevent their cold inner tube (6.35 mm diameter) from

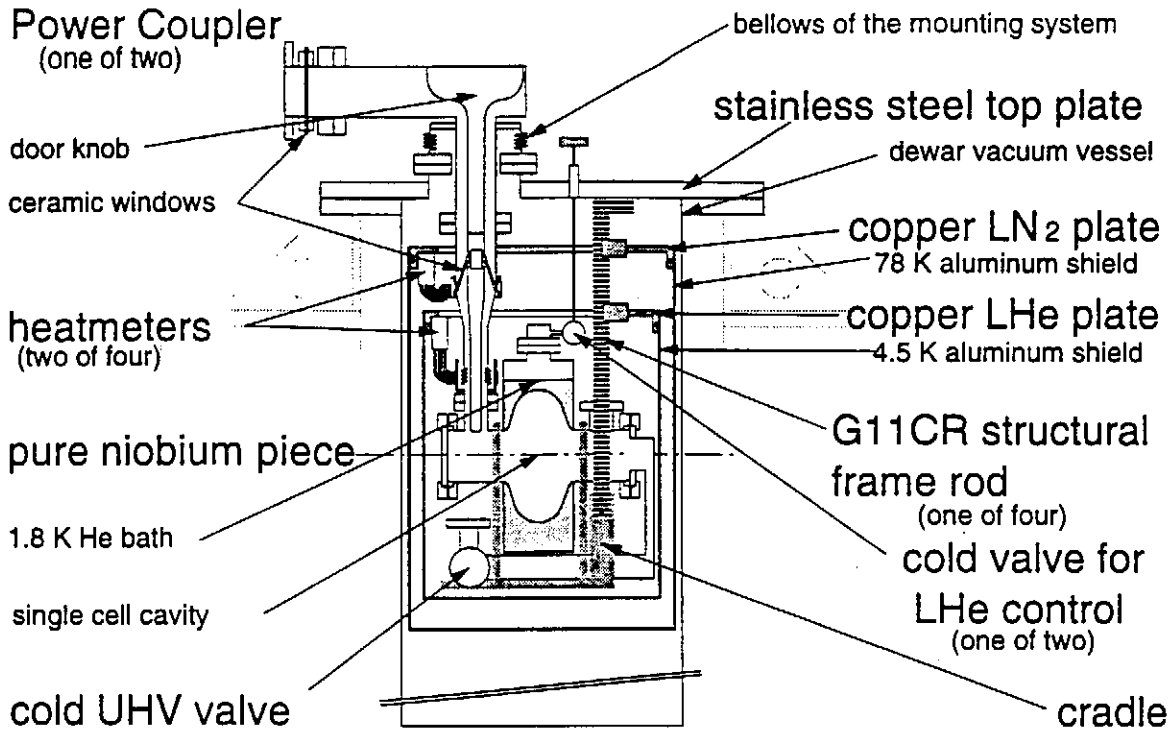

Figure 2. General mechanical structure of the cryostat

cooling the plate. Since thick frosted coating on these lines was not a concern, "Hytron" thermoplastic hoses (manufactured by Imperial Eastman) have been used here with good results although these temperatures are well below their specifications . The rotary "Ferrofluidic" feedtroughs are used to permit the control of the two cold valves through 6.35 mm diameter G11CR rods that extend their stems inside the cryostat.

The **copper plates** are 9.53 mm thick discs of OFHC copper to which are brazed two copper-magnet-bus-hollow conductors and two small OFHC copper discs. Through the hollow conductors will flow the cryogens that determine the temperature of the plates. One of these is 2.16 m long and has 5.79 x 5.79 mm cross section with a 3.18 mm diameter hole, the other has a 14.3 x 25.4 mm cross section with a 6.35 mm diameter hole and form the rim of the plate. The outside of this rim is then machined at a 2.0 ° angle to form a conical surface for thermal contact with its aluminum shield. The two small discs add thickness to the plates locally for the 1/2-14NPT pipe threaded hole used for the attachment of the heatmeters

The **78 K** and **4.5 K shields** are made from 3.18 mm thick aluminum plate rolled and welded to form flat based cylindrical cans. The rims are internally machined at a 2.0 ° angle to closely contact the conic surfaces of the respective plate rims. Three race-track shaped holes equally spaced around are machined partially intersecting the conic surface to permit the introduction of a tool for the uncoupling of this binding conic contact. These holes are also used by special fasteners to prevent gravitational induced de coupling. The conic surfaces are lightly coated with Apiezon L grease to improve thermal contact and ease of disassembly. The thermal contact of these conic surfaces, helped by the copper/aluminum differential thermal expansion coefficient proved to be completely satisfactory.

The **pure niobium piece** was formed at the Laboratory for Nuclear Studies of Cornell University and further modified by e-beam welding to it the LHe reservoir, the pulled-out tubes and flanges . These latter operations were done at Fermilab. Noteworthy are the seals to the stainless steel mating flanges that use Helicoflex "O-rings". In particular, one of them seals the superfluid He containing reservoir from the insulating vacuum. This piece together with the Ultra High Vacuum (UHV) manifold and its all metal valve are held to a cradle that allow us to position it easily on a table or attach it and the lower parts of its two couplers to the cryostat frame or to a shipping frame. So the niobium piece consists of a beam tube with two radial pullouts (for the couplers) between which it expands in an

elliptical single cell cavity. This cavity is coaxially surrounded by a cylindrical liquid He container also with a radial pull-out which is parallel and in between the other two. The extremities of the beam tube and pull-outs have shoulders that fit into special stainless flanges designed to seal with Helicoflex metal "O-rings". The entire piece is made exclusively of high purity niobium stock and electron-beam welded together. The niobium piece, its cradle and the ceramic-window-sealed colder halves of the two couplers, plus a manifold ending in an all metal valve, V1, are detachable as one UHV system that can be shipped for chemical polishing and assembly in a clean room.

The four supports that form the **structural frame** of the cryostat were machined out of a G11CR plate. They have the shape of an inverted long and narrow L. The foot of each L is attached to the bottom of the stainless top plate by means of a 1/4-20 screw into a threaded hole 12.7 mm deep. The long vertical legs have a 12.7 x 25.4 mm cross section. Horizontal threaded holes are used to hold the copper plates and heat-sink the supports at the copper plates temperatures. This is accomplished by means of copper coated screws and copper coated stainless adapters. The LN2 cooled copper plate is at 76.2 mm below the stainless top plate and the LHe cooled copper plate is 102. mm further down. The horizontal holes used for the attachment of the cradle and its pure niobium piece (at 1.8 K) are 241. mm further down.

The **four heatmeters** are very similar. The two, designed for the 80 K region, have a 2.1 mm long stainless steel body segment between copper segments containing 100 Ω Pt RTDs (Resistance vs. Temperature Devices). The other two, designed for the 5 K region, have a 0.5 mm long stainless steel body segment between copper segments containing 100 Ω, 1/8 w Allen Bradley carbon composition RTDs.

Each heatmeter has a 45 Ω calibration heater and an aluminum thermal shield. The contact to the heat sinking plates is by means of 1/2-14 NPT pipe threads (copper to copper) and to the couplers through copper braided cables and copper clamps. Copper powder loaded grease is used in these contacts and care is taken to prevent the braided cables from touching anything.

Not shown in figure 2 is the **cavity ultra high vacuum pumping line,** it is composed of three sections. The section from 300 K to 80 K is formed by a zigzag of three coaxial vertical tubes in order to reduce heat conduction. The middle section is a 31.75 mm diameter 0.11 m long horizontal stainless tube joining the other (vertical) sections through mitered welds. The lowest section has a brazed copper sleeve .32 m long around it. This sleeve has a cooling channel that makes it act as a cryopump. This line terminates with Conflat 2.75 flanges. The flange at room temperature is after an elbow adapted to the top plate and the flange at low temperature connects to the all metal valve of the detachable UHV system.

The **1.8 K bath pumping line**, also not shown in figure 2, starts as a 6.35 mm diameter stainless tube leaving radially from the cap of the bath and connecting to the shell side of the **heat exchanger**. The shell of this heat exchanger is made out a 15.9 mm

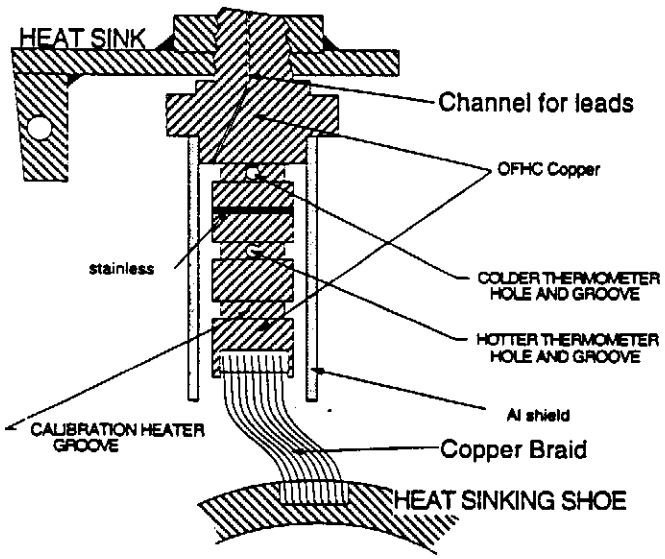

Figure 3. Heatmeter mechanical schematic.

diameter, .89 mm wall, 0.53 m long stainless tube curved in a semi-circle. This semi-circle lays below and along the inner edge of the copper LHe plate without touching it. Inside the heat exchanger, seven stainless capillary tubes each 0.79 mm OD x 0.15 mm wall x 1.70 m long are connected in parallel and coiled. They carry and cool the liquid helium to the JT valve. After the heat exchanger this line continues as a 19.0 mm OD stainless tube to a bayonet type port on the top plate. Care was taken to insure that this line slopes up all the way to prevent formation of liquid pools above the bath.

The **cap of the 1.8 K** bath is a rather busy component that contains an electrical feedthrough with 9 wires, the pumpout tube, the refill tube, the cooldown tube and the supports for three electrical connectors one inside and two outside besides the shoulder for the sealing flanges. The feedthrough is made from Stycast 2850 in a well tested style[4]. One of the outside connectors is of SMA type and is used for the twisted pair leads of the capacitive liquid Helium level sensor. The other two are commercial 9 pin connectors based on diallyl phthalate. So, before sealing the cap to the bath, a cable with the 4 leads from a RTD, 2 leads from the level sensor and two leads from the immersed bottom heater is plugged in the inner connector. Also, before sealing the cap to the bath, a Teflon tube gets connected to the cooldown tube so that the cold helium is directed to the bottom of the bath. Therefore, the end of the cooldown tube inside the cap points directly down ready for connection to the Teflon tube that will extend it to the bottom of the bath. The refill tube however brings the expanding cold mixture from the JT valve pointing it horizontal and tangential to the inner wall for a phase separation action and minimum disturbance of the accumulated liquid. The pumpout tube leaves the cap from the cylindrical side wall radially.

The **capacitive liquid helium level sensor** is made out of 3 stainless steel strips (.13 mm thick, 12.7 mm wide shims 260. mm long) separated with 1.59 mm x 9.52 mm spacers, 25.4 mm apart, each made out of 7 layers of adhesive Teflon tape buildup to a thickness of 0.62 mm. The outer strips form the external grounded plate of the capacitor. This flexible probe is inserted in the bath space along the external equator of the single cell cavity. Therefore its response to the level is non-linear in a calculable way. The circuit used has been described by S.J. Collocott[5] . In this system we placed the front end frequency to voltage converter (an integrated circuit) on the connector inside the cryostat to reduce the parasitic capacitance and reduce noise pick up.

MODES OF OPERATION AND FLOW DIAGRAM

The cryostat is cooled and run by continuously flowing liquid He from a 500 liter storage dewar and liquid N_2 from an existing storage trailer. Figure 4 is the flow diagram of the system showing these components and the cryostat plumbing. Non conventional schematic symbols and lines are used to give a more pictorial representation of the actual system. Valve V1 is an all metal valve which is operated only when the system is at room temperature and is kept open when the system is in the dewar for cooling or running. It is not part of the helium flow system. The liquid from the storage dewar and the part of it that is vaporized by the transfer tube heat leak are handled differently according to the operational mode.

After establishing the plumbing connections, vacuum leak testing the different volumes, leaving them with the appropriate gas and valve settings the cool down starts by flowing nitrogen from the storage trailer through the LN_2 .copper plate. In the first stage of the *cool down mode*, the vent plumbing, valves V3 and V2 are closed directing the cold helium to cool the lower section of UHV pumpline (cryopump) and the copper LHe plate exiting through the **exhaust exit plumbing**. In the second stage, once the UHV cryopump is cold, valve V3 is open directing the helium to further cool the copper LHe plate and the pure niobium piece leaving the system via the bath pumpout line. This stage should be paced by the conduction cooling of the heavy end-flanges of the cavity.

In the *operating mode*, valve V3 is closed and the incoming mixture reaches the **phase separator** where the gas is directed to the now open **vent exit plumbing** while the liquid continues to be used to cool the cryopump section of the UHV pumping line and the copper LHe plate leaving the cryostat via the exhaust exit plumbing. Part of this flow is diverted to the 1.8 K bath via the cold heat exchanger and the V2 valve which here acts as a the Joule Thompson expansion valve (JT). The aperture of this valve is adjusted to maintain

the level in the bath stable above the cell wall. The time constant characteristic of this control is suitable for manual control, but future upgrade includes an automatic control for this function.

In figure 4, the heat exchanging parts of the flow lines are indicated with their diameter and length in inches. The connections are made with 6.35 mm OD x 0.89 mm wall stainless tubes welded or brazed. The heat exchanger before the V2 valve has been described above as part of the 1.8 K bath pumping line. The phase separator has a volume of less than 50 cm^3 and is probably not optimal. The vent tube coming out of it is being redesigned to go trough a serpentine cooling line in the LHe shield prior to exiting the cryostat.

The general control of the operation is done by the pressure in the LHe storage dewar and the flow limiting rotameter valves downstream in the exhaust and vent exit plumbing. These helium flows determine the 4.5 K shield temperature and enable the JT valve (V2) effective operation, which together with the pumping on the helium bath surrounding the cavity and the heat load determines the cavity temperature.

Besides the thermometers and heaters in the heatmeters that have been described above and the sensors in the helium bath there are RTDs installed in the shields and plates. Sixteen RTDs are multiplexed into four hardware channels. Other instruments installed are four pressure gauges, two flow meters, and two liquid level indicators.

The data acquisition system is based on hardware and software designed and built at

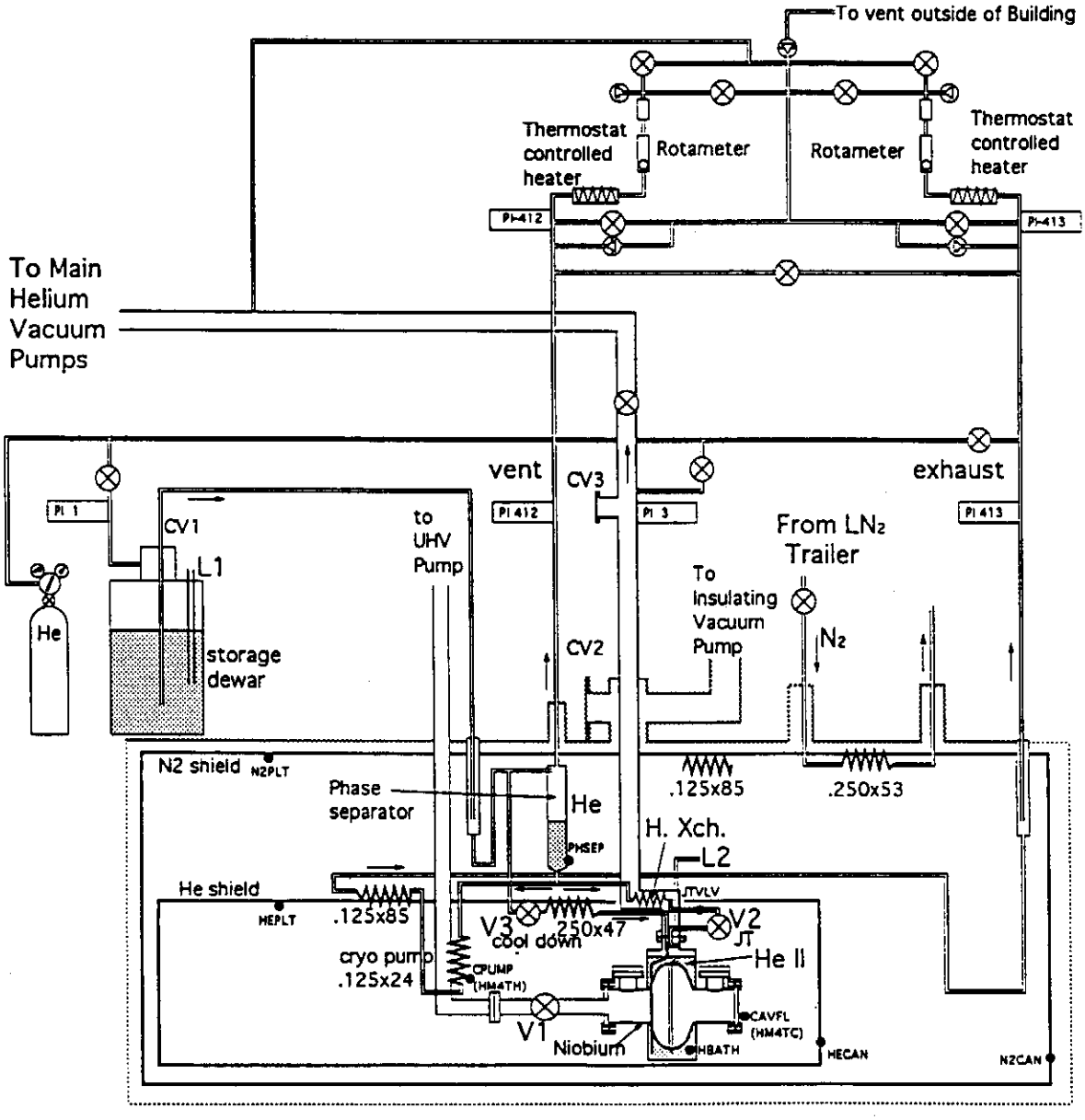

Figure 4. Flow diagram of the cryostat

Fermilab for control of its Linac[6]. The hardware consists of two modules both of which are nodes in the Internet. One of them is an RF wave form digitizer and the other is the Internet Rack Monitor (IRM) which has been used here for the cryogenic data acquisition. A special set of instrumentation amplifiers[7] and IRM software[8] was developed and implemented to handle RTD thermometry. The Parampage[9] software used is specifically written for MacIntosh computers and communicates with the rest of the hardware by local network or the Internet. So data acquisition (and control if properly authorized) can be monitored independently and simultaneously from anywhere. Most of the time, trouble shooting and resetting operations have been done by the specialists in the Linac Control group at their desks a few kilometers away.

RESULTS

Besides a commissioning run without power couplers, only one attempt has been made to run this cryostat in the proposed resonant ring mode but the low Q due to the yet unpolished cavity surface prevented resonance. So the data acquired so far are the heat loads of the first two power couplers (carrying no RF power) and the operational parameters for the cryostat itself.

These heat loads include contribution of the infrared radiation exchange between the braided copper connection and its surroundings. They are a function of the temperature distribution throughout the cryostat and are shown in Table 1. We estimate the order of the uncertainty here to be less than 30 % . More running experience and tests are needed to reduce this estimate uncertainty. At this time we are not in need of a more precise result.

Table 1. Power Coupler heat loads

	window load	at	base load	at
Coupler #1	6.7 W	102 K	1.01 W	6.7 K
Coupler #2	5.8 W	101 K	0.96 W	6.8 K

Measurements were also made of the temperature of the He bath surrounding the cavity as a function of the power deposited in its internal heater. The steady state temperature was 1.43 K and Table 2 presents its value as a function of power. The level of the superfluid in the bath went down under the 2 W and 4 W loads but it took of the order of 15 minutes to empty.

Table 2. Cavity He Bath temperature under several power loads

Watt	0.00	.129	.254	.380	.498	1.00	2.00	4.01
K	1.43	1.45	1.48	1.50	1.52	1.60	1.71	1.86

The operation of the cryostat is best when it is not left to warm up much overnight. This involves an overnight liquid helium consumption rate of 4 liters/hour but it prevents contamination problems and long cooldown times. Under typical measuring conditions, the consumption rate is 32 liters/hour. One feature of the system worth mentioning is how this rate is measured: The American Magnetics superconducting wire level sensor used here is part of an adapter to the commercial 500L liquid He container. Its analog voltage output seen as a function of time and the zooming capabilities in the Parampage graphical display provide great sensitivity to the level of the Liquid He supply (± 0.1 mm). This sensitivity allows for the observation of many factors affecting the level. The most obvious the consumption rate reflected in the slope.

CONCLUSION

A special cryostat has been built and tested at Fermilab capable of measuring the heat

loads of TESLA input power couplers. The relevance of these measurements is related with the number of these couplers required. The test facilty now under construction in Hamburg requires 32 and the projected accelerator over 20,000.

ACKNOWLEDGMENTS

We thank the Cornell U. Laboratory for Nuclear Studies for providing the niobium cavity. A large number of people from Fermilab contributed to this project. In particular we want thank Helen Edwards and Frank Turkot for general support. The following contributions are acknowledged: design and drafting by Clare Miller; machining and welding by Fermilab village machine shop; coordination of assembly and operation by Al Rusy; level capacitive sensor, heatmeters wiring, cryostat wiring and superinsulation by Dan Assell; level probe electronics by Dyrrell Lewis; heat meter drafting by Clark Reid; general support by Fermilab Lab 2 personnel; data acquisition system setting up and maintenance by Mike Kucera and Bob Florian.

REFERENCES

1. H. T. Edwards, TESLA Parameters Update - A Progress Report on the TESLA Collider Design, in: "6th Workshop on RF Superconductivity," R.M. Sundelin, ed., CEBAF, Newport News, VA (1993), vol. 1, p. 361.
2. M. Kuchnir, J. D. Gonczy, J. L. Tague, Measuring heat leak with a heatmeter, in: "Advances in Cryogenic Engineering," vol. 31, Plenum Press, New York, (1986), p. 1285.
3. J. Graber, et al., High peak power RF processing studies of 3 GHz niobium cavities, in: "5th Workshop on RF Superconductivity," D. Proch, ed., DESY, Hamburg (1991), vol. 2, p. 758.
4. M. Kuchnir, Fabrication of cryogenic electrical feedthroughs, Fermilab TM-596 (1975).
5. S. J. Collocott, *Cryogenics*, 327 (1983).
6. R. W. Goodwin, M. J. Kucera, M. F. Shea, *Nucl. Instr. and Meth. in Phys. Res. A* 352, 189 (1994).
7. R.D. Oberholtzer and B.M. Wisner - private communication
8. R.W. Goodwin - private communication
9. R. E. Peters - private communication

VARIOUS METHODS OF MANUFACTURING SUPERCONDUCTING ACCELERATING CAVITIES

C. Benvenuti, Ph. Bernard, D. Bloess, E. Chiaveri,
C. Hauviller and W. Weingarten

CERN, European Organization for Nuclear Research
1211 Geneva 23, Switzerland

ABSTRACT

We report on experience in superconducting cavity production methods gained in shaping, joining and thin film coating with various materials and techniques (Pb, Nb, Nb_3Sn, NbN, NbTiN) with emphasis on their potential to reduce mass production costs.

INTRODUCTION

Production technology of superconducting (sc) cavities has entered a new phase: the number of manufactured cavities has jumped from a low value (recyclotrons, heavy ion accelerator facilities, intermediate sc RF systems such as in TRISTAN, HERA) to a large series of hundreds (CEBAF, LEP2) and even thousands (proposed TESLA). This necessitates reconsideration of production and quality control methods with respect to performance requirements and cost effectiveness.

The maximum attainable gradient is not necessarily that for which the construction cost is a minimum. If the total RF voltage, V, and the current are fixed, the total investment costs are given by three terms. The first one is proportional to the total length L of the cavities and cryostats ("linear" costs), the second one is proportional to the total RF power P_{RF} to be transmitted to the beam (independent of L), and the third one is proportional to the cooling power ("cryogenic" costs), which is essentially the power P_d dissipated in the RF cavities. Since $V = E_a \cdot L$ is constant, E_a being the accelerating gradient, the first term is inversely proportional to E_a. If E_a is increased, the RF losses will go up quadratically with E_a. On the other hand the length L is inversely proportional with E_a, because V is constant. Hence P_d increases only linearly with E_a and consequently the cooling power to be installed. The cost minimum is located where the first and third term are equal. The following example is based on numbers, which are close to CERN's experience[1] for LEP. Fig. 1 displays these three terms and their dependence on E_a. It shows that a gradient between 8 and 10 MV/m is an optimum choice for this particular application.

However, having in mind even larger applications, such as the sc linear collider TESLA under design, at higher frequency (1.3 GHz) and higher energy (500 GeV), costs must be reduced substantially. The cooling power may be reduced (technical Q-values being in the 10^9 range) by slowly pulsing the accelerator, which reduces the cryogenic costs. One can see from Fig. 1 that for a duty cycle of 1% (close to that envisaged in TESLA) a gradient of 25 MV/m would yield the cost minimum provided that the linear costs go down

by a factor of 10. To obtain such a factor would be a challenge. Under these assumptions the total costs (for $V = 2$ GV) would go down by a factor of 40.

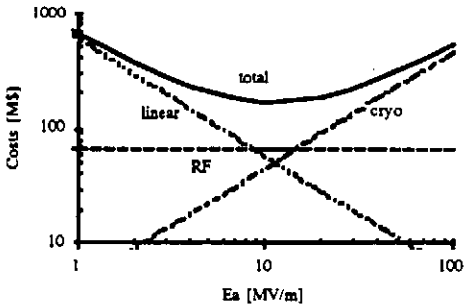

Figure 1. Estimate of investment costs for an sc RF system ($f = 352$ MHz, $V = 2$ GV, 12 MW RF power, 5 W/m standby heat load, $Q_0 = 4 \cdot 10^9$): The total costs are the sum of three terms, linear, RF and cryogenic costs.

The purpose of this paper is to review the state of the art of producing sc cavities. It will focus on the manufacturing of the sc accelerating structure itself. Methods with the potential to save costs will be looked at more closely.

THE MECHANICAL STRUCTURE

The sc cavity consists of two essentials: the "mechanical structure" and the layer which carries the RF current, the "sc surface".

Table 1. Comparison of niobium and copper [1)]

	Cavity grade Nb	OFE Cu
Thermal conductivity @ 4.2 K [W/(mK)]	10 (RRR = 40) - 100 (RRR = 400)	400 - 500
Electrical resistivity @ 295 K [10^{-8} Ωm]	14.4	1.68
Density [g/cm^3]	8.57	8.96
Linear expansion (L_{273}- $L_{4.2}$)/$L_{4.2}$ [‰]	1.43	3.3
Atomic weight	92.91	63.54
Atomic number	41	29
Melting point [°C]	2468 - 2497	1080
Recrystallization temperature [°C]	830 - 1230	400 - 600
Stress relieving temperature [°C]	780 (1h)	200 - 250
Tensile strength [N/mm^2]	207 - 274	196 - 245[3)]
Elongation [%]	6 - 42	6 - 50
Yield point [N/mm^2]	20 [2)]- 196	15 - 300

1) Some data are taken from refs. 2, 3
2) annealed for several hours at 1800 [°C] and 10^{-8} Torr
3) annealed

The mechanical structure has to provide three features. At first it must be sufficiently stable and rigid at low temperatures to sustain with a safety margin the pressure in the helium tank (usually 1 bar) outside, the radiation pressure inside and to block mechanical vibrations. Secondly the thermal conductivity must be such that heat is effectively removed without generating too large temperature gradients (thermal stability). Thirdly it must be shaped economically with reasonable effort and joints between pieces must be vacuum tight and reliable.

Up till now two materials have been used for the mechanical structure; niobium and copper (Table 1). Niobium can simultaneously provide the mechanical structure and the sc surface. In addition it is the element with the largest transition temperature T_c. Copper is relatively cheap, can be manufactured and shaped without tremendous effort and has a large thermal conductivity.

The wall thickness of the mechanical structure assures its mechanical stability. It has to be designed according to contradicting constraints. Thin walls are less costly, easier to handle and effectively cooled, but on the other hand prone to buckling from pressure spikes inside the He tank and mechanical and ponderomotive oscillations (cf. below). Modern accelerating structures are made from several mm thick material (niobium or copper). A Finite Element Analysis software such as CASTEM[4] allows the mechanical behaviour of the structure, in particular the buckling modes, the maximum tolerable pressure, and the natural resonant frequencies to be understood (Fig. 2)[5]. Main modes of vibration can be suppressed by imposing forces of constraint on well-chosen points of maximum amplitude. A complete suppression of all the mechanical vibration modes is impossible. These modes add phase shifts on the tuner feedback loop and can make it unstable. A way out is to shift their resonant frequencies to larger values beyond the tuner bandwidth. This could be done by increasing the rigidity of the stiffening bars and hence the resonant frequency.

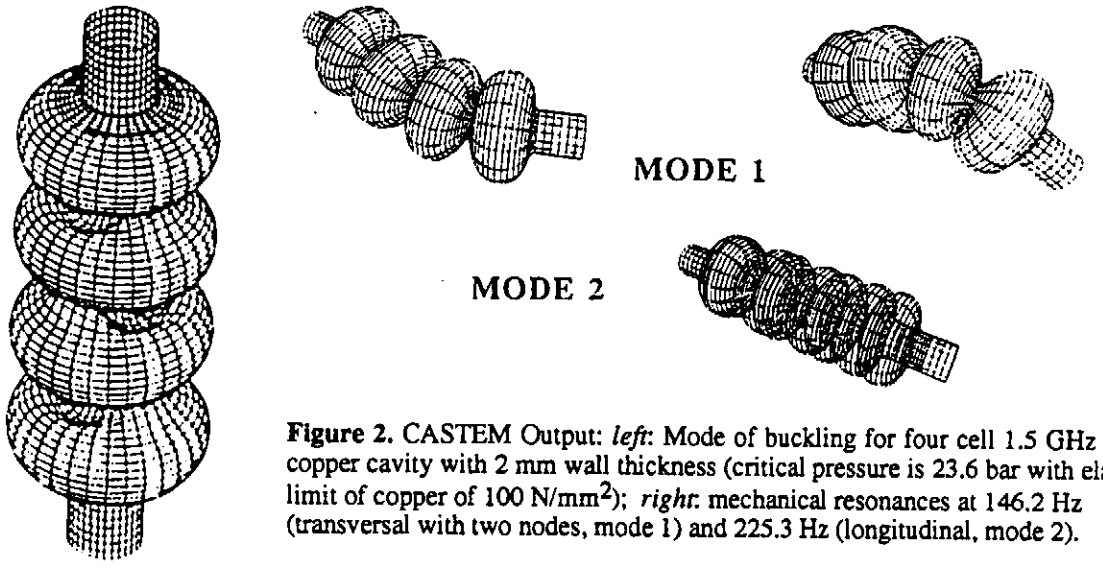

Figure 2. CASTEM Output: *left*: Mode of buckling for four cell 1.5 GHz copper cavity with 2 mm wall thickness (critical pressure is 23.6 bar with elastic limit of copper of 100 N/mm^2); *right*: mechanical resonances at 146.2 Hz (transversal with two nodes, mode 1) and 225.3 Hz (longitudinal, mode 2).

Ponderomotive forces[6] depend on the square of the accelerating gradient. By increasing the accelerating gradient, the cavity is driven out of resonance, for example by the radiation pressure acting on the cavity wall (Lorentz force). It takes a certain time before the wall moves (there is a delay). The RF amplitude will fall, and the resonant frequency will be shifted back to tune again, which closes the loop. The delays present can make the system unstable.

Thermal Conductivity

The temperature T near a localized heat source falls inversely proportional to the thermal conductivity λ and the distance r from that heat source. This may be a normal-conducting inclusion, a poorly-cooled welding bead, peeled-off flake etc., or a region of electron impact. If the source dissipates too much heat, the transition temperature of the sc surface can be surpassed, by which effect the stored energy (100 J for a LEP cavity at 6 MV/m accelerating gradient) is dumped near the defect (quench). The cavity can only be operated at a gradient well below the quench. Therefore the thermal conductivity near T_c of the material in the intimate vicinity of the heat source is the important parameter.

It becomes immediately clear that, to increase the maximum gradient, the number and size of the surface defects have to be reduced, and, on the other hand, sc metal of increased thermal conductivity must be made available (thermal stabilization of defects). It is known[7,8] that the thermal conductivity of niobium is most severely affected by interstitial impurities such as oxygen, nitrogen and carbon. These impurities can be considerably reduced by repeated furnace treatments on the manufacturer's premises[9-11] and/or solid-state

gettering by wrapping a foil of metal with a large affinity to these impurities around the cavity in a furnace at 1200–1400 °C. Yttrium and titanium are used as getter material[12,13].

Shaping and Joining Techniques

There exists a wealth of knowledge on shaping and joining techniques[2,14-25], which will not be repeated here. Niobium can be machined by the usual high speed steel tools. It turns very much like lead or soft copper. It has nevertheless the tendency to gall; tool angles, cutting speed and lubrication have to be carefully chosen. Normal techniques of metal spinning are applied, and the metal takes up the contour of the former. Deep drawing is also used and gives satisfactory results (no "orange peel") for fine grain material (ASTM < 4).

Hydroforming is a common manufacturing procedure (e.g. production of bellows). The principle is to push the part against a rigid die by applying a large pressure through a liquid. Monolithic pieces can be produced, and welding can be avoided. Reproducibility is superior compared to welded parts, but the tooling is expensive. This fact is of no consequence for a large series. However, repeated annealing is necessary and increases the cost. Cavities in the frequency range from 300 MHz to 3 GHz have been produced from OFE (Oxygen Free Electronic grade) copper tubes[22]. The frequency of the fundamental mode of 1.5 GHz five-cell cavities has a standard deviation of ±0.3‰[26]. The final deformation is more than 200%. The ultimate elongation of copper being only of the order of 50% (Table 1), this process has been achieved in several stages: swaging has been followed by three expansion and intermediate annealing steps at 600 °C for one hour.

Swaging means that an oil-pressurized membrane pushes the annealed copper tube on to the internal core creating a toroidal groove. The problem is to prevent plastic buckling due to high compressive stresses creating ripples. The process has been modelled by the BOSOR5[27] software and experimentally checked. Good correlation has been obtained for the critical buckling values in the case of uniform thickness. Thirty-five percent reduction of the iris diameter has been achieved in only one stage with a pressure up to 650 bars.

The expansion is obtained by a multi-part die which is initially open and closed progressively during expansion. The closed die has the exact external shape of the final cavity. The internal hydraulic pressure progressively increases up to 200 bar. The number of expansion steps depends on the radial deformation needed and on the behaviour of the annealed copper. CASTEM software[4] was used for modelling. A precise prediction of the behaviour during all stages has been possible.

OFE copper has high purity and high conductivity at cryogenic temperatures. The parameters of the heat treatment were determined using standard tensile tests. The heat treatment starts to influence material properties from 400 °C. The hydroforming phases were then simulated on test samples (initial annealing, 32% elongation and second annealing, 32% elongation and third annealing).

Hydroforming niobium was first used at HEPL (Stanford)[28]. This metal has very similar properties to copper (Table 1) except the characteristic temperatures such as, for example, the melting point. Heat treatment should be done at 1000°C for about one hour. The procurement of high quality niobium tubes is not easy. Seamless tubes and rotary swaged longitudinally welded ones are presently being investigated.

Spinning is another method for cheap mass production. A seamless nine-cell 1.5 GHz cavity starting from a planar disk of Al has been spun without annealing[29], and Cu and Nb nine-cell cavities are under preparation. The thickness uniformity was about a factor of two.

Galvanoplastic shaping[30] is another technique to build the whole structure without welds in one stride: an organic glass mandrel (shaped like the inner surface of the cavity) is sputter coated with a copper layer, on to which the bulk copper is deposited by the galvanoplastic technique. Subsequently the mandrel is dissolved. A 3 GHz nine-cell cavity has been produced and sputter-coated with a niobium film inside. RF results are not yet published.

THE SUPERCONDUCTING SURFACE

The superconducting surface has to comply with the following three features: it must tolerate high electric fields and currents at sufficiently low RF losses (large Q-values); it

must be operated at a temperature which can be produced by the evaporation of a cryogenic liquid with reasonable effort; it must be operated at a temperature sufficiently below the critical temperature T_c of the sc material (safety margin). There are three different ways of complying simultaneously with these demands, which reflect the historical progress of the technology. The most straightforward way is to use the structure material as the sc surface as well. The second one is to modify the structure material (towards larger T_c and Q-value which means less effort for cooling). The third one separates the function of the structure and the sc surface completely and opens up an avenue towards new materials for the sc surface (thin films).

Identical Superconducting Surface and Structure Material

The metal (exclusively niobium) has been machined as, for example, for the CERN-Karlsruhe RF separator[25], or has been shaped by deep drawing and machined, as for the Stanford HEPL recyclotron[28], or is shaped by deep drawing or spun from sheet metal like, for example, the CEBAF, CERN-SPS-LEP (first phase), Darmstadt-Wuppertal, DESY-HERA, KEK-TRISTAN structures. Some effort with TIG welding has been made, but EB welding of the half cups[23] (preferably from the inside[24]) and irises gave more reliable results. The best results in Q-value and maximum gradient E_a, obtained in an industrial series production, are shown in Fig. 3 (a) and (c).

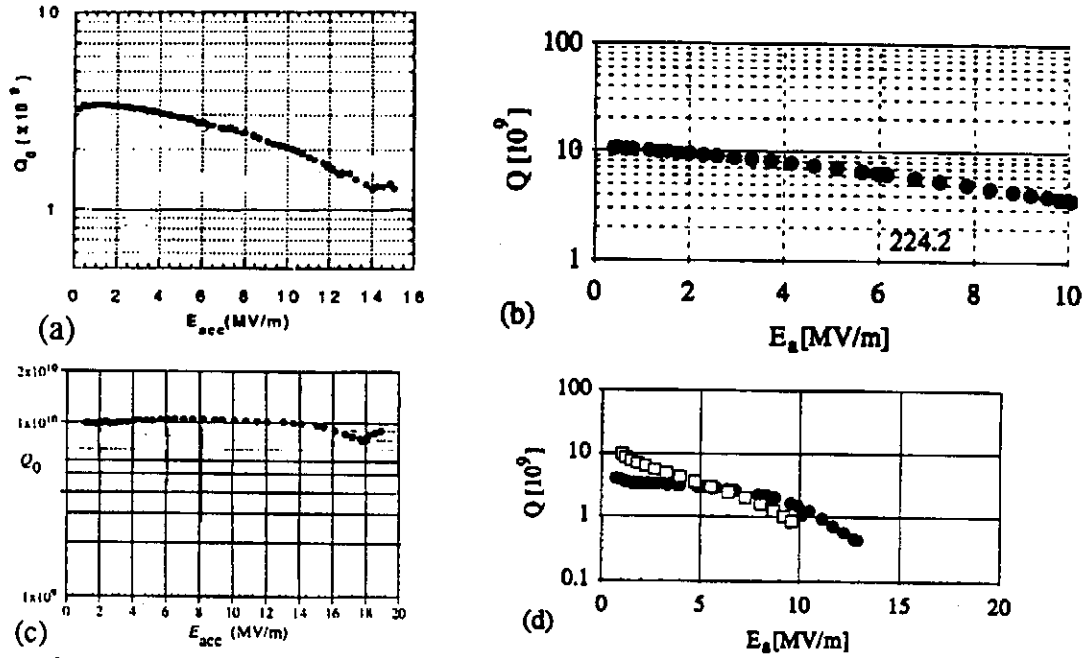

Figure 3. Q_0-E_a plots in vertical tests (best results) for cavities from serial production in industry [except (d)]: (a) a 508 MHz five-cell niobium sheet cavity for TRISTAN[31] (4.2 K); (b) a 352 four-cell niobium coated copper cavity for LEP[32] (4.2 K); (c) a 1500 MHz niobium sheet cavity for CEBAF[33] (1.8 K); (d) 1500 MHz hydroformed niobium coated copper cavity (from industrial production feasibility study)[21] (1.8 K).

The processing of the surface. When the structure and the sc surface are identical, the properties of the sc surface pay tribute to those of the mechanical structure (inclusions from rolling and shaping, thermal conductivity). Nevertheless, the methods of surface processing have been refined in such a way that the maximum gradients obtained in multi-cell accelerating structures have been pushed up to 16 MV/m in a five-cell 508 MHz cavity at KEK[31] and about 22 MV/m in a nine-cell 1.5 GHz cavity in the TESLA collaboration[34]. The first result wasobtained by electropolishing, heat treatment (1.5 h at 700°C) to remove the embedded hydrogen, and rinsing with ultra-pure water under ultrasonic agitation. The second one was obtained by chemical polishing, solid state getter furnace treatment (to improve the thermal conductivity) before welding, rinsing with ultra-pure water (under low and high pressure), and pulsed operation under high RF power (high power pulsed processing)[35].

In the presence of hydrogen (accumulated by slow chemical polishing), cavity grade Nb with high thermal conductivity forms compounds which during slow cool down precipitate as hydrides at low temperatures (~ 100 K) and degrade the Q-value[36]. These cavities have to be annealed to chase the hydrogen or the cool down has to be done fast.

Cavities with identical mechanical structure and sc surface could be taken out one by one, coated by compounds based on the structure metal with improved surface properties (as Nb_3Sn, see below), and retrofitted into the accelerator again.

Acceptance rates in initial vertical tests in an industrial series production for CEBAF are 98% (E_a = 5 MV/m and Q = 2.4·10^9)[33].

Superconducting Surface from Reprocessed Structure Material

A15 and B1 compounds. The surface resistance R_s is composed of the theoretically well understood BCS surface resistance R_{BCS} (which can be calculated by using the BCS theory) and the residual surface resistance R_{res}. At a given operating temperature R_{BCS} falls exponentially with increasing Cooper pair energy 2Δ (2Δ is the energy gap of the sc metal). The BCS theory tells us that Δ is proportional to T_c, Δ = 3.5 kT_c, hence superconductors with a larger pairing energy Δ should allow a smaller surface resistance at the same temperature, provided the pre-exponential constant is about the same. This is the reason why both the B1 and A15 compounds NbN and Nb_3Sn are also being investigated for RF applications.

Table 2. BCS surface resistance of some metals

	T_c [K]	A	n	Δ'
Nb (RRR = 100)	9.25	105	2	18
Nb_3Sn	18.1	105	2	40
Pb (Ref. 37, Fig. 1)	7.2	74	1.75	14.6
PbSn (4 at% Sn)[38]	7.5	68.5	1.9	15.1

The BCS surface resistance (in μΩ) of sc metals for $T < T_c/2$ is given by $R_{BCS} = A \cdot f^n \cdot \exp(-\Delta'/T))/T$, with the temperature T measured in K, the frequency f in GHz, and the constants from Table 2. There is a large potential of attaining a low surface resistance in these compounds, provided that R_{res} can be made sufficiently low (Fig. 4).

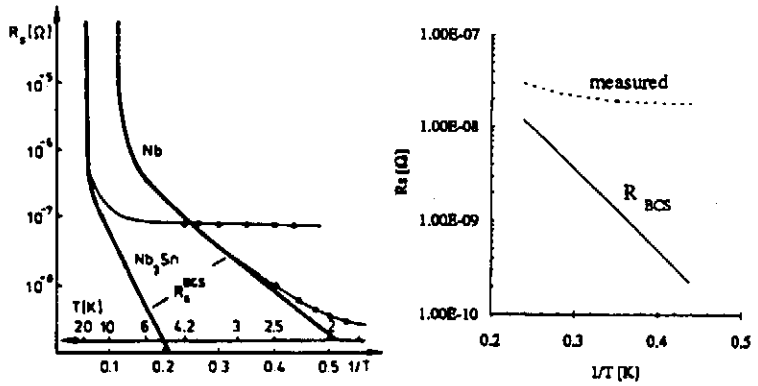

Figure 4. The surface resistance at 500 MHz of a re-entrant cavity with niobium and Nb_3Sn surface (left)[39], and that of a NbTiN layer on a copper accelerating mono-cell cavity (right)[40].

Thin coatings of these materials on RF cavities are produced by thermal diffusion out of the vapour phase at a temperature of 930-1160 °C and 1400°C for Nb_3Sn[39,41,42,43,44] and NbN[45], respectively. Recently, CEBAF has obtained in a Nb_3Sn coated single-cell 1.5 GHz cavity (in collaboration with Wuppertal) a Q-value at 4.2 K, which exceeds the design Q-value for Nb at 2 K[46] at the design field of 5 MV/m.

In an sc metal the London penetration depth λ of the RF field is independent of the frequency in a wide range up to tens of GHz, 39 nm (Nb) and 37 nm (Pb). Therefore, to keep the RF losses low, an sc layer of say ten times the penetration depth is largely sufficient. Such films can be produced by several methods, as follows (we do not consider composite materials, as for example niobium clad copper, the RF performance of which is very similar to bulk niobium).

Coating by electroplating. Lead can be deposited on a copper substrate by electrodeposition. Although niobium is superior to lead (larger T_c, B_c and lower BCS surface resistance, Table 2), nevertheless lead is particularly used for heavy ion structures[37] in small series at low frequencies (where BCS losses are low), if the geometry is such that high thermal gradients may occur, or when the full potential of RF superconductivity technology is not of paramount importance. Several pre-plating, plating and post-plating treatments have been developed, including plating with Pb-Sn[38] and Pb-Bi[47] alloys.

Coating by sputtering. At CERN[48], coating a cavity made of OFE copper by a niobium film has been chosen for several reasons. First, a thermal breakdown (quench) is improbable. Secondly, the material costs would have amounted to about 22 % of the total cavity and cryostat production costs if made from niobium sheet. They are negligible if made from copper sheet. Sputtering has been chosen because the sputtered atoms have a large kinetic energy, which favours the adhesion. DC Magnetron sputtering has been preferred to diode sputtering because of relatively large deposition rates, easy application to multi-cell cavities, and good thickness uniformity. A Q vs. E_a curve is shown in Fig. 3 (b). Compounds as NbN and NbTiN have also been investigated [Fig. 4 (b)][48,49].

In the final phase of the industrial series production for CERN, the acceptance rates in initial vertical tests is 60 - 70 % (E_a = 6 MV/m and Q = $4 \cdot 10^9$)[32].

CONCLUSION

Cost-effective mass production is a key issue for accelerating structures for linear colliders. A strong development effort is needed for the following:

- fabrication methods which allow a substantial reduction in production costs (such as, for example, hydroforming, spinning, galvanoplating) and
- more stringent quality control in a fully automated production chain.

REFERENCES

1. W. Weingarten, Superconducting cavities, *Int. J. Mod. Phys. A (Proc. Suppl.)* 2B:678 (1993), or Proc. XVth Int. Conf. High Energy Acc., J. Rossbach, ed., World Scientific, Singapore (1993), p. 678.
2. W. Bauer, Fabrication of niobium cavities, Proc. 1st Workshop RF Supercond., M. Kuntze, ed., Karlsruhe (1980), KfK 3019, p. 271.
3. M. G. Rao and P. Kneisel, Thermal and mechanical properties of electron beam welded and heat-treated niobium for TESLA, Proc. 6th Workshop RF Supercond., R. Sundelin, ed., CEBAF, Newport News VA, USA (1993), p. 643.
4. A. Combescure, Manuel d'utilisation CASTEM 2000, Rapport CEA DEMT 88/176.
5. J. Genest, private communication.
6. P. H. Ceperley, Ponderomotive oscillations in a superconducting helical resonator, *IEEE Trans. Nucl. Sci.* NS-19:217 (1972).
7. K. K. Schulze, Preparation and characterization of ultra-high-purity niobium, *Journ. of Metals* 33:33 (1981).
8. H. Padamsee, The technology of Nb production and purification, Proc. 2nd Workshop RF Supercond., H. Lengeler, ed., CERN Geneva (1984), p. 339.
9. M. Hörmann, The production of high thermal conductivity niobium on a technical scale for high frequency superconductors, available from W.C. Heraeus GmbH, Produktbereich Sondermetalle, P.O. Box 1553, D-6450 Hanau 1, Germany.
10. E. Drost and M. Hörmann, Mass Production of Superconducting Materials Nb and NbTi, available from W.C. Heraeus GmbH, Produktbereich Sondermetalle, P.O. Box 1553, D-6450 Hanau 1, Germany.

11. P. Kneisel, Improvements in materials and fabrication methods - large scale production and testing - Proc. 5th Workshop RF Supercond., DESY 1991, D. Proch, ed., Hamburg (1992), DESY Report M-92-01, p. 163.
12. H. Padamsee, A new purification technique for improving the thermal conductivity of superconducting Nb microwave cavities, *IEEE Trans. Magn. MAG-21*:1007 (1985).
13. P. Kneisel, Use of titanium solid state gettering process for the improvement of the performance of superconducting RF cavities, *J. Less Common Metals* 139:179 (1988).
14. Columbium (Niobium) Alloys and special products from Teledyne Wah Chang Albany, OR, USA.
15. Columbium (Niobium) from Kawecki Berylco Industries, Inc., Reading PA, USA.
16. Niobium / Columbium from Companhia Brasileira de Metalurgia e Mineração, São Paolo, Brazil.
17. J. P. Bacher et al., Brazing of niobium to stainless steel for UHV application in superconducting cavities, Internal Report CERN/EF-RF 87-7, Dec. 1987.
18. J. Susta, Development of Fabrication Methods, ibid. ref. 8, p. 597.
19. J. Kirchgessner, Forming and Welding of niobium for superconducting cavities, Proc. 3rd Workshop RF Supercond., K. W. Shepard, ed., Argonne Nat. Lab. (1988), ANL-PHY-88-1, p. 533.
20. T. Furuya, Preparation and handling of superconducting RF cavities, Proc. 4th Workshop RF Supercond. KEK, Tsukuba, Japan, 1989, KEK Report 89-21 (January 1990), p. 305.
21. D. Bloess et al., Superconducting, hydroformed, niobium sputter coated copper cavities at 1.5 GHz, Proc. 4th European Particle Acc. Conf. London 1994, V. Suller, Ch. Petit-Jean-Genaz, eds., Singapore (1994), p. 2057.
22. C. Hauviller, Fully hydroformed RF cavities, Proc. Particle Acc. Conf. Chicago 1989 (IEEE, New York, 1989), p. 213.
23. E. Chiaveri and H. Lengeler, Welding of Niobium Cavities at CERN, ibid. ref. 8, p. 611.
24. E. Chiaveri et al., Welding of radio frequency cavities with an internal EB gun, Proc. First Int. Conf. Power Beam Technology, Brighton, UK, 1986, The Welding Institute, London.
25. A. Citron et al., The Karlsruhe-CERN superconducting RF separator, *Nucl. Instr. Meth.* 164:31 (1979).
26. Ph. Bernard et al., Superconducting hydroformed niobium sputter coated copper cavities at 1.5 GHz, ibid. ref. 3, p. 739.
27. D. Bushnell, BOSOR5 Program for buckling of complex , branched shells of revolution including large deflections, plasticity and creep, Lockheed Applied Mechanics Lab.
28. J. Turneaure et al., Performance of 6-m 1300 MHz superconducting niobium accelerator structures, *Appl. Phys. Lett.* 25:247 (1974).
29. V. Palmieri et al., A new method for forming seamless 1.5 GHz multicell cavities starting from planar disks, ibid. ref. 21, p. 2212.
30. A.I. Ageev et al., Development of production technology for weldless copper shells of sc cavities, ibid. ref. 3, p. 802.
31. E. Kako et al., Long term performance of the TRISTAN superconducting RF cavities, Proc. 1991 IEEE Particle Acc. Conf. San Francisco, USA, 1991, (IEEE, New York, 1991), p. 2408.
32. E. Chiaveri et al., Analysis and results of the industrial production of the superconducting Nb/Cu cavities for the LEP2 project, Proc. XVIth Int. Conf. High Energy Acc., Dallas TX, USA, 1995, in press.
33. C. Reece et al., Performance of Production SRF Cavities for CEBAF, Proc. 1993 IEEE Part. Acc. Conf. , Piscataway, NJ, USA (1993), p. 1016.
34. B. Aune, private communication.
35. M. Leenen, The infrastructure for the TESLA Test Facility (TTF) - a status report, ibid. ref. 21, p. 2060.
36. B. Bonin and R. W. Röth, Q-degradation of niobium cavities due to hydrogen contamination, ibid. ref. 11, p. 210.
37. J. R. Delayen, RF properties of superconducting Pb electroplated onto Cu, ibid. ref. 19, p. 469.
38. L. Dietl and U. Trinks, The surface resistance of a superconducting lead-tin alloy, *Nucl. Instr. Meth.* A284:293 (1989).
39. G. Arnolds-Mayer and N. Hilleret, Field emission and secondary electron emission from Nb_3Sn surfaces, *Advanc. in Cryog. Eng. Mat.* 28:611 (1982).
40. C. Benvenuti et al., (NbTi)N and NbTi coatings for superconducting accelerating cavities, ibid. ref. 11, p. 518.
41. G. Arnolds-Mayer, ibid. ref. 8, p. 643.
42. M. Peiniger et al., Nb_3Sn for superconducting accelerators at 4.2 K, Proc. First European Acc. Conf., Rome 1988, S. Tazzari, ed., Singapore (1989), p. 1295.
43. G. Arnolds-Mayer and E. Chiaveri, On a 500 MHz single cell cavity with Nb_3Sn surface, ibid. ref. 19, p. 491.
44. B. Hillenbrand et al., Superconducting Nb_3Sn cavities *IEEE Trans. Magn.* MAG-11:420 (1975).
45. G. Gemme et al., RF surface resistance measurements of binary and ternary niobium compounds, *J. Appl. Phys.* 77:257 (1995).
46. H. Piel, private communication.
47. J. Sikora et al., Lead/Tin Resonator Development at the Stony Brook Heavy-Ion Linac, ibid. ref. 19, p. 419.
48. C. Benvenuti et al., Niobium films for superconducting accelerating cavities, *Appl. Phys. Lett.* 45:583 (1984); C. Benvenuti et al., Superconducting 500 MHz accelerating copper cavities sputter-coated with niobium films, *IEEE Trans. on Magn.* MAG-21:153 (1985).
49. S. Cantacuzène et al., Elaboration et caractérisation de couches minces de $(Nb_xTi_{1-x})N$ pour des applications en hyperfréquences, thesis, Université de Paris Sud, centre d'Orsay (1995).

STATUS REPORT OF THE TTF CAPTURE CAVITY CRYOSTAT

S. Bühler, P. Blache, R. Chevrollier, T. Junquera[1],
N. Colombel, R. Panvier[2]
J. Gastebois[3]

[1]Institut de Physique Nucléaire
Orsay, 91406 cedex, France
[2]Laboratoire de l'Accélérateur Linéaire
Orsay, 91405 cedex, France
[3]CEA /DAPNIA / SEA
Gif-sur-Yvette, 91191 cedex, France

ABSTRACT

We describe the capture cavity cryostat, for the Tesla Test Facility at DESY in Hamburg, which was designed and is presently under assembly in France. We also discuss the construction of an ancillary feed box which is required for a preliminary cryogenic test prior to delivery.

INTRODUCTION

The capture cavity is the first cryogenic device on the beam line of the Tesla Test Facility (TTF) at DESY in Hamburg and will connect the "warm" injector to the first cryomodule.

Design, manufacture and integration of the different parts of the cryostat are substantially done in France and will be completed locally in order to perform two cryogenic tests prior to the delivery to DESY. This decision, however, implies the construction of major ancillary equipment for supply and control of the cryogenics in this first phase.

REFRIGERATION

The capture cavity is mounted in a separate cryostat at the end of the injector. For its final installation at DESY (1) a common feed box provides the cooling for Cryocap as well as for the subsequent cryomodules, connected partly in parallel, partly in series at the following three temperature levels :

- a supply of two-phase He at 1.8 K, 16 mbar which maintains a constant level of superfluid LHe around the cavity,
- a second loop, fed with supercritical He at 3 bar, enters at 4.5 K and cools a heat sink on the RF input coupler,
- a third loop uses He gas at 14 bar and 60 K for cooling a single radiation shield.

For initial cool-down or final warm-up of the cavity a small feed line is connected to the bottom of the LHe tank.

CRYOSTAT

Figure 1 shows the composition of Cryocap.

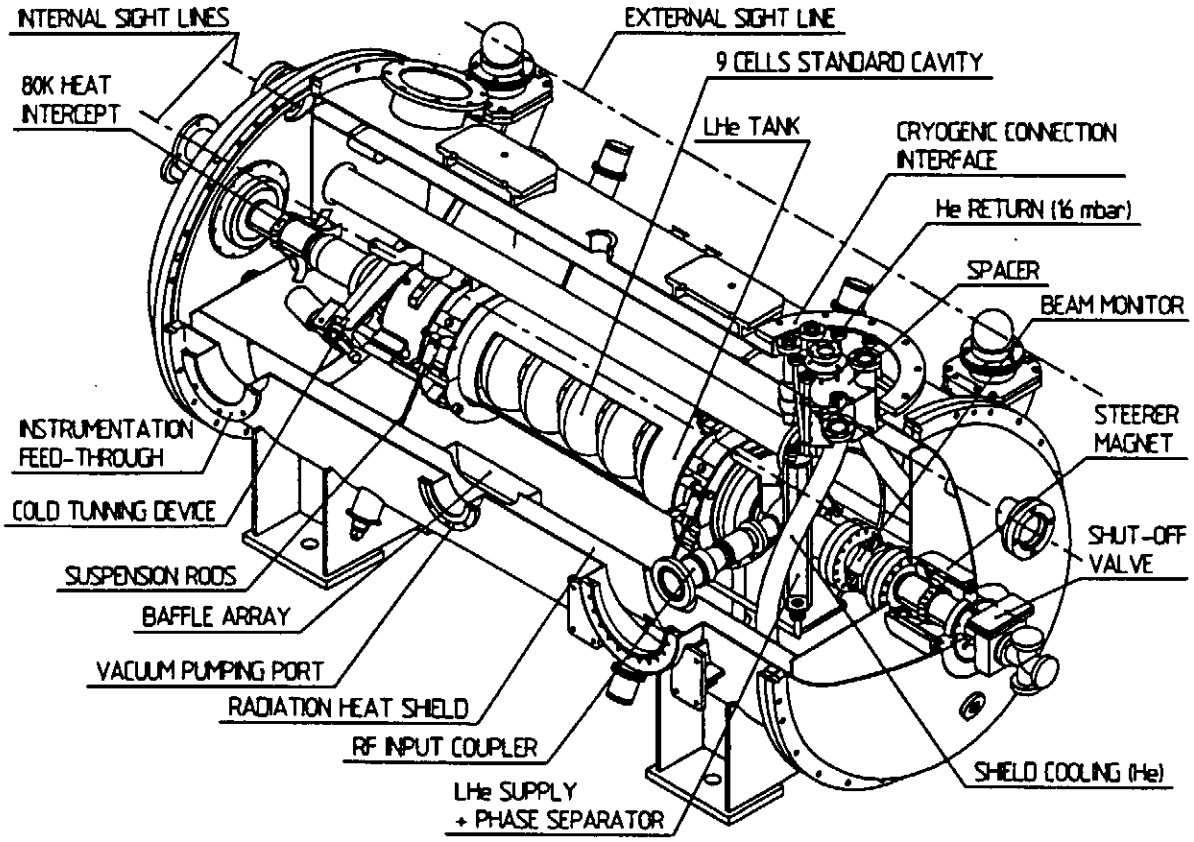

Figure 1. Capture cavity cryostat (CRYOCAP).

LHe tank with cavity

The capture cavity consists of a single but standard 9 cell 1.3 GHz cavity and features the new concepts developed for the TESLA project, i.e. integration into a cylindrical helium vessel with a reduced capacity (23L), with all RF couplers located outside in the vacuum space and thus cooled by conduction only through the niobium walls of the cavity.

The LHe tank is made from titanium, easy to weld to niobium and of a similar thermal contraction. But as niobium turns brittle at very low temperature, the composed titanium-niobium reservoir is not accepted as a pressure vessel, therefore the outer vacuum tank has to assume the duty of a containment volume.

Fine RF tuning of the cold cavity is obtained with a mechanism which compresses the whole 9-cell assembly by approximately ± 1.5 mm.

Passive magnetic shielding of the cavity is provided with a sheet of Cryoperm placed on the LHe tank.

10 layers of superinsulation are wrapped around the fully equipped LHe vessel.

Suspension system

Two split suspension rings are clamped onto the LHe vessel. A radial suspension device with 2 x 4 rods of epoxy-fibreglass, in an antagonistic array which permanently blocks any thermal contraction, maintains the cavity in its adjusted initial position. Such a mounting is acceptable since the low Young's modulus of the composite induces only moderate thermal

stresses which may occasionally be measured with a set of 4 strain gauges mounted in the upper fixture of the suspension rods.

In the axial direction, the LHe tank is blocked with a finger device which penetrates from the vacuum tank into one of the suspension rings.

Radiation heat shield

The thermal radiation from ambient temperature to the cavity is intercepted by a single copper radiation shield cooled to 80 K with forced flow He or LN circulation on its cylindrical part. It integrates into the vacuum tank where it stands on 4 nylon bases. Both removable end covers are conduction cooled.

Heat flow from the surroundings is reduced with a blanket of 40 layers of superinsulation.

The insulating vacuum is autonomous ; a specially devised barrier, located in the cryogenic connection line, separates it from the feed box vacuum space.

A blackened baffle array on the radiation shield allows an efficient evacuation of the innermost vacuum space.

Its basic function apart, the radiation shield also serves other purposes :

- it provides a heat sink for thermal intercepts,
- it supports a solenoidal coil for active magnetic shielding during cool down,
- it may be used to accelerate a warm-up of the cryostat with a thermocoax resistor soldered onto the copper cylinder.

Vacuum tank

The vacuum tank, made from stainless steel, is designed for a service pressure of 1.2 bar abs. As a containment vessel for the fragile cavity reservoir it is protected with a big safety valve against any excessive overpressure.

The removable end caps define the primary alignment axis for the cavity with two permanent sight lines through the entire cryostat, thus allowing an occasional check of the cavity position even in a cold state.

Heat load

A thermal budget estimate limited to the fully equipped CRYOCAP is given in Table 1.

Table 1. Heat load estimate for Cryocap

Temperature level (K)	Nature of heat flow	Static heat flow with no RF power (W)	Static heat flow with full RF power (W)
80	Conduction (supports, heat intercepts)	15	18
	Radiation	37	37
	Total	**52**	**55**
4.5	Intercept on RF input coupler	**0.3**	**0.5**
1.8	Conduction (supports, electric leads)	1.1	1.1
	Radiation	0.4	0.4
	RF power dissipation in cavity	-	1.3
	Total	**1.5**	**2.8**

ANCILLARY FEED BOX (AFB)

For the first cryogenic tests in France, a special ancillary feed box was built which substitutes for the DESY feed box and provides the cooling for Cryocap at 1.8 K and 4.5 K with liquid helium (LHe) and at 80 K with liquid nitrogen (LN) corresponding to the flow scheme of Figure 2.

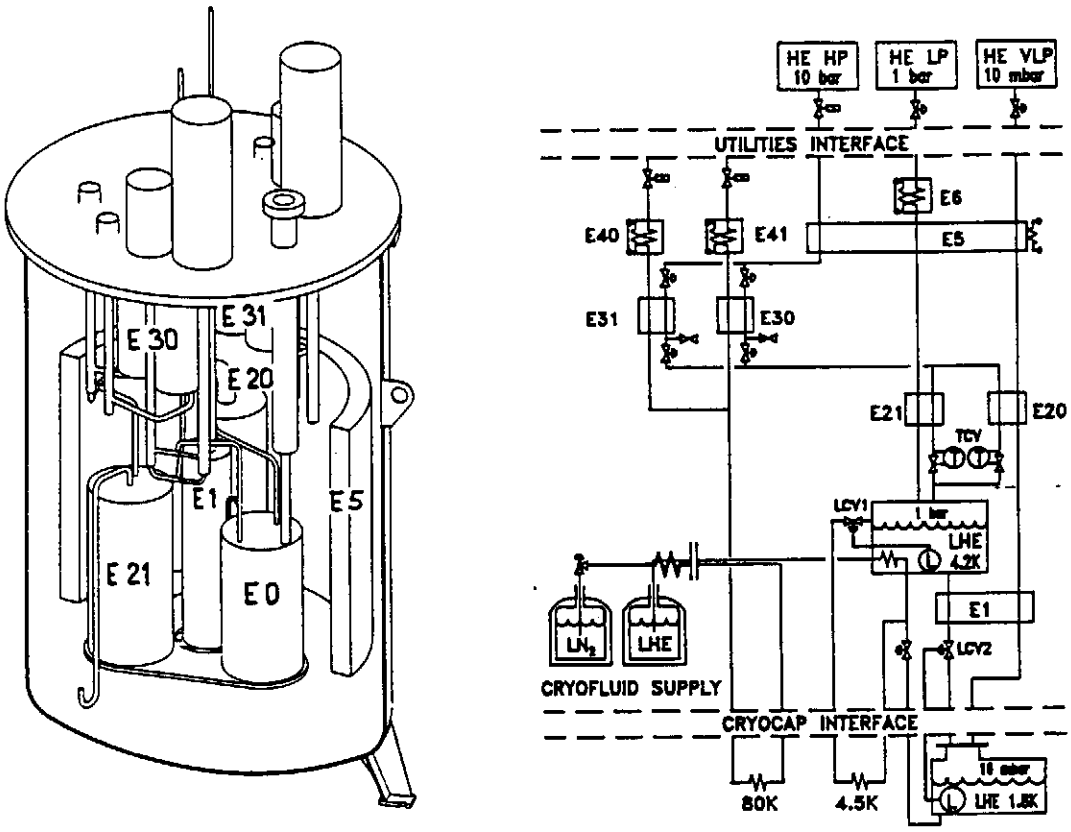

Figure 2. Ancillary feed box for Cryocap and its flow scheme

LHe under 1.2 bar is siphoned continuously from a standard storage vessel, passes a recondensing coil immersed in a LHe pool at 4.2 K and then divides into two flows.

The first flow is only used occasionally for an initial cool-down of the cavity.

The second flow supplies the 4.5 K cooling loop in Cryocap where it partially vaporizes, then returns to AFB where the residual liquid maintains a constant LHe level of the 4.2 K bath, adjusted with the control valve LCV1.

LHe for the 1.8 K bath is taken from the 4.2 K reservoir. A passage through heat exchanger E1 cools it to 2.2 K and thus substantially reduces the flashing losses during expansion to 16 mbar in LCV 2. This valve remotely controls a constant LHe level of the 1.8 K cooling bath in Cryocap.

A second storage vessel provides LN which is essentially used for radiation shield cooling. Thus a continuous feed of LN passes, first in an annular gap through the coaxial LHe transfer line, then through the cooling loops soldered onto the radiation shields of both AFB and Cryocap and finally cools the charcoal adsorbers, alternately E30 or E31, where it entirely vaporizes.

The cold He vapour from Cryocap and those from the 4.2 K cooling bath in AFB may be handled in two different ways :

a) they are simply warmed up to ambient temperature in an electric heater,
b) their potential cooling capacity is recovered in an economizer.

With the construction of the feed box we wanted to combine our long term interests with our short term obligations, so we decided to equip the cold box from the very beginning with a line of heat exchangers which might be operated arbitrarily as an economizer or as a simple heater.

The economizer principle consists essentially in a counter-current heat exchange of the available enthalpy in the escaping low pressure stream to an inflowing high pressure stream whose final Joule-Thomson expansion produces a substantial amount of LHe which in turn reduces the supply from the external storage for the same useful cooling capacity.

Our arrangement consists of two separate Hampson type heat exchangers of high efficiency, operating between 4 to 80 K and a single heat exchanger with a comparatively poor efficiency which operates between 80 to 300 K as a counter-current heat exchanger. The latter is made from two coaxial flexible hoses of 20 m length wound on a cylindrical mandrel. High (HP) and low pressure (LP) gas flows inside of the flexibles hoses, whereas the very low pressure (VLP) gas passes externally and perpendicular to the windings which are, moreover, equipped with an electric heater of 3 kW. Therefore, if no economizer is used, the same apparatus might only be used to warm up the cold vapours to ambient temperature.

Two sets of commutative charcoal traps are provided to purify the incoming high pressure He and to maintain its temperature down to 80 K.

For optimum performance of the economizer the HP mass flow has to be permanently adjusted to the fluctuating LP and VLP cold gas returns. Two identical autonomous control valves have been developed which maintain the temperature of the incoming HP flow at an optimum value (i.e. 6 K).

PRESENT STATUS (July 1995)

Some problems in developing the cavity and its RF coupler induced a substantial delay in our initial planning. Thus assembly of Cryocap has just started and will be completed in next autumn.

The ancillary feed box has been assembled and a first cryogenic test of this particular unit is in progress.

REFERENCES

(1) G. Grygiel, U. Knopf, R. Lange, B. Petersen, D. Sellmann, J. Weisend
"Status of the TTF Cryogenic System", presented at the CEC Conference, July 17-21, 1995, Columbus OH.

TU-A3-5

STATUS OF THE TTF CRYOGENIC SYSTEM

G.Grygiel[1], U.Knopf[1], R.Lange[1], B.Petersen[1],T.Peterson[2],
D.Sellmann[1], and J.Weisend II.[1]

[1]Deutsches Elektronen-Synchrotron (DESY)
Hamburg, 22603, Germany
[2]Fermilab, Batavia, Illinois 60510, U.S.A.

ABSTRACT

As part of the TESLA-Collaboration, components of a 1.8 K cryogenic plant, designed for testing superconducting RF cavities at the DESY laboratory, have been designed and built at the CEN SACLAY, LAL ORSAY, FERMILAB, INFN FRASCATI and DESY. Some additional components are being fabricated at IHEP PROTVINO and industry. The general layout of a 1.8 K Test Facility for the test of superconducting RF cavities has been described earlier[1].

The first stage of the cryogenic facility has been brought into operation. During tests of the prototype cavities, the cryogenic performance of the main components of the cryogenic plant was monitored and is presented. This includes vacuum compressors, vertical and horizontal test dewars, a collection box and a helium heater.

For the second stage, required for the operation of the TTF-500 MeV-linac, the construction of the first module cryostat, the capture cavity cryostat, the 6-fold transfer line and the TTF-feedbox is almost finished. The construction of TTF-module transfer lines, TTF-module end caps and a large low pressure heat exchanger has begun. The design of these components and the present status of the installation at DESY is reported.

INTRODUCTION

The cryogenics of a 1.8 K TESLA Test Facility (TTF) for the test of superconducting RF cavities and the operation of a superconducting 500 MeV test linac has been described recently [1,2]. After the rebuilding of a 900 W 4.4 K helium plant and the installation of a vacuum compressor system and a helium distribution system, a vertical test dewar[3] and a horizontal test dewar (CHECHIA)[4] were brought into operation.

The vertical dewar is used to test the RF performance of single superconducting RF 9-cell cavities at a temperature of about 1.8 K in a liquid helium bath. In addition High Peak Power (HPP) processing and temperature mapping measurements take place in this dewar[2]. In CHECHIA single cavities are tested again, after they have been equipped with their individual helium tanks , the main RF couplers and the higher order mode (HOM) couplers. After the installation of the main couplers, the RF quality Q_{RF} can only be detected by cryogenic heat loss measurements.

The continuous supply of 1.8 K liquid helium which is precooled by means of a low temperature heat exchanger and expanded via a Joule-Thomson valve into a helium bath at a constant level is common for all test cryostats of the facility as well as for the later TTF-test linac. During the first tests of cavities experience can be gained in the operation of the Helium plant, which is valuable for the later operation of the other components.

The complete TTF-linac will consist of a beam-injector including a superconducting capture cavity (CRYOCAP) and four module cryostats (see fig. 1). The detailed status of CRYOCAP and the module cryostats is reported separately in this conference[5,6,7]. Each module cryostat includes eight superconducting cavities and one superconducting quadrupole. The first module cryostat[6,7] is under construction at INFN. The module vacuum vessel, thermal shields , supports, tubing and a 300 mm diameter return tube will be delivered to DESY for final assembly, were also a chain of eight eqipped cavities and a quadrupole will be inserted into the vacuum vessel.

The operation of the linac will start in several steps. As a first step the injector and one module cryostat will be operated. With the installation of a 100 m long transferline, a TTF-feedbox and the transferlines to CRYOCAP and the first module the cryogenic supply will be similar to the supply of the test cryostats. For the supply of the complete test linac

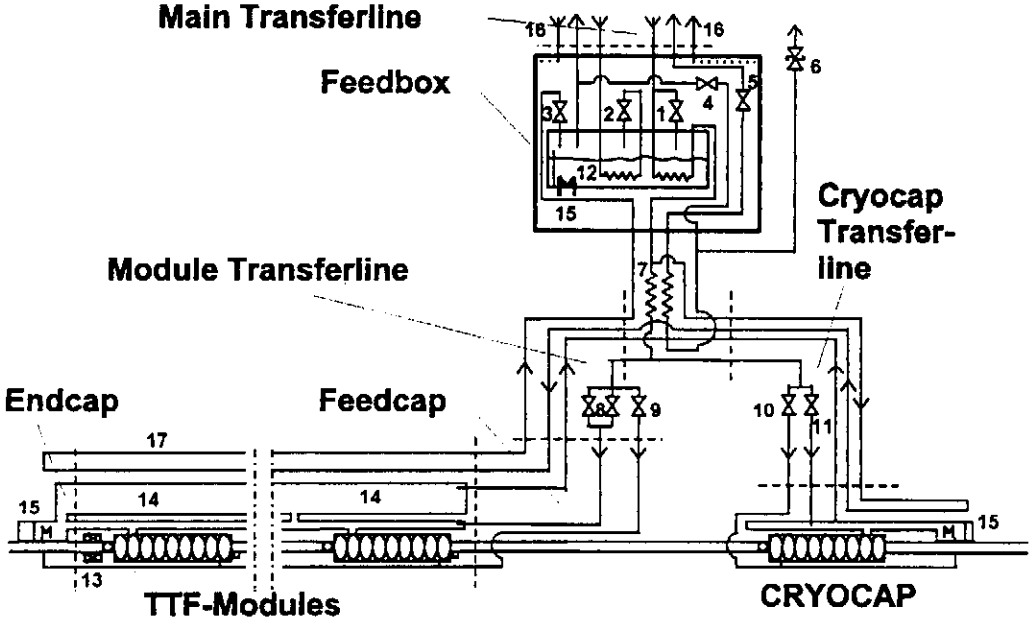

Figure 1. Simplified flowscheme of the cryogenic supply of the TESLA Test Facility.
(1) 5 K supply Joule Thomson (JT) valve, (2) 7.5 K supply JT-valve (from large heat exchanger), (3) 4.4 K return JT-valve, (4) cool down bypass valve, (5) 1.8 K return isolation valve, (6) relief valve system, (7) low temperature heat exchanger, (8) 1.8 K supply JT-valves, (9) cool down bypass valve, (10) cool down bypass valve, (11) 1.8 K supply JT-valve, (12) subcooler, (13) module quadrupole, (14) ∅ 300 mm module return tube, (15) liquid level sensor and heater, (16) 70/80 K thermal shield supply (details not shown), (17) 4.4 K thermal shield.

the liquefaction mode of the plant will be changed into refrigeration mode by means of an additional large heat exchanger . The heat load capacity at 1.8 K will thus be enhanced from about 100 W to 200 W .

VACUUM COMPRESSOR SYSTEM

The vacuum pumping assembly is designed to meet the demands of all phases of the TTF project. For helium mass flows in the range of 0.2 to 10 g/s the pressure can be regulated from 10 mbar to 30 mbar with a relative stability better than 1 %. For mass flows lower than 10 g/s the pressure can be lowered to about 1 mbar.
Although cold compressor systems for this pressure range and mass flows up to 10 g/s are available, warm vacuum compressors were chosen for the TTF due to their flexibility and simplicity of operation. After crossing low temperature heat exchangers and a gas heater in the first stage or a large low pressure heat exchanger in the second stage the helium gas is at a temperature of more than 253 K before entering the vacuum compressors.
As shown in fig. 2 the vacuum compressor system consists of four stages. At the low pressure end the gas is compressed by two roots blowers (LEYBOLD RA 16000) in parallel followed by two stages of single roots blowers (RA 13000/RA9001). All roots blowers are dry pumps, only the bearings are oil lubricated. In the last stage four rotary vane pumps (LEYBOLD SOGEVAC 1200) in parallel feed the gas back to the main gas circuit of the helium refrigerator at a pressure of 1.05 to 1.3 bar, which corresponds to the suction pressure of the screw compressors.
The helium mass flowrate is measured at room temperature by one of two parallel flowmeters at the outlet of the vacuum compressor assembly.
Under full stationary load the maximum electrical power consumption does not exceed 150 kW (with 340 kW power installed).
All pump stages are separated by gas coolers. The rotary vane pumps are cooled in addition by oil/water heat exchangers . The oil contamination of the gas is lower than 60 ppm at the

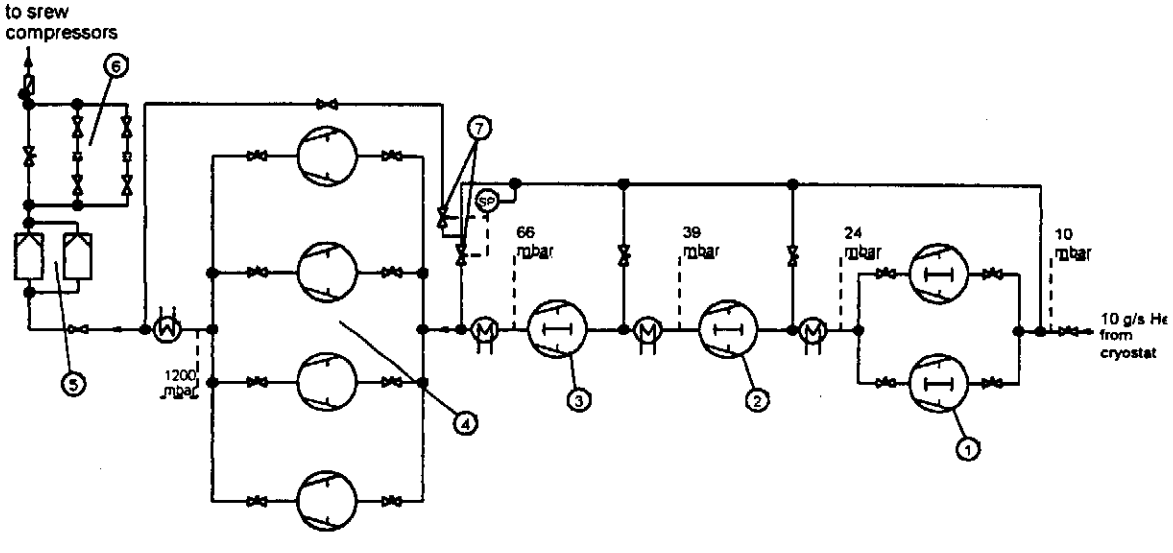

Figure 2. Vacuum compressor assembly. The vacuum compressor assembly consists of two parallel RA16 000 (1), one RA 13000 (2), one RA 9001 (3) rootsblowers and four parallel SV 1200 rotary vane pumps (4), a set of oil filters (5), warm mass flowmeters in the range 0 - 2 g/s and 2 - 20 g/s (6) and two bypass valves (7). Pressures are indicated for the nominal inlet pressure of 10 mbar and maximal massflow of 10 g/s. (Simplified flow scheme)

outlet of the rotary vane pumps and is further reduced to <1 ppm by additional filter elements to avoid any risk of oil condensation in the cold parts of the refrigerator. Breox B 35 oil is used in all vacuum compressors as well as in the screw compressors of the refrigerator.

The suction pressure of the vacuum compressor assembly is regulated by two bypass valves in parallel to the rotary vane pumps and the roots blowers respectively.
The whole system is operated by an internal process control system (SIEMENS SIMATIC S5) which communicates with the process computer of the refrigerator. With the desired suction pressure set, the system reacts to changes of mass flow and pressure by operating the bypass valves and switching pumps on and off.

The vacuum compressors are housed in an extra building attached to the TTF-experimental hall but separated by its own foundation with a distance of about 20 m to the test linac. The beam of the linac will be extremely sensitive to any kind of external vibrations. To avoid vibrations as far as possible, the frame of the vacuum compressors is separated from the floor by special damping elements (BARRYMOUNT SLM) in addition, resulting in more than 90 % damping of the vibrations . (The RMS oscillation velocity of 2 mm/s at the frame is reduced to less than 0.1 mm/s at the floor).
The complete vacuum compressor assembly was designed and constructed by the LEYBOLD AG in Germany and delivered to the TTF-collaboration in time and on schedule.

After the vacuum compressor assembly had passed initial acceptance test on the manufacturer's side and at DESY and an operational test of 1000 hours without severe failures the plant has now reached about 4000 hours of operation.

VERTICAL DEWAR

The vertical test dewar has a depth of 3.8 m and an inner diameter of 0.6 m. During the RF tests of 9-cell cavities the dewar is filled with 620 liters of liquid helium at a temperature of 1.8 K.
The vertical test dewar consists of the dewar itself, the outer vacuum vessel with a thermal shield cooled by liquid nitrogen and the top plates. The supply and return tubes, cryogenic valves and the low temperature heat exchanger are installed outside the helium dewar and inside the outer vacuum vessel, leaving free all space inside the helium dewar for the cavity insert, the RF connections and the vacuum equipment. The transferlines including the vacuum insulated helium pumping tube are welded to the outer top plate of the dewar. A more detailed description of the vertical dewar can be found elsewhere [3]. The dewar has been designed and built at FERMILAB.

Helium of about 4.4 K and a pressure of 1.2 to 3 bar is supplied by the 900 W plant, precooled by a low temperature heat exchanger to about 2.2 K and expanded via a Joule-Thomson valve into the helium dewar. The operation of the JT Valve is controlled so as to keep the liquid level constant during steady state operation. The vapor pressure of the liquid helium bath is lowered to a pressure of 16 mbar by means of the vacuum compressor system. The helium is pumped through the low temperature heat exchanger, the collecting box and the helium heater.

The helium dewar and the insert are equipped with several temperature sensors, a level sensor and pressure gauges. Additional heat load of up to 100 W can be supplied by an electrical heater in the bath. This heater can be used complementary to the changing RF-Power to obtain constant heat loads and more stable conditions.

For the performance tests different helium massflows were adjusted by the heat load of the electrical heater in the helium bath. The liquid helium level was kept constant at a reading of 95 % of the level sensor (this means that a 9-cell cavity is covered with about 20 cm of liquid at its top end). Each setpoint was maintained for several hours to insure stationary thermal conditions.
In fig. 3 the maximum obtainable extra heat load as well as helium bath vapor pressures are plotted versus the pumped helium massflow at 9.5 mbar and 5 mbar pressure setpoint at the vacuum compressors. For a vapor pressure of 16 mbar (1.8 K) the maximum extra heat load turns out to be about 79 W at a setpoint of 5 mbar at the vacuum compressors (about 40 W at a setpoint of 9.5 mbar).

Heat loads in the vertical dewar as well as in CHECHIA can be obtained from the measured liquid level drop while the supplies are closed, or from the absolute pumped helium massflow measured at constant liquid level of the helium bath. Using the second method, it has to be taken into account that a fraction of the pumped massflow is caused by the quality of the fluid at the JT-expansion. This quality can be calculated from thermodynamic state functions if temperature and pressure of the helium in the supply of the JT-valve is known.

The total heat loss results from the static heat loss of the helium dewar including the cryostat insert (cavity, waveguide, couplers, vacuum tubes, supports and cables), thermal radiation and thermal conduction across the helium vessel and the tubing connected to the vessel, and the extra heat loads due to RF operation of the cavity (or the electrical heater): During continuous wave RF operation of a nine cell cavity in the vertical dewar the Q_{RF}-value was calculated from the corresponding heat loss measurements in the helium bath.

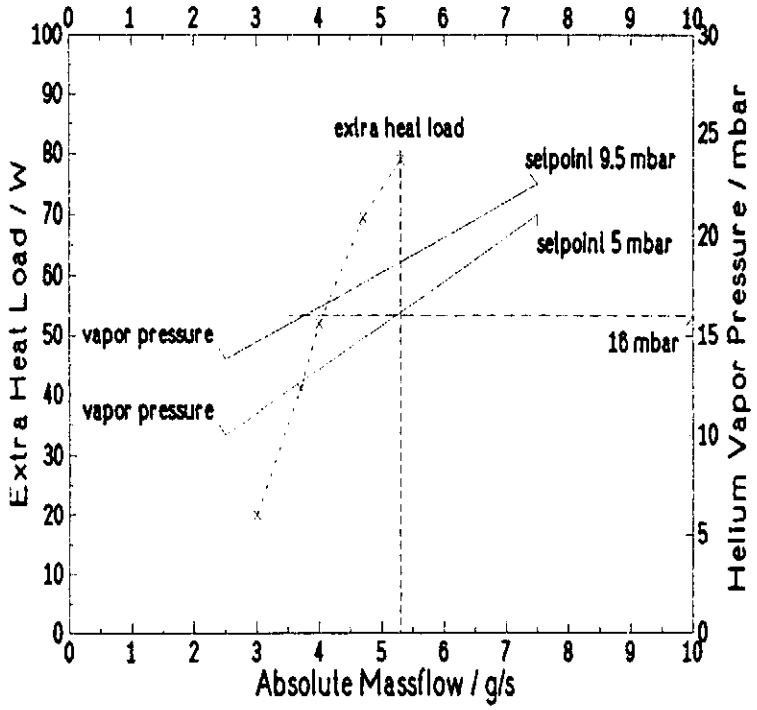

Figure 3. Vertical dewar cryogenic performance. The helium vapor pressures of the vertical dewar and the external heat loads are plotted versus the corresponding helium massflows at two setpoints of pressure at the vacuum compressors. For a given vapor pressure in the dewar the maximum external heat load can be obtained from the diagram. For the design vapor pressure of 16 mbar (1.8 K) 79 W external heat can be applied.

The deviation of the Q_{RF} calculated from electrical measurements to the Q_{RF} calculated from the heat losses is smaller than 10 %. In CHECHIA the Q_{RF} can only be monitored by cryogenic measurements after the main RF coupler has been installed[4].
From the data in fig. 3 a static heat load of 20 - 25 W results for the vertical dewar with a 9-cell cavity if the liquid helium level is in the range of 95 % . This static heat loss can be lowered to about 10 W if the level is decreased further. With a maximum of about 80 W for continuous RF cavity heat load left at 1.8 K, there is enough cryogenic capacity for all RF measurements, HPP preparation and temperature mapping. In addition, was demonstrated during the first cw-tests of the 9-cell prototype cavities that the regulation system will return to stable operation even if heat loads up to 300 W are transferred into the helium bath for some seconds. With minor changes in the design, a second vertical test dewar is under construction at Fermilab.

The continuous supply of helium into the dewar resulting in a constant helium level during the subatmospheric operation has some important advantages in comparison to the more common method of lowering the level during pumping on a helium bath: the time to test superconducting RF cavities at 1.8 K is not limited by an emptied helium bath and about one meter of cryostat length corresponding to about 200 l of liquid helium could be saved. Detailed results of heat loss measurements of the CHECHIA cryostat are presented in a separate paper at this conference[4].

MAIN TTF TRANSFERLINE

For the cryogenic supply of the TTF-linac a 6-fold 100 m transferline is required to connect the 900 W refrigerator, the helium heater (stage I) or a heat exchanger (stage II) and a feedbox close to the first TTF module cryostat. This transferline has been designed and is under construction now at the DEMACO company in the Netherlands. Fig. 4 shows a cross section of this transferline. At the 70 K level 2 W/m and on the 4.4 K level 0.2 W/m are specificated for the overall heat losses of the transferline.

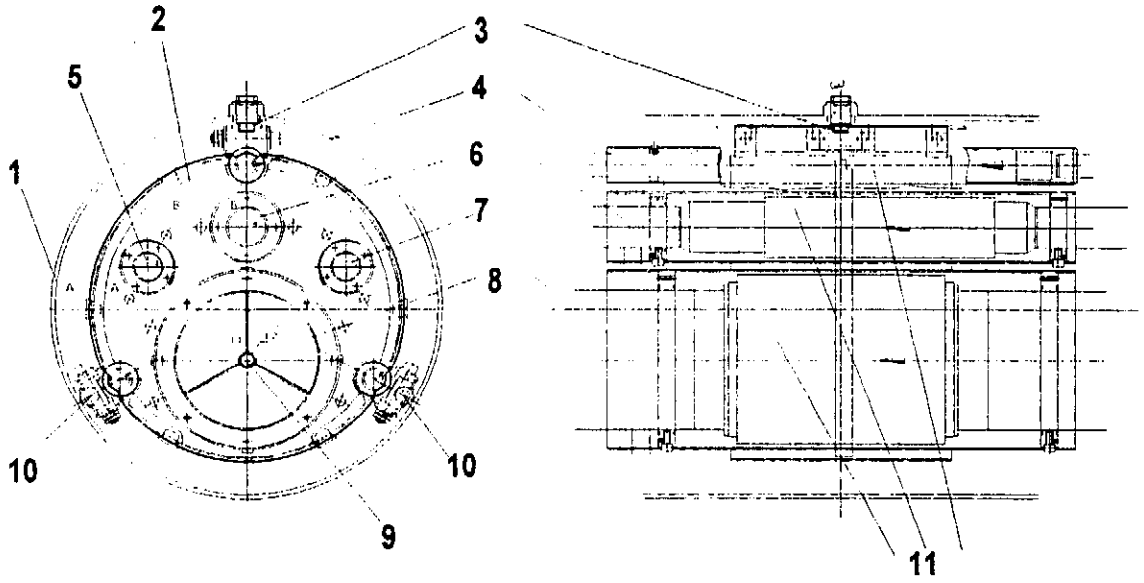

Figure 4. Cross section of main transferline. (1) Vacuum vessel, (2) 80 K thermal shield, (3) glass fiber reinforced plastic (GFRP) suspension, (4) 80 K return tube, (5) 70 K supply tube, (6) 4.4 K return tube, (7) 5 K supply tube, (8) 3.5 K / 16 mbar return tube, (9) 7.5 K supply tube (from large heat exchanger), (10) moving supports, (11) tube compensators.

TTF FEEDBOX

The feedbox is needed to branch the 70 K, 4.4 K and 1.8 K helium circuits to the first module cryostat and CRYOCAP. The simplified flow scheme of the feedbox is shown in fig. 1. In addition the 4.4 K has to be recooled in the feedbox to get stable conditions for both the 4.4 K shield of the modules as well as for the JT-supply of the 1.8 K bath. The return gas from the 4.4 K shield of the modules is expanded via a JT-valve into the liquid bath of the subcooler. After the installation of a large low pressure heat exchanger in the second stage 7.5 K/14 bar helium coming from this heat exchanger will also be preecooled to about 5 K and than be expanded into the subcooler bath. The low temperature heat exchanger for the supply of the modules is attached to the feedbox. The feedbox has been designed and is under construction at FERMILAB.

MODULE TRANSFERLINES, FEED & END CAPS

Transferlines from the feedbox to the first module (8 m) and to cryocap (3 m) include JT-valves and bypass valves for cool down and warm up (see fig. 1) . By means of flexible hoses only small transversal forces will act on the suspensions of the module cryostat. A sketch of the feed cap connection to the first module is shown in fig. 5. The flanges of feed and end cap have to support 14 000 kg vacuum force. The end flanges are equipped with feedthroughs for optical alignment and a stretched wire monitor system. The module transferlines and the feedcap are designed and constructed at DESY and the endcap at INFN.

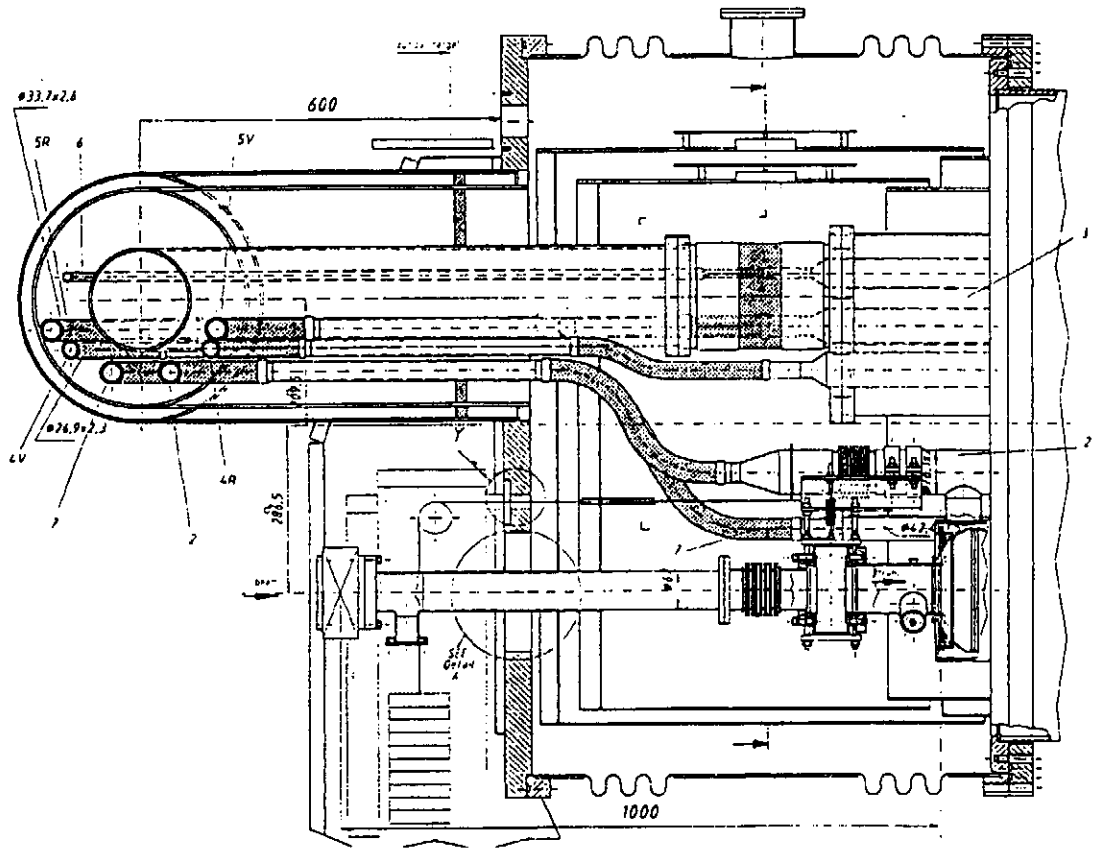

Figure 5. The connection of the module transferline to the first TTF-module (feedcap)

LARGE LOW PRESSURE HEAT EXCHANGER

To increase the cooling capacity from about 100 W to 200 W at 1.8 K for the later supply of the complete test linac, the enthalpy of the low pressure gas has to be transformed to a pressure and temperature level which can be used in the cryoplant by means of a Large Low Pressure Heat Exchanger.
In this heat exchanger incoming warm 14 bar helium gas is cooled to a temperature of less than 7.5 K by the counterflow of low pressure gas which enters the heat exchanger at a temperature of about 3.5 K.
At a maximum mass flow of 10 g/s of the low pressure gas the high pressure mass flow has to be tuned to the performance of the heat exchanger resulting in a mass flow of about 9 g/s. The high pressure gas is expanded via a JT valve into the subcooler of the TTF-feedbox (see fig. 1). The high pressure gas flow rate is controlled by the gas temperature in the supply of this JT valve.
At a low pressure mass flow of 10 g/s a pressure drop of only 3 mbar can be allowed, a large thermal stress due to the high temperature gradient is expected. The performance of the heat exchanger will be seriously affected by internal heat flow along the tubes. A small gas heater of 1.5 kW at the warm outlet of the low pressure flow is added to give more flexibility.
The Large Low Pressure Heat Exchanger is installed into a vacuum isolated box, separated from the 4.4 K Cold-Box and from the feedbox of the test linac. IHEP Protvino is in charge for the design of the heat exchanger which will be built in Russian industry.

CONCLUSION

The cryogenic system for the TESLA Test Facility is well underway. The first vertical dewar and CHECHIA have been successfully operated. A second vertical test dewar, the TTF feedbox, main transferline, module transferlines, feedcap and endcap are to be delivered by the end of 1995. Delivery of the large low pressure heat exchanger is planned for summer 1996. Cryogenic operation of the first part of the TTF Linac (first module and CRYOCAP) is expected in the first quarter of 1996.

REFERENCES

1. Horlitz, G., et al.,'A 1.8 K Test Facility for Superconducting Rf Cavities', Adv. in Cryogenic Engineering, Plenum Press, New York, 1993, Vol. 39 , (Proc. of the CEC/ICMC Conference 1993 in Albuquerque, N.M.)
2. Grygiel, G., et al., 'A 1.8 K Test Facility for Superconducting RF Cavities', TESLA-COLLABORATION, TESLA 94-08, April 1994
3. Nicol, T.H., et al, ' TESLA Vertical Test Dewar Cryogenic and Mechanical Design', IEEE Proceedings of the 1993 Particle Accelerator Conference, Vol. 2, pp. 989-991, Piscataway, N.J., 1993
4. Duthil, R., et al.,' Cryogenic and Electrical Test Cryostat for Instrumented Superconductive RF Cavities (CHECHIA)', Adv. in Cryogenic Engineering, this conference
5. Buhler,S.,'Status Report of the TTF Capture Cavity Cryostat', Adv. in Cryogenic Engineering, this conference
6. Nicol,T.H.,' TESLA Test Facility Cryostat Design', Adv. in Cryogenic Engineering, this conference
7. Alessandria,F., et al.,'Design,Manufacture and Test of the TESLA-TTF Cavity Cryostat', Adv. in Cryogenic Engineering, this conference

Presented at the CEC/ICMC ConferenceColumbus, Ohio USA, July 17-21, 1995
Revised on September 20, 1995 for publication.

A NOVEL ROTATING TEMPERATURE AND RADIATION MAPPING SYSTEM IN SUPERFLUID He & ITS SUCCESSFUL DIAGNOSTICS

Q. S. Shu[1], T. Junquera[2], , A. Caruette[2], G. Deppe[1], M. Fouaidy[2]
W-D. Moeller[1], M. Pekeler[1], D. Proch[1], D. Renken[1], C. Stolzenburg[1]

[1]Deutsches Elektronen-Synchrotron (DESY)
Notkestrasse 85, 22607 Hamburg, Germany
[2]Institute of Nuclear Physics
(CNRS - IN2P3) 91406 ORSAY cedex, France

ABSTRACT

An novel rotating temperature and radiation mapping system in He II has been developed to investigate field emission (FE) & thermal breakdown (TB) in TESLA 9-cell SRF cavities. More than 10,000 spots on a cavity surface can be analyzed in one turn with 5° stepping. 116 special surface scanning thermometers have been developed to measure surface temperature in He II. 32 photodiodes are employed to study the X-rays induced by FE electrons. Each rotating arm holds 14 thermometers and 4 photodiodes. A unique driving and suspension system is designed to gently turn the 9 arms around the cavity and uniformly press the thermometers against cavity surfaces. A moving adapter device (pancakes) is designed for rotating a large number of electronic cables which become inflexible in superfluid He.

The T-R mapping system has successfully detected and diagnozed serious problems caused by FE and TB, and has played a significant role in cavity processing.

INTRODUCTION

Main Obstacles of High Gradient Cavities

Field emission (FE) and thermal breakdown (TB) are still the main obstacles preventing SRF cavities from confidently reaching Eacc = 25 MV/m (TESLA's goal) from existing operating levels of 5-10 MV/m[1,2,3]. Most of the FE sources and TB defects on the inner RF surfaces of cavities were found to be submicro-sizes [4,5] and activated only at high RF fields while cavities are in a superconducting state. It is impossible to directly observe the FE and TB on the inner surface of cavities during RF operation. Therefore, the main approach to understanding the FE and TB of cavities is to study the hot spots and X-rays (induced by impacting FE electrons) generated on the cavity surfaces during RF operation.

DESY's Rotating T-R Mapping System

Various temperature (T) mapping and X-ray (R) mapping systems have been developed at many laboratories around the world[3,4,6,7,8]. The systems can be classified

into two categories: (1) Fixed Mapping - thermometers or photodiodes are fixed on the surfaces of the cavity. (2) Rotating Mapping - thermometers or photodiodes are rotating against the surfaces of the cavity.

The Rotating T-R mapping system developed at DESY for TESLA 9-cell cavities combines measurements of T & R and employs special rotating scanning thermometers which were developed at INP Orsay.

Advantages.

(1) Greatly reduce the number of sensors: The DESY T-R mapping analyzes 10,000 spots on the cavity surface using only 116 scanning thermometers. A stystem using fixed thermometers would require 10,000 thermometers to analyse the same spots on cavity.

(2) Once an area is suspected, the sensors in DESY mapping system can be relocated to the suspect location during cryogenic-RF operation for additional analysis.

(3) The mapping combines T-R diagnostic systems to give information on both heating and x-rays for understanding the dynamic progress of cavity processing.

Challenges.

(1) Fixed contacts and use of grease as bounding agent to enhance thermal contact between thermometer and surface being measured are essential to reach a high efficiency (particularly, in the case of He II). In a rotating system, neither fixed contact nor grease can be applied. A new type of thermometer was needed[9].

(2) Due to TESLA cavity structure, thermometers can not reach the high risk areas of FE at cavity irises. A combined measurement of T & R was required.

(3) The TESLA cavity has 9 cells (the largest cell number for low frequency cavities) with complex surface curves. The space in the cavity test cryostat is tightly constrained. Assuring satisfaction of 3-dimension tolerances at all moving contact points is a challenge.

(5) A fast data acquisition system was also needed to trace the dynamic progress.

We have overcome the above challenges and developed the rotating T-R mapping system. Since December 1994, the system has been successfully employed in diagnostic tests and played a significant role in cavity processing[10].

TECHNOLOGIES DEVELOPMENT

Surface scanning Thermometer and Photodiode

The surface thermometer design as shown in Figure 1(A) is very close to the model developed earlier for the CERN's SRF cavity project by INP Orsay[10,11,12]. The sensitive part is an Allen-Bradley carbon resistor (100 Ohm, 1/8 W) housed in a silver block with a sensor tip of 1 mm diameter for the thermal contact to the external surface of the cavity. This housing is thermally insulated from the surrounding He II by an epoxy envelope (Stycast) moulded around the silver block and into a bronze piece which allows the sensor

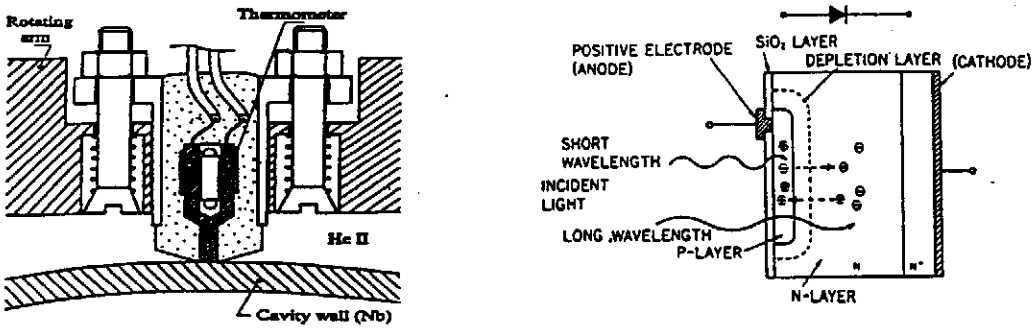

Figure 1 (A) Cross section of a HeII surface scanning thermometer, (B) cross section of a photodiode

to be mounted in the rotating thermometric arm. The thermometer's tip must present a good contact with the cavity wall when scanning. Each thermometer has two independent manganin wires thermally anchored to the silver block with ~ 15 cm free length for connecting to each cell board (14 thermometers).

The complementary calibration test was performed by mounting the thermometers in the real operating conditions of the scanning device at different spring pressures and heat fluxes in He II and subcooled He (2.3K and one bar). The detailed results are presented in another paper[9]. In the case of He II, the efficiency is heater power dependant.

Commercial PIN silicon/S 1223-01 photodiodes are used as x-ray detectors in the mapping because of their small size (3mm x ϕ10 mm) and ultra-fast response. A simplified photodiode cross-section is shown in Figure 1(B).

Rotating T-R Arms

As shown in Fig. 2, 14 thermometers and 4 photodiodes are mounted in each arm which is precisely machined to have the same curved surface as the cavity cell. Due to the reinforced structure of TESLA cavity, the thermometers can not directly touch the surfaces of the cavity iris. Considering that the electrical fields reach maximum at the iris, 4 photodiodes are located in the end of each arm to monitor FE induced X-rays while 14 thermometers are used to monitor the temperatures in the entire region between the irises of each cell[13]. Two springs located inside two holes in the body of the rotating arm are used to adjust the contact pressure. A printed circuit board is mounted on the side of the arm. All cables for the sensors are fed through a device, called moving adapter device or "pancakes", and then connected to a feedthrough on the top flange of the cryostat. Fig. 3 is the T-R mapping system.

Driving and Suspension Frame (DSF)

A total of 116 surface scanning thermometers (14x7 + 9x2)[13] and 32 photodiodes are assembled into 9 rotating arms which are mounted in the DSF as shown in Figure 4 (A). The most important consideration in the mechanical design is to assure the three dimension tolerance between the cavity surface and the tips of the 116 thermometers over the entire

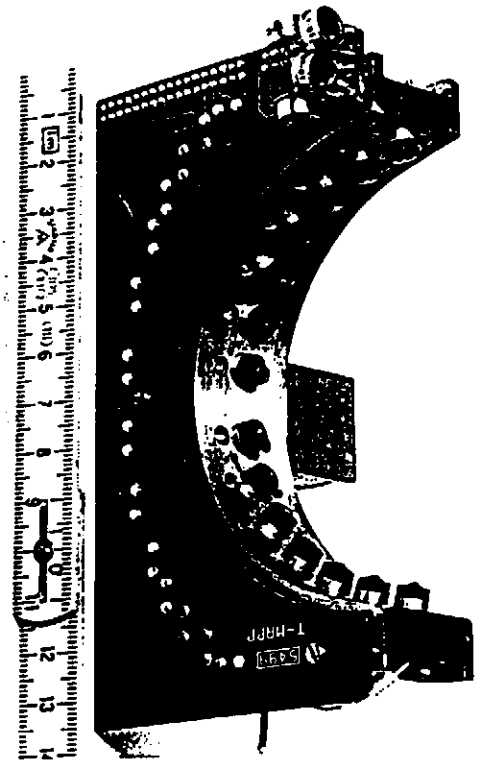

Figure 2. A picture of the rotating arm.

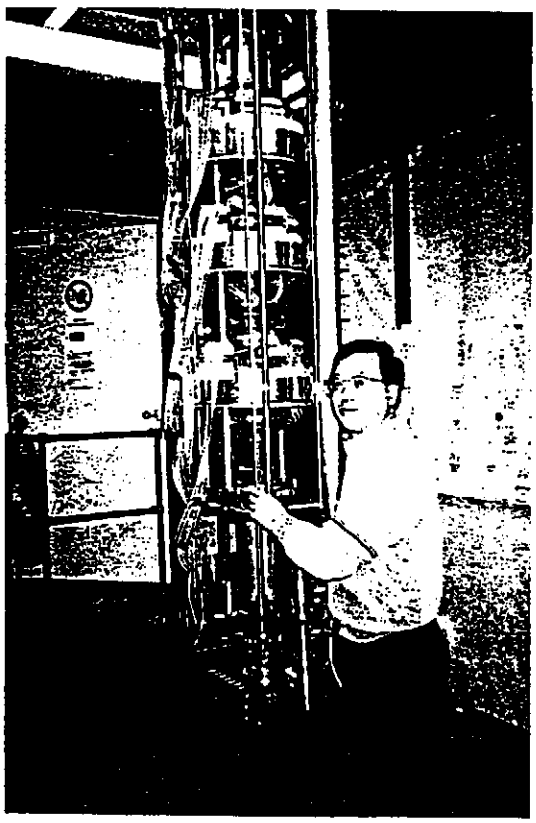

Figure 3. A picture of the T-R mapping system

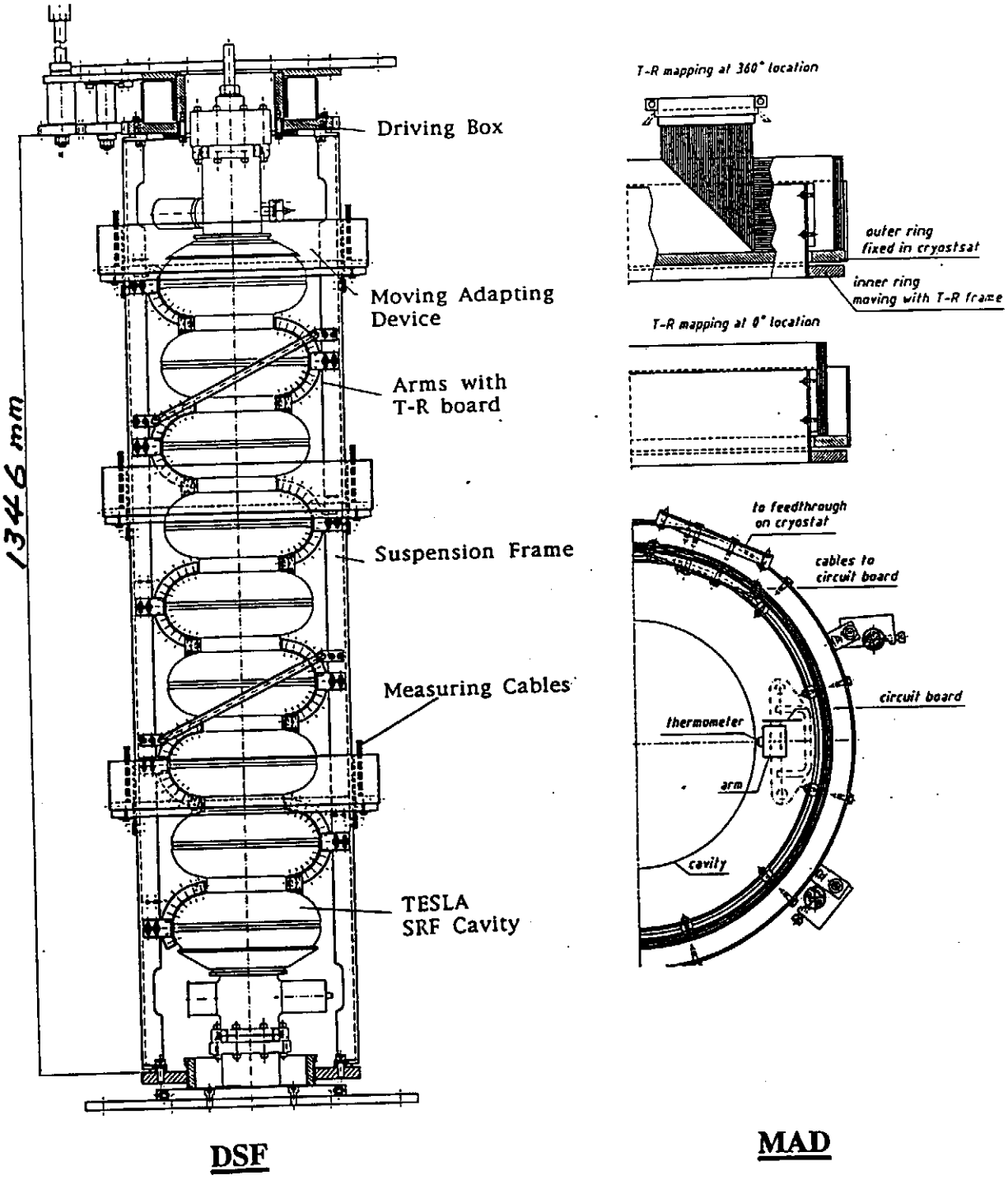

Figure 4. Schematic cross sections of the DSF and MAD

cavity surface (i.e. more than 10,000 points) are within ±1mm. The DSF has two centering rings to allow the axis of DSF as close to the axis of the cavity cells as possible.. The rotating frame is suspended on two disks made of low friction materials. These structures enable the DSF in superfluid He to gently turn the arms around the cavity and uniformly press the thermometers (through the spring-holder structure, force=100 g per thermometer) against the cavity surfaces. Driven by a computer-controlled stepping motor, the T-R arms can be automatically turned to any position on the cavity surface with a accuracy of ±1 degree.

Moving Adapter Device (MAD)

A large number of electronic measuring cables have to move with the rotating arms when the T-R mapping rotates. These cables become very rigid in LHe. A moving adapter device[13] was successfully designed to overcome the problem as shown in Figure 4 (B). Each pancake has two rings. The inner ring is mounted in the moving DSF and turns with the DSF around the cavity. Its outer ring is fixed with cavity supports. One end of each 64-wire-cable is connected to the inner moving ring and the cables make 9 turns around the inner ring of the MAD while the other end of the cables connects to the outer fixed ring. When the DSF turns 360° around the cavity, the cables only make relatively short movement inside the MAD. The space in the TTF vertical cryostat is very constrained which makes the MAD design even more difficult. The MAD has been tested and functions well in many cavity experiments.

Fast Data Acquisition and Test Procedure

Two Ge-thermometers and three additional scanning thermometers are used to monitor the change of bath temperature during measurement. To check the photodiodes two small lights are placed in the DSF. Maps can be taken with auto-scanning of entire cavity surface or scanning with time in a fixed position. The temperature change ΔT is made by comparison of measurements of RF power on and off (also, the bath temperature changes are subtracted from the total ΔT). The effective resolution of temperature measurement is less than 5 mK. One longitudinal measurement in a fixed angular position can be completed in less than 10 ms. All data taken, control and display are performed through a multiplexer by a Sun-station computer with a LabView™ language program[14].

RESULTS, ANALYSIS & DIAGNOSTICS

The T-R mapping has been successfully employed in the diagnostic testing of TESLA SRF cavities. We will briefly introduce some of the more interesting results here. A detailed test report will be presented in the "1995 SRF Superconducting Workshop".

Detection of Thermal Breakdown

We use the TESLA 9-cell cavity (D-6) as an example shown in Figure 5. This cavity has been heat treated with Ti-purification at 1400° C for 4 hrs and a test sample has a RRR of about 500. At first, the cavity was limited by severe FE at Eacc = 4 MV/m and Q dropped to 8×10^7, Fig. 5 (A). With RF power processing, the FE events were eliminated and the T-maps show the heating areas by FE gradually disappeared. Finally the cavity reached Eacc = 12.5 MV/m through a high RF pulse peak power processing (HPP) and then limited only by a quench.

While scanning the entire surfaces of the 9-cell cavity, the T-mapping located a strong heating area centred at the equator of the cell-5 over 10 thermometers between the 10° to 50° longitude as shown in Fig. 5 (C). To further study the TB event, we relocated the T-R arm to the heating area, moved it by 5° angular steps and found the hottest spot to be near 35°. Finally we moved the arms to 35°, turned on the RF power in CW mode and observed continuing quenches and recoveries of the cavity as shown in Fig 5 (B). Simultaneously, we continuously took temperature measurements at this fixed location. Fig. 5 (D) shows a dynamic progress of the temperature changes at 35° as a function of time. The highest temperature measured on the outer surface of the cavity is above 5 K and the quench was limited to one cell and did not propagate to adjacent cells.

These results indicate that HPP is very effective in eliminating FE[15], but not for TB. The tests tell us that there may be a combination of local defects at cell-5 and existence of a low thermal conducting thin layer (due to Ti-purification) on the cavity. Optical observation after test showed a deep scratch on the inner surface near the equator and close to 35° of cell-5 . We are planing to take an additional 50 μm of material from the inner surface and test it again.

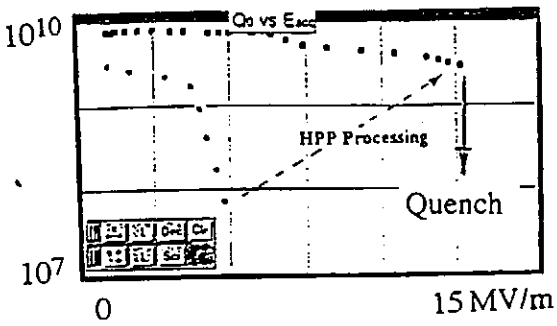

(A) Overall performance of the 9-cell cavity D6.

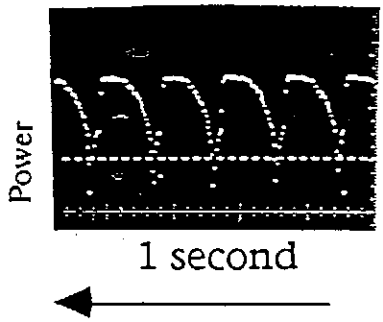

(B) Oscilloscope traces of transmitted power during continuing TB (quench) of the cavity.

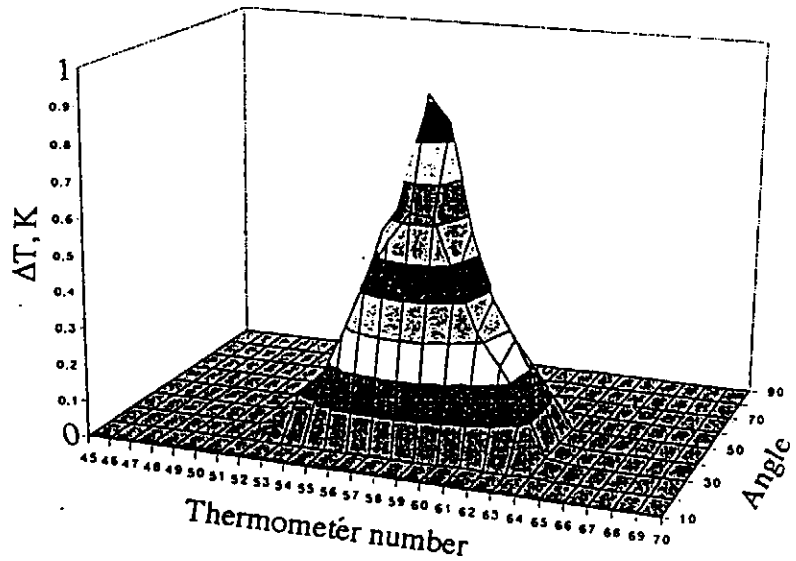

(C) The detected heating area due to TB (quench) at the equator of the cell-5,

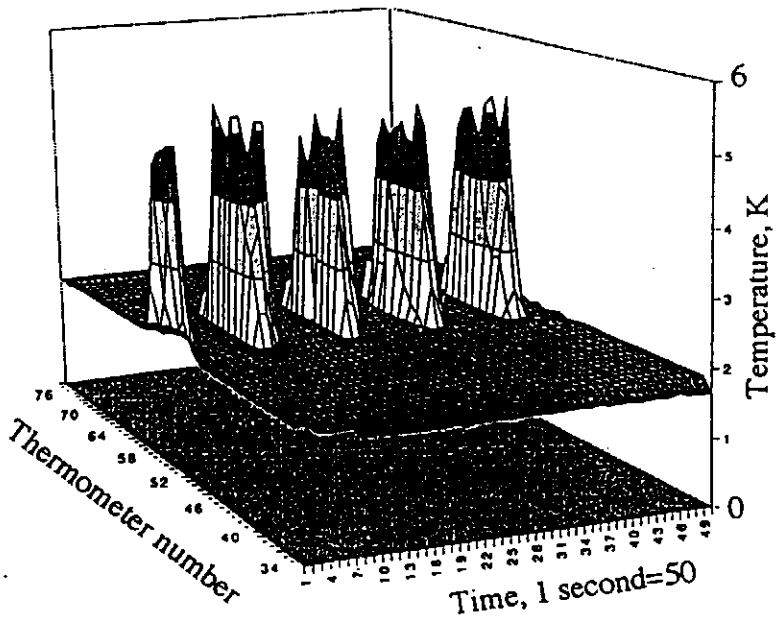

(D) Temperature changes as a function of time at longitudinal of 35° of the cell-5 during continuing quench & recovery.

Figure 5. The dynamic progress of a cavity thermal breakdown (quench) detected by the T-R Mapping.

Identification of FE Heating and Emitter Location

In investigating FE, we first use T-R mapping to identify the landing areas of FE electrons and then find out the locations of emitters with simulations of FE electron trajectories. we use a TESLA prototype 9-cell cavity (-1) as an example. It has reached 20 MV/m as shown in figure 6 (A). Previously, cavity -1 had been limited by thermal breakdown at about Eacc = 10 MV/m. Afterwards, the cavity -1 was heat treated at 1400° C with Ti-purification. We then removed 80 μm of material from the inner RF surface and 30 μm from outer side by chemistry, followed by high pressure rinsing.

Locating of Heated Areas and Intensity

In the test, cavity -1 was initially stopped by heavy field emission at point A (figure 6) at 11.2 MV/m with a Q of 8.5×10^8. The T-map, figure 6 (B) indicates an important heated region delimited by 12 thermometers (#53 to #64) centred close to the equator of the 5th cell, between the 110° to 200° angles. Outside of this region the heating is very low. The ΔT value in this region is 100mK - 3.3K. The y-axis of figure 6(B) is the thermometer number from 0, close to the top iris of cell-1, to 116, close to the bottom iris of cell-9. The x-axial represents the angular location on the cavity surface.

Analysis of Thermal Performance

The experimental data obtained with the T-R mapping is consistent with the thermal analysis if we make the following assumptions: high efficiency of thermometer at high heat flux, heat transfer governed by Kapitza regime, and electron trajectories impacts over a large area. The magnetic field heating at equators of the 5th cell, for Eacc=11.2 MV/m and Rs=30 nΩ, gives only ΔT=5 mK. The power related to the electron FE, Pelec=173 W, is focusing on local region.

The very high value ΔT measured in this region (100mK-3.3K) can only be explained by assuming that the efficiency of a scanning thermometer increases strongly with the heat flux density at the interface between the cavity wall and HeII. Such a high heat flux density is slightly less than the critical heat flux densities reported in experiments with metallic flat heaters in HeII[16]. So it is believed that the heat transfer is in the regime governed by Kapitza conductance. The integration of the product of Kapitza conductance and ΔT over the heated region leads to a total heat power going to He bath: Q~100 W. This value is consistent with the RF measurements of the experiment.

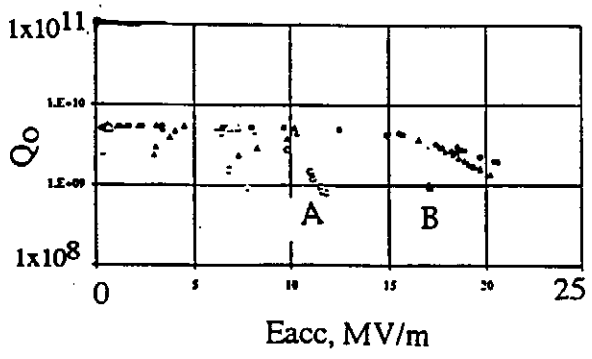

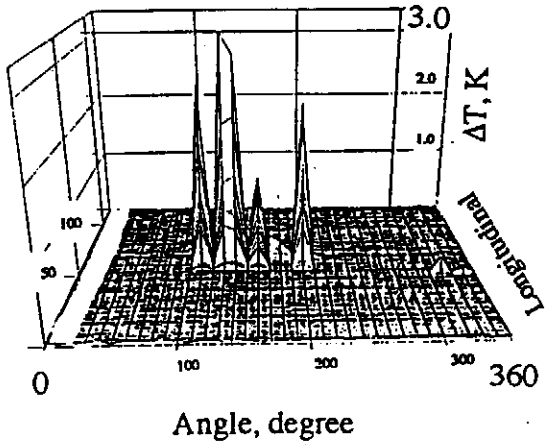

Figure 6. (A) Overall RF performance of the TESLA cavity -1.

(B) FE heating area responsible for the Q dropping and limit of Eacc

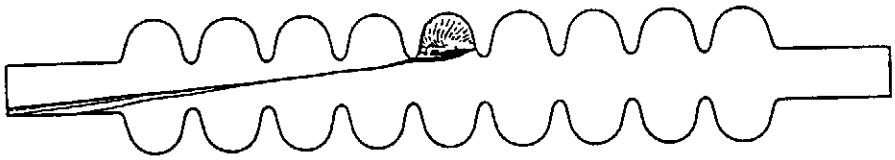

(A) FE electron trajectories of the emitter located at So = 8 cm and the emitter is responsible for the Q degradation.

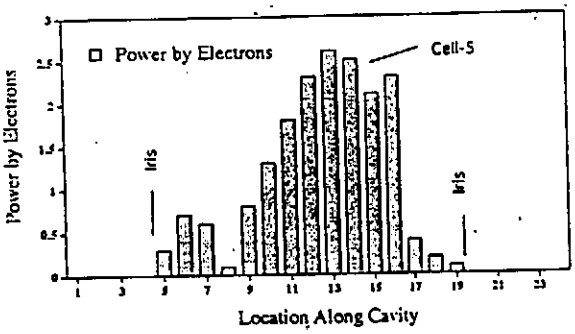

(B) Power distribution contributed by impacting FE electrons from So = 8 cm.

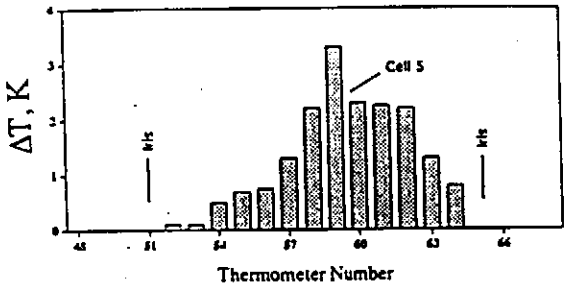

(C) Experimental longitudinal ΔT plot from T-map data of Figure 6 B fixed at 140°.

Figure 7. A comparison of computer simulation of the FE emitter with the experimentally heated areas.

Identifying of FE Emitter Location

Locating origins of FE and TB is very important to understand the influence of various cavity processing and also to a guided reparation of defected cavities. However, the measured hot spots only indicate the landing of impacting FE electrons, but not the emitter.

The simulation of FE electron trajectories demonstrate the following interesting results: FE electrons from an emitter can impact over a very large area, the shape of trajectories are sensitive to emitter location (So), and emitters responsible for the heating areas (shown in figure 6 B) can be successfully identified. Since electron trajectories, impacting electron energy and power deposition distribution (dP/ds vs. s) are controlled by the Eacc and So. A series of simulations are performed by changing So at Eacc=11.2 MV/m, assuming emission enhancement $\beta = 200$, Se (emitter area) = $1 \times 10^{-13} m^2$. It is found that an emitter located at So=8 cm (at the iris area) has electron trajectories shown in figure 7 (A). Its power distribution (dP/ds vs. s) in Figure 7 (B) seems to be very close to the shape of the measured temperature distribution, Figure 7 (C). It indicates that heated areas at the equator (usually by defects) can also be caused by FE. The β and Se of the candidate emitter were adjusted to fit with the thermal analysis and RF experimental data. For instance, at Eacc=11.2 MV/m, if Se=1×10^{-13} m^2, $\beta = 400$, the total mean power landed over RF period is 10W.

Finally, the high pulse RF power processing (HPP) was introduced to the cavity (150KW) and successfully eliminated the field emitters. Another T-map also witnessed the FE elimination. After HPP, the cavity finally reached 20 MV/m in CW mode.

Information from X-Ray Maps

A large number of radiation maps of X-rays induced by FE electrons were also observed. In general, information from X-ray maps are in consistent with that obtained from T-maps. As we mainly discuss the technical areas relevant to low temperature science here, the X-ray maps and analysis will be presented at the 1995 SRF superconducting workshop (Saclay, France). Figure 8 (A) shows an X-ray map recorded during a cavity processing, while figure 8 (B) presents the T-map taken on the same cavity and in the same time.

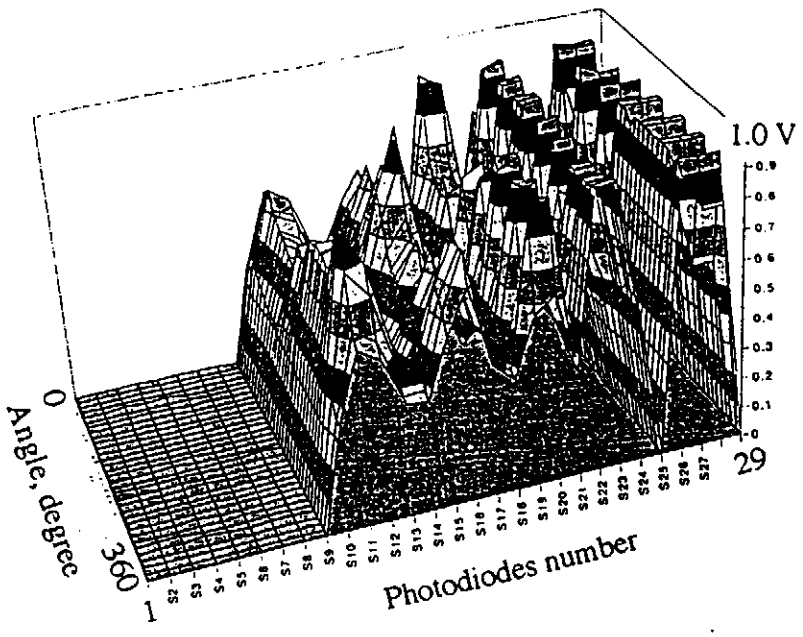

(A) An X-ray map in which the strong radiation closed to the cavity irises.

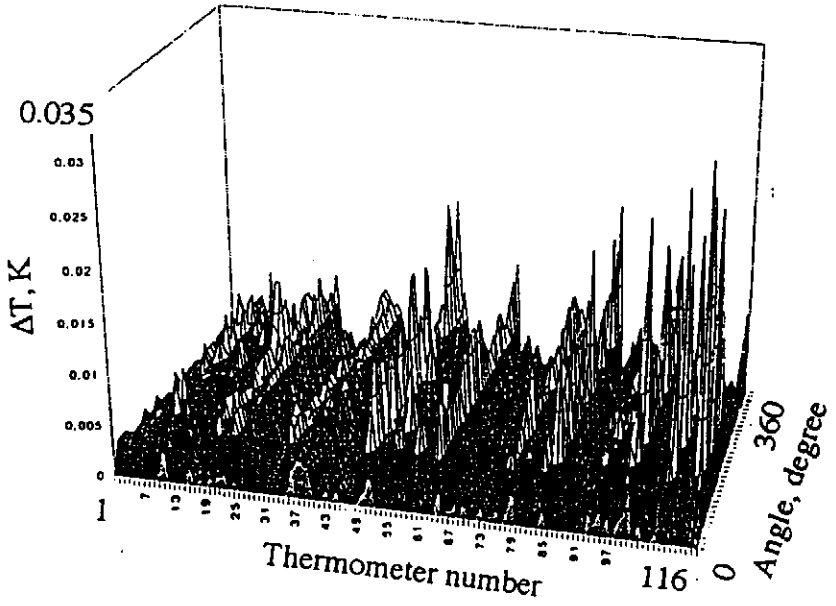

(B) A T-map taken in the same time as Fig 8(A) shows that the FE heated areas are also located mainly in cavity irises.

Figure 8. A comparison of the X-ray map with the T-map in the same 9-cell cavity.

CONCLUSION

The T-R mapping system for TESLA 9-cell cavities was commissioned and successfully analysed and diagnosed the problems with the TESLA cavities caused by FE and TB. The information learned from T-R mapping results has played a significant roles in cavity processing and will be very valuable in further guided reparation of some cavities.

ACKNOWLEDGEMENT

We sincerely thank P. Kneisel (CEBAF), W. Weingarten (CERN), H. Padamsee, M. Champion (Fermilab), C. Pagani (INFN), B. Bonin (Saclay) and G. Mueller, R. Roeth (Wuppertal) for many fresh discussions and hints. Sincere thanks are also presented to our DESY colleagues in the cryogenic group, vacuum group, mechanical group, MHF group for their support.

REFERENCES

1. D. Proch (editor), Procceedings of the 5th workshop on RFS, Hamburg, Aug., 1991. (status report, p5, p23, p37, p44, p84, ans p245) published by DESY.
   R. Sundelin (editor), Procceedings of the 6th workshop on RFS, Newport News, Oct., 1993 (status report, p33, p49, p67, p77, p131, p173) published by CEBAF.
2. H. Pademsee, Applied Supercond. Conf., Boston, 1994.
3. Q.S. Shu et..al., IEEE transaction, Vol. 27, No. 2, 1991
4. B. Bonin et. al., Procceedings of the 6th workshop on RFS, 1993.
5. R. Roth and G. Muller et. al., Procceedings of the 5th (and 6th) workshop on RFS, DESY 1991 (and CEBAF, 1993).
6. Ph. Bernard et. al, Nucl. Inst. & Methods in Phys. vol 190.
   Ph. Bernard et. al. & S. Buhler et. al, the 5th (and 6th) workshop on RFS, DESY 1991 (and CEBAF, 1993).
7. Q.S. Shu et.al., Nucl Inst & Methods in Phys A278. 1989.
   J. Knobloch, et. al., SRF 94-0419-03, Cornell Univ., 1994
8. M. Fouaidy et al Proc 5th workshop on RFS, DESY,1991.
9. T. Junquera et. al. TTP 14, Dallas, TX. PAC/95, May 1995.
10. Q.S. Shu. et. al., TTP 19, Dallas TX. PAC/95, May 1995.
11. R. Romijn, W. Weingarten, IEEE Trans. on Magnetics, Mag. p. 1318, 19 (1983).
12. S. Buehler, et. al., Procceedings of the 6th workshop on RFS, Newport News, published By CEBAF, Oct., 1993.
13. Q. S. Shu, et al. TESLA Weekly Meeting, February, 1995, DESY, Hamburg.
14. M. Pekeler, internal tech. note to be in Ph. D. thesis, 1995.
15. J. Graber et. al., Nucl. Inst. & Methods in Phy. A278. 1989.
16. A. Kashani, S. W. Van Sciver, Cryogenics 25, 1985.

CRYOGENIC AND ELECTRICAL TEST CRYOSTAT FOR INSTRUMENTED SUPERCONDUCTIVE RF CAVITIES (CHECHIA)

P. Clay, [1] J.P. Desvard, [1] R. Duthil, [1] J. Gastebois,[2] G. Grygiel, [3] U. Knopf,[3] R. Lange,[3] F. Lejars, [1] C. Mayri, [1] P. Pailler, [1] B. Petersen,[3] D. Sellmann,[3]

[1]CEA - CE/Saclay - DSM/DAPNIA/STCM
91191 Gif-sur-Yvette Cedex (France)

[2]CEA - CE/Saclay - DSM/DAPNIA/SEA
91191 Gif-sur-Yvette Cedex (France)

[3] DESY - Notkestrasse 85
22603 Hambourg (Germany)

ABSTRACT

This facility has been designed to carry out cryogenic RF quality factor (Q_{RF}) measurements, cold tuner tests, high order modes coupler tests, main coupler tests and full RF tests of superconducting cavities under real accelerator conditions (pulse mode, feedback loops, etc). The cryostat is built to receive one horizontally positioned cavity equipped with its helium vessel, its tuner and various RF couplers. The maximum heat load is ≈ 58 W (2.5 g/s) at 2 K for high power peak processing and ≈ 6 W (0.25 g/s) under normal conditions. Q_{RF} will be obtained from heat load measurements by LHe level variation and gas flow measurement at known temperature and pressure. The calibration is given by a DC electrical heater. The paper describes the design and the preliminary results of cryogenic performance tests of the cryostat itself.

INTRODUCTION

The cryostat is built to receive a 9 cell cavity fully equipped with its welded helium vessel, main coupler, HOM couplers and cold tuner before final assembly of 8 cavities together in the TTF (Tesla Test Facilities) cryomodule.

It will allow measurement of cavity performances, tuning range, accuracy and speed of the cold tuner, depending on bath pressure variations and Lorentz forces action in the cavity.

It may also allow a more detailed study of RF electron trajectories and X ray production, due to surface emitters.

In this simplified layout the quench behaviour of cavities at high fields can be studied and first tests on the handling of quenches and adequate protection systems can be performed, involving not only RF signals, but also the bath pressure and cavity vacuum.

MAIN FEATURES OF THE CRYOSTAT

The vacuum vessel made of mild steel is equipped with a large hinged cover, giving full access for the cavity assembly. All connections are placed close to the cover (input coupler, helium supply vacuum pipe and cabling).

Two thick aluminum shields, one cooled at 77 K with liquid nitrogen, the second at 4.5 K with liquid helium insure the thermal insulation of the cavity (fig 1).

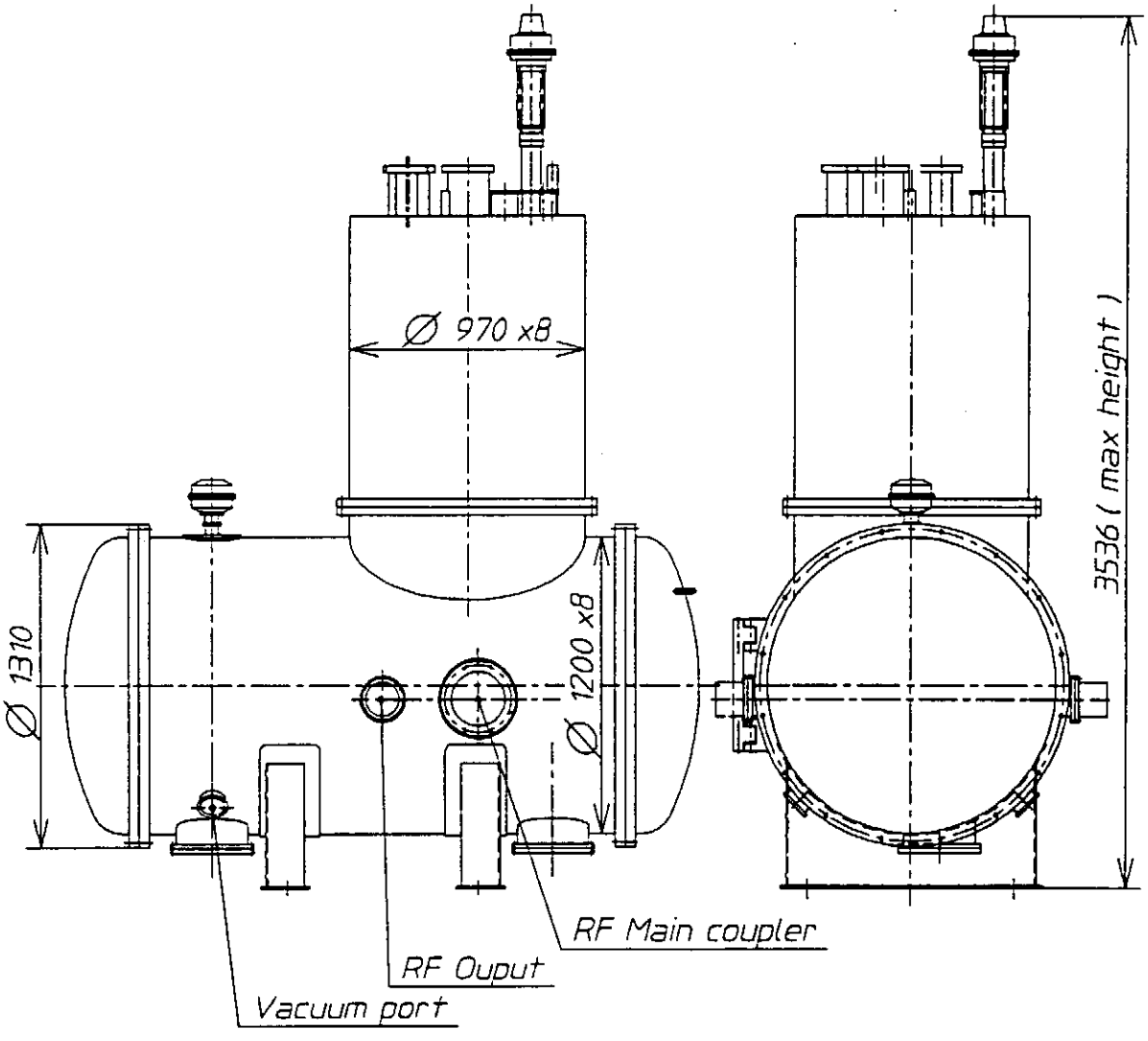

Figure 1. Outside view of the cryostat

The cavity is fixed on a bench supported by two insulating posts. Each post has two intercepts one at 4.5 K and one at 77 K.

The cryogenic equipment is placed in a vertical turret . All components are easily accessible by lifting the vacuum turret sleeve (fig 2 & 3).

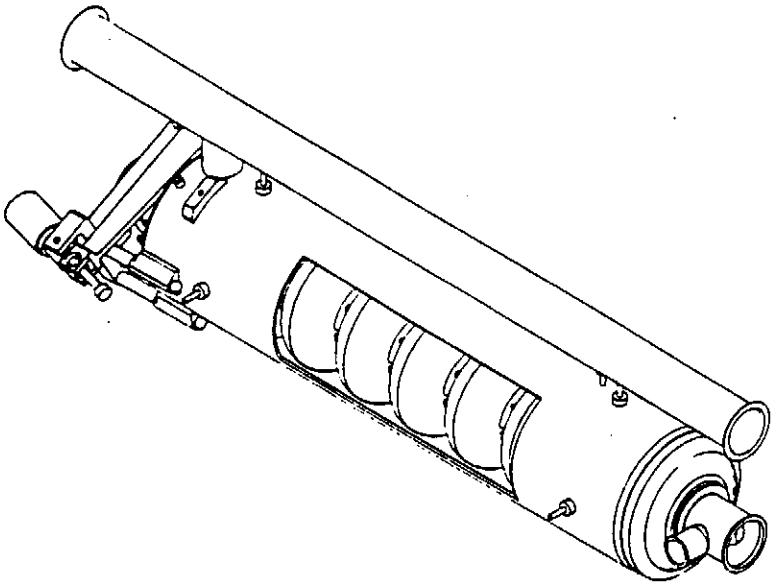

Figure 2. Dressed RF cavity, with cold tuning system.

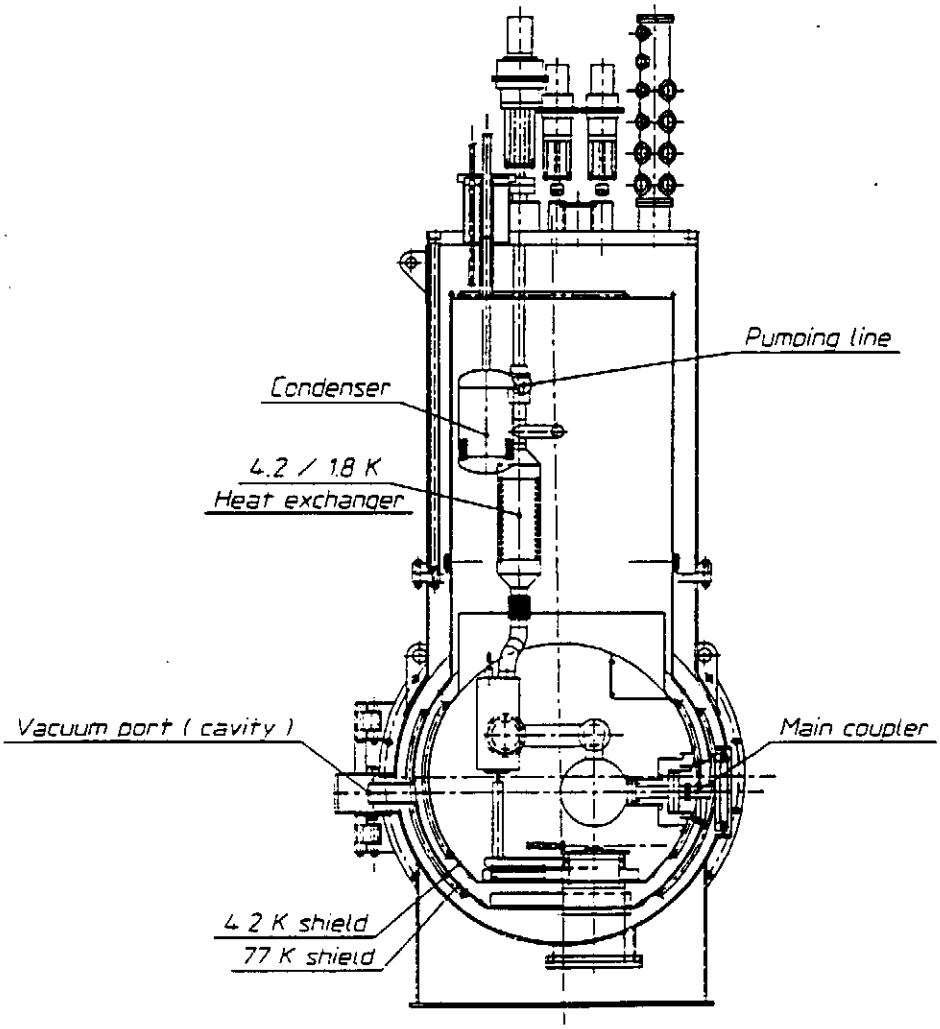

Figure 3. Cross section of the turret.

Table 1. Main characteristics of Chechia

Item	Unit	Value
Length	mm	2 612
Height	mm	3 536
4.5 K shield dimensions	mm	Ø 954 x 1850
Design pressure		
1.8 K section	bar abs	2
4.5 K section	bar abs	3
77 K section	bar abs	3
Heat consumptions		
1.8 K section	g/s	0.012
	W	0.28
	l/h	0.29
4.5 K section	g/s	0.49
(including transfert line)	W	9.9
	l/h	14.25
4.5 K shield temperatures		
Temperature inlet	K	≈ 4.5 K
Temperature outlet	K	≈ 6.5 K

CRYOGENIC FLOW CHART

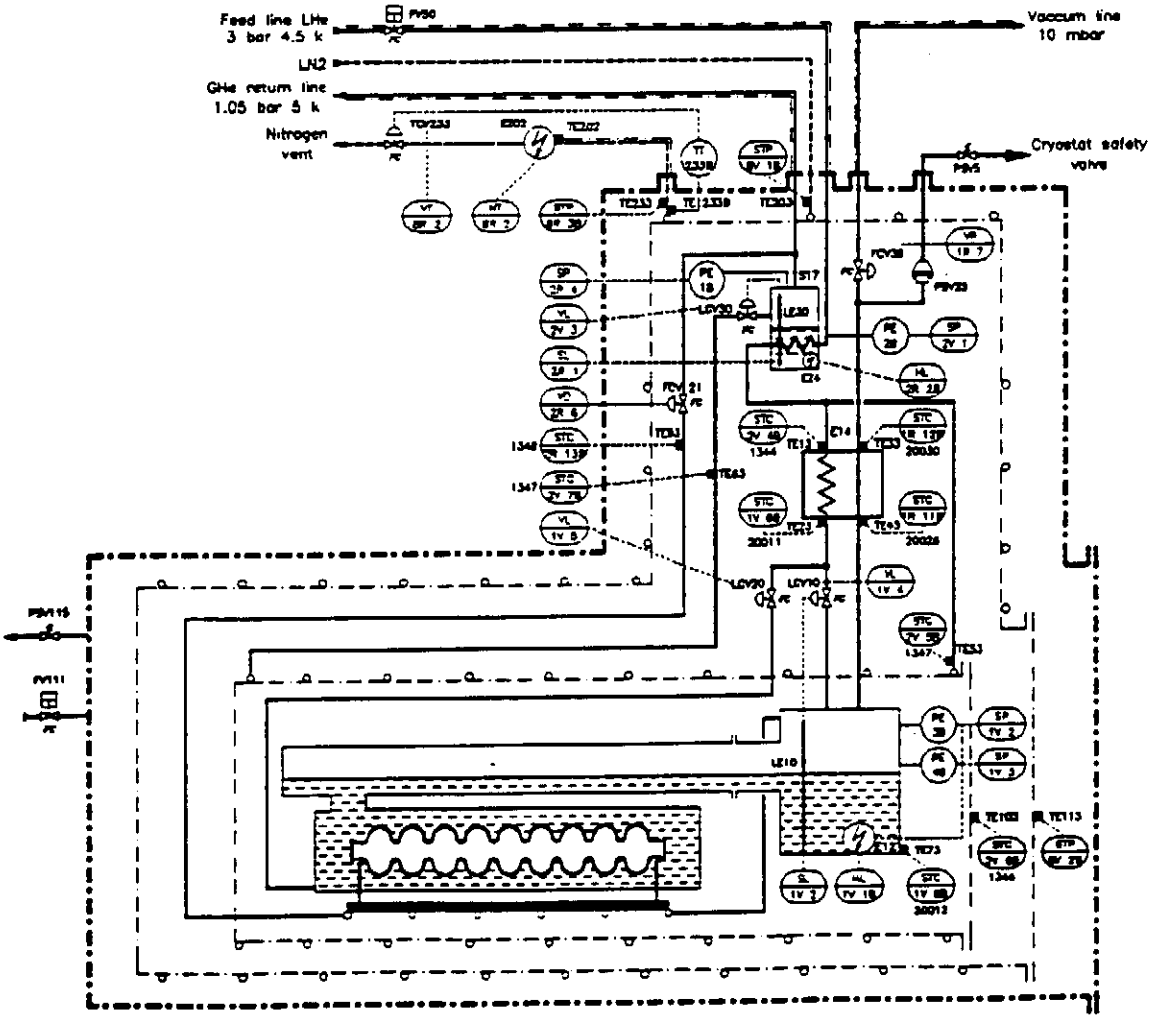

Figure 4. General flow chart of CHECHIA.

The flow schematic for CHECHIA is shown in fig. 4.

The helium is supplied by a 4.4 K/900 W refrigerator at a pressure of about 3 bars and a temperature of 4.4 K.

Before being expanded into the two phase volume, the mass flow is passed through the 5 K heat shield. After having absorbed the heat load of the shield, the helium returns at about 5K to the condenser inlet and expands through the valve LCV 30. The vapor is returned to the refrigerator or to the helium recovery circuit (fig. 4).

From the liquid phase of the condenser a flow of about 2.5 g/s is forced into the heat exchanger where it is subcooled to about 2.2 K by means of the 2 K vapor return flow from the cavity helium vessel.

The final pressure in the cavity will be 16 mb at 1.8 K, after expansion through the Joule-Thomson valves LCV 10 and 20.

Table 2. Instrumentation

Sensors	Quantity	Type
Thermometers		
HOM	2x2	Carbon sensor RIVA®
Main coupler	2	»
Spare	5	»
He vessel		
Shields		
J.T. valves	1	Carbon sensor RIVA®
Pumping line	1	»
Cold tuner	2	»
Heater (2 K circuit)	1	»
Level sensors		
2 K sump	1	SC wire sensor
2 K sump	1	»
Pressure sensors		
1.8 K circuit	1 + 1	WIKA® MKS®
4.5 K circuit	2	WIKA®

UTILIZATION OF THE CRYOSTAT

Cavity performance measurement.

The aim is to measure a few points of the curve Q_{RF} versus accelerating field. As the input coupler will not have the right coupling coefficient, cryogenic measurements have to be done to determine the heat load at 2 K with and without RF.

The Q_{RF} input power is simulated by an electrical heater placed in the 2K sump.

The goal is to reach an accuracy of ≈ 0.4 W which means that the static heat load has to be at most about 4 W.

Two methods will be used:

1. For a steady liquid level, one measures the flow rate out of the cryostat. A good accuracy is expected in measuring the pumped helium gas flow, with mass flow meters, provided the measurement is made during sufficiently long time.

2. With no helium flow in, one measures the liquid helium level change. To increase the accuracy, the level probe is installed in the 2 K sump. This container is placed higher than the cavity vessel which can be kept full of helium during the measurement. The cross section of the sump is small enough to amplify the level variations.

High peak processing treatment.

The HPP technique offers the possibility of cleaning up residual emission. Controlled exposures that test the survival of the benefits of HPP will be carried out to establish a protocol for the assembly of cavities. The helium consumption at 2 K will then be much higher than under normal RF processing. A compromise has been set at 2.5 g/s for the maximum helium flow at 2 K, corresponding to 58 watts.

RESULTS

Determination of Q_{RF} with the flow meters.

Two mass flow meters are used, one covering the range of 0 - 1 g/s and the second the range of 0 - 20 g/s.
Equivalent Q_{RF} input is computed from the voltage on the heater. The flow was measured for various values of Q_H input power. The steady flow is obtained after 1 hour stabilization. For 1 watt after integration of the flow-meter signal during 1 hour, the precision is better than ≈ ±0,2 W in the range of 20 to 40 watts of input power.

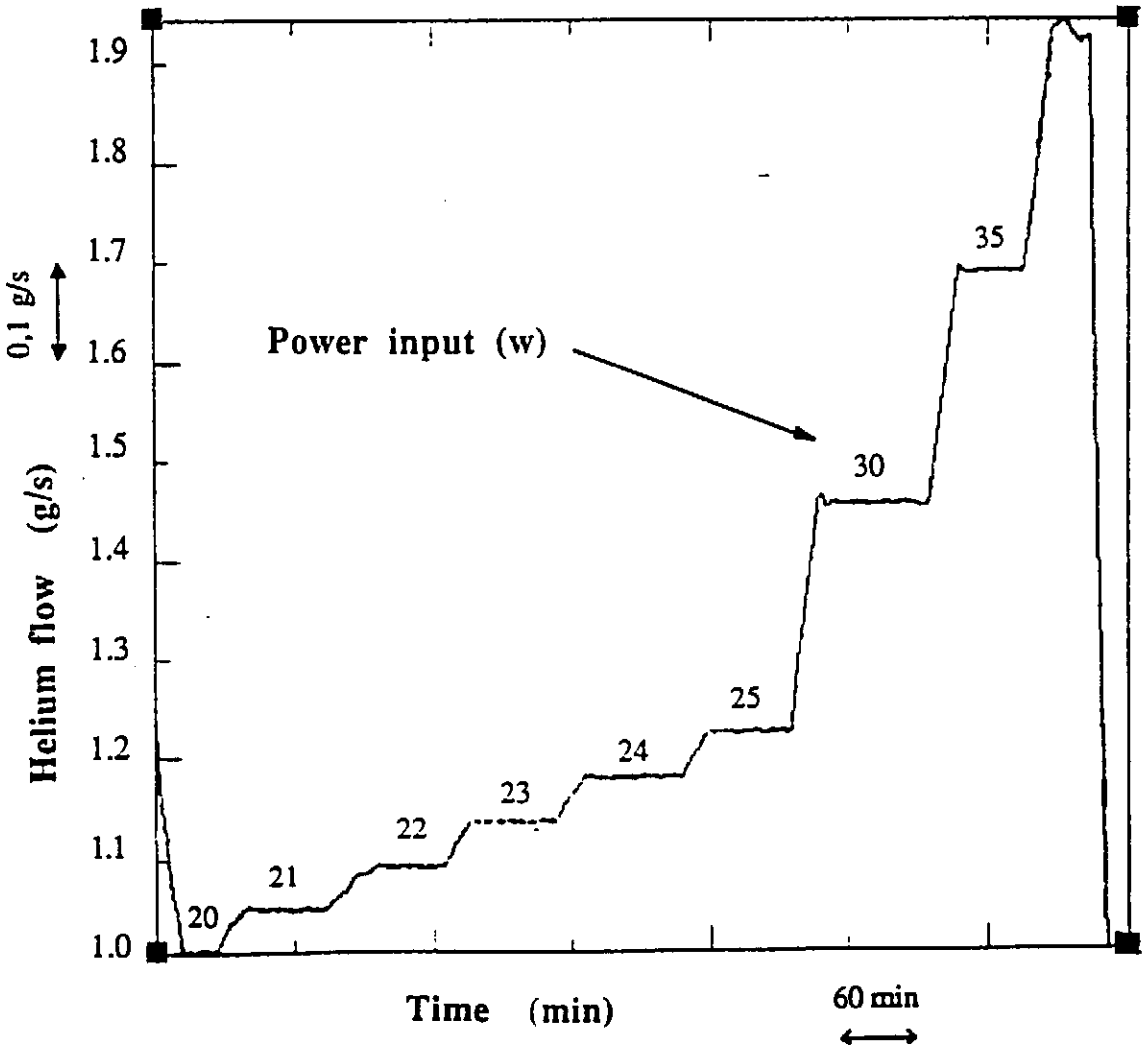

Figure 4. Flow measurements function of Q_H input (computed), with mass flow method

If a calibration is made before the test of the cavity, an accuracy of ≈ ±0.1w can be reached.

Determination of Q_{RF} with level difference

The level is measured with a superconducting sensor in the sump, the internal diameter is 150 mm.

The precision of level measurement is ≈ 1 mm over a height of about 80 mm, which gives an accuracy better than ≈ ±0.2 w (over 4 mn). This measurement requires no additional calibration.

Table 3 - Measurement of Q by level difference at 1.8 K

Q input (w)	0	1	2	18	34
Total evaporated He flow (g/s)	0,012 (1)	0,053	0,095	0,82	1,48
Corrected flow (g/s)		0,042	0,084	0,81	1,47
Q measured (w)		0,97	1,95	18,2	34,2

(1) Static losses

The precision of this method is altered by the decrease of heat losses coming from the piping when the input power increases.

CONCLUSION

Both mass flow and level difference measurements can reliably be used to determine the Q_{RF} values. The accuracy of mass flow measurements depends on the calibration before the tests. The level difference method gives a better accuracy in the low range values (0 - 10 watts).

REFERENCES

1. A proposal to Construct and Test Prototype Superconducting R.F. Structures for Linear Collider, DESY/Hamburg, April 1992.
2. Tesla Test Facility Linac - Design Report, March 1995, TESLA 95-01.

SAFE AND EFFICIENT OPERATION OF MULTISTAGE COLD COMPRESSOR SYSTEMS

M. Kauschke, C. Haberstroh, H. Quack

Technische Universität Dresden
Lehrstuhl für Kälte- und Kryotechnik
D-01062 Dresden, Germany

ABSTRACT

Large refrigeration rates in the temperature range of super fluid helium can only be obtained with the help of centrifugal cold compressors. For the large 2 K systems, four compression stages are necessary to reach atmospheric pressure. Centrifugal cold compressors are quite sensitive to mass flow and suction temperature variations; but these have to be expected in a real system. The first step in the systems design is to find safe and efficient quasi-stationary modes of operation.
The system which is being proposed for the TESLA refrigerators relies on two features. The first is to allow the room temperature screw compressor, downstream of the cold compressors to work occasionally with a subatmospheric suction pressure. The second is to stabilise the suction temperature of the third stage of compression at about 10 K. With these features it is possible, that in all modes of operation all four compressor stages operate exactly at their design point.

INTRODUCTION

In the linear collider project TESLA electrons will be accelerated up to a collision energy of 500 GeV. TESLA will work with superconducting cavities operating at 1.3 GHz. This e^+e^--collider will be built from nine-cell cavities with an acceleration gradient of about 25 MV/m. For a final energy of 500 GeV a total accelerator length of 32 km is required.
The liquid helium for the linac will be made available by 16 refrigerators in 8 refrigerator stations. This means that each refrigerator supplies a length of 1.8 km of the linac. The refrigerator specification is mainly given by the cooling demands of the cavities and the quadrupoles. The superconducting cavities have to be cooled below 2 K [1]. The quadrupole magnets for focusing the beam are designed for a working temperature of 4.4 K. An 80 K cooling shield is proposed in order to reduce radiation losses.
The provisional specifications for one refrigerator are given in Table 1.

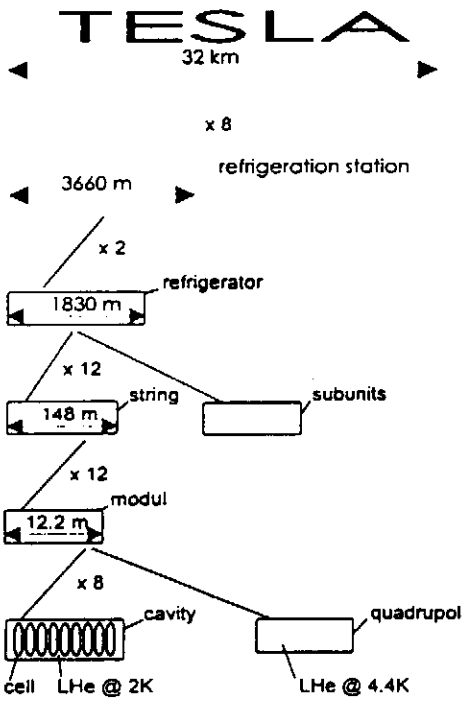

Figure 1: TESLA refrigeration scheme

Table 1: Heat loads of TESLA at the three temperature levels per refrigerator

	static load	total load
2 K	500 W	4.2 kW
4.4 K	2 kW	4.4 kW
80 K	6.5 kW	22 kW

It is important to note that additionally to the static load, dynamic loads are induced by the 1.3 GHz excitation of the cavities. So the refrigerators will have to cope with strongly and rapidly changing loads. Nevertheless the refrigerators should have a very good efficiency, because the running costs of the collider are a major cost factor and they contribute strongly to the viability of the total project.

So the challenge is to invent a refrigerator scheme, which is thermodynamically efficient, but also flexible to cope with rapidly changing loads.

COLD COMPRESSORS

The temperature of 2 K corresponds to a vapour pressure of helium of 31 mbar. The large refrigeration capacity required for TESLA can only be obtained with a multi-stage cold compression system [2]. The total pressure ratio up to atmospheric pressure is about 36, so using a four stage system an average pressure ratio of 2.5 per stage is required. Actually the colder stages will have a somewhat larger pressure ratio.

The main difficulty of the task comes from the fact, that such turbocompressors have a very narrow safe operational band, quite different from the load changes, which one has to expect. The cold compressors are very sensitive to changes in the suction temperature, because the suction temperature influences strongly the necessary enthalpy head which has to be covered by the single compressor.

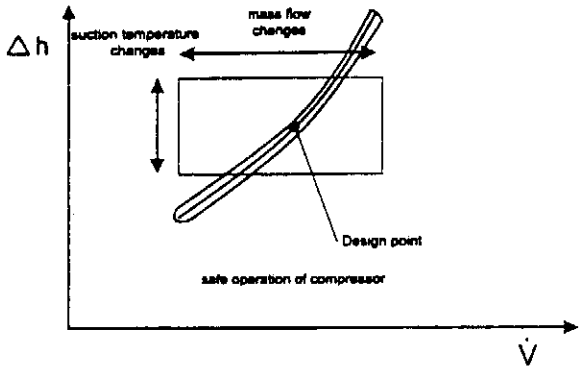

Figure 2: Required duties and safe operational regime of cold compressors

Figure 2 demonstrates the dilemma caused by the ranges of mass flow and suction temperature which have to be covered. Figure 2 shows even only half of the problem, because it does not yet describe the dynamics, i.e. the speed at which the changes may occur.

QUASI-STATIC SOLUTIONS

The task has to be solved in two steps:
First a solution has to be found for the quasi- static operation, i.e. for the required operational range shown in figure 2, where the speed of change is not yet taken into account.

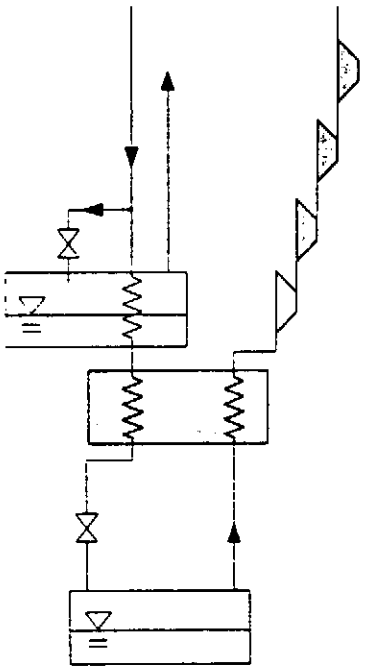

Figure 3a

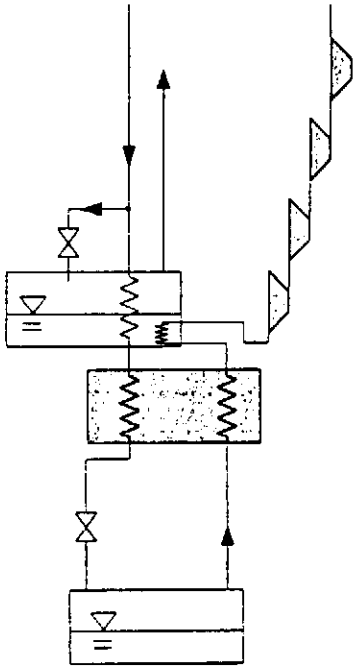

Figure 3b

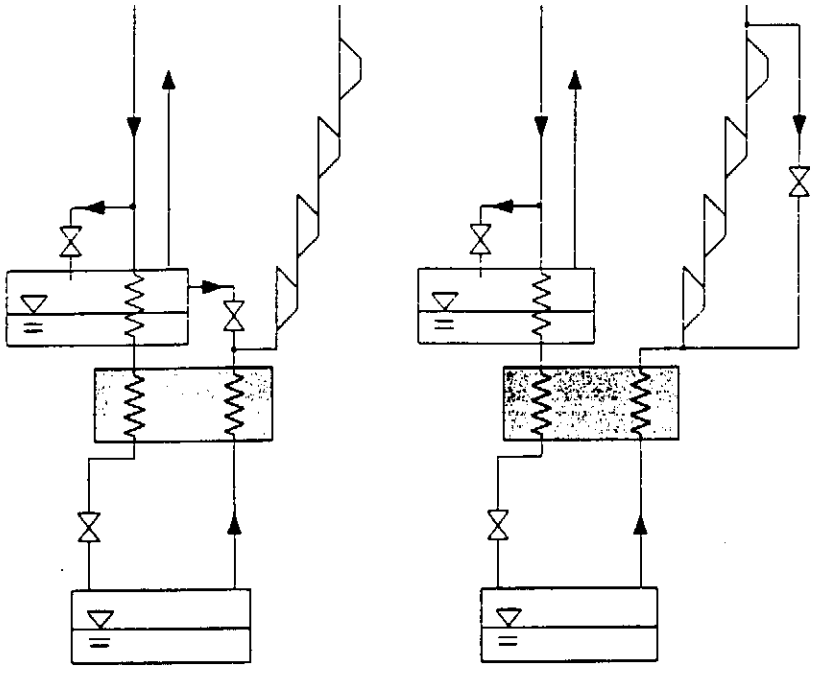

Figure 3c Figure 3d

Figure 3: Diverse approaches of controlling safe operation of cold compressors

In figure 3, a number of previous approaches are shown [3]. Figure 3a shows the starting system with the characteristic of figure 2. In figure 3b the suction temperature of the first stage of compression is stabilised by a thermal anchoring to a 4.4 K bath. By this method the disturbing influence on the required enthalpy head is removed, but

- the changes in the mass flow rate are not addressed
- in the heat exchanger thermodynamic losses due to heat transfer from 4.4 K to 3.5 K are produced
- and this is a very expensive heat exchanger causing additional pressure drop for the low pressure gas.

Figure 3c shows the proposal for a bypass valve from the vapour space of the 4.4 K bath to the suction side of the first compression stage. This way the fluctuations of the mass flow rate are reduced, to a certain degree also the suction temperature is stabilised. But still this operation is thermodynamically not acceptable over longer periods of operation.
Figure 3d shows a bypass valve over all four stages of compression. This may stabilise the suction mass flow, but it has a detrimental effect on the suction temperature and efficiency.

Our approach was led by the search for a solution with a minimum of loss producing features at least for the quasi-static operation. To cope with the mass flow variation, we intend to work with the speed control of the compressors only: If less flow comes the speed is reduced, if more flow comes the speed is increased. And if the suction temperature rises or falls we live with that pressure ratio, which the compressor is able to handle under such flow and speed conditions.

With this control method, the total pressure ratio cannot anymore be reached under all mass flow conditions, the exhaust pressure of the fourth stage is being reduced at smaller than design flow rates. But this fits well with the volumetric suction characteristic of the main refrigerator screw compressor. At lower mass flow rates it may go to subatmospheric suction pressure. At higher than design flow rates, the cold turbo compressors provide a higher than design pressure ratio and the screw compressor may operate at an elevated suction pressure.

To make this scheme possible, the flow between the cold compressors and the associated screw compressor needs its own channels in the plate-fin heat exchangers.

DAMPENING HEAT EXCHANGER

The pressure ratio which can be reached with this scheme can be stabilised by anchoring the suction side of the third compression stage to the 10 K level of the main refrigeration cycle. This is the temperature range, where the high pressure stream has its peak specific heat. Therefore it is a quite stable range - similar to a condenser in a vapour compression system. At low flow rates, the first two stages of compression provide a relatively low pressure rise and therefore also a small temperature rise to the low pressure stream. Thus the low pressure stream will be warmed up in the 10 K anchor exchanger. So the third stage gets a larger suction volumetric flow rate and can produce a higher pressure ratio.

At high flow rates, the low pressure stream comes at a higher pressure and temperature to this heat exchanger. It is cooled down to 10 K and the duty of the third and fourth stage of compression is reduced.

For the design of the anchoring heat exchanger, we propose to use a plate fin exchanger in cross flow configuration. Since no internal distributors are needed in this design, pressure drop is minimised. Because this heat exchanger is situated at a relatively high pressure and temperature level, the thermodynamic losses are minimal.

FLOW DIAGRAM

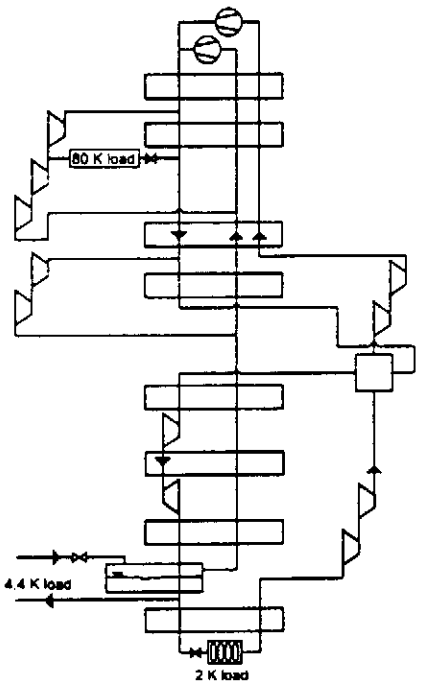

Figure 4: Proposed flow diagram

In figure 4 the flow diagram of one of the refrigerators is shown. The screw compressor downstream of the cold compressors is allowed to work with a suction pressure below atmospheric pressure.

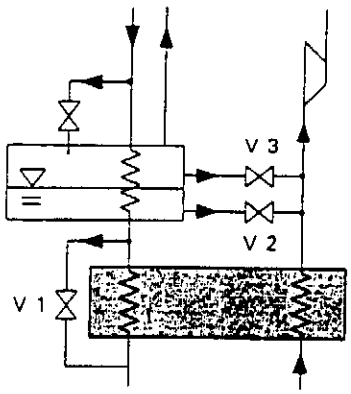

Figure 5: Means for handling of dynamic loads

HANDLING OF DYNAMIC LOAD CHANGES

Having established a scheme, which allows efficient and safe operation at all foreseeable quasi- static modes of operation, further dampening means have to be provided which give the refrigerator enough time to adjust to quick load changes. The operation of 3 valves is provisionally foreseen for this purpose:

- V1- a HP bypass valve around the final heat exchanger
- V2- an injection of liquid helium into the cold compressor suction line
- V3- the throttling of 4.4 K vapour into the cold compressor suction line

The arrangment of the valves is shown in Figure 5. The questions, which of the these valves will be operated under what conditions will be studied in a dynamic numerical simulation investigation.

ACKNOWLEDGEMENTS

We would like to thank DESY (Deutsches Elektronen-Synchrotron) for supporting this research project.

REFERENCES

[1] D. Trines et al: Conceptual design of the cryostat and cryogenic supply for a superconducting linear collider. High Energy Accelerator Conference, 1992

[2] H. Quack. Cold compression of helium for refrigeration below 4 K, Advances in Cryogenic Engineering, Vol. 33 (1987), 647-653

[3] Jean- Philippe Guignard: Contribution a l'etude de la stabilite de fonctionnement et de l'adaptation de charge des compresseurs centrifuges cryogeniques multietages. CERN AT Group Report 93-05 (CR)